[Frontiers In Bioscience, Landmark, 22, 1379-1426, March 1, 2017]

Photosystem II and terminal respiratory oxidases: molecular machines operating in opposite directions

Sergey A. Siletsky[1], Vitaliy B. Borisov[1], Mahir D. Mamedov[1]

[1]Belozersky Institute of Physico-Chemical Biology, Lomonosov Moscow State University, Leninskie Gory, Moscow 119991, Russian Federation

TABLE OF CONTENTS

1. ABSTRACT

In the thylakoid membrane of green plants, cyanobacteria and algae, photosystem II (PSII) uses light energy to split water and generate molecular oxygen. In the opposite process of the biochemical transformation of dioxygen, in heterotrophs, the terminal respiratory oxidases (TRO) are at the end of the respiratory chain in mitochondria and in plasma membrane of many aerobic bacteria reducing dioxygen back to water. Despite the different sources of free energy (light or oxidation of the substrates), energy conversion by these enzymes is based on the spatial organization of enzymatic reactions in which the conversion of water to dioxygen (and vice versa) involves the transfer of protons and electrons in opposite directions across the membrane, which is accompanied by generation of proton-motive force. Similar and distinctive features in structure and function of these important energy-converting molecular machines are described. Information about many fascinating parallels between the mechanisms of TRO and PSII could be used in the artificial light-driven water-splitting process and elucidation of energy conversion mechanism in protein pumps.

2. INTRODUCTION

Almost all of production of molecular oxygen and most of its consumption by living organisms on Earth are carried out by photosystem II (PSII) and terminal respiratory oxidases (TRO) respectively. Due to PSII, photoautotrophs are capable to use light energy to split water and generate molecular oxygen. It is the primary light-driven enzyme in the photosynthetic electron transport chain in thylakoids of cyanobacteria and chloroplasts which extracts electrons from water and transfers them to the primary (PQ_A) and secondary (PQ_B) plastoquinone molecules. The protons derived from water are released into the thylakoid lumen. As a result, the chemiosmotic gradient (proton motive force or $\Delta\mu H^+$) is formed and maintained. The reduced plastoquinone (plastoquinol) acquires reducing ability to transfer electrons further along the chain of chloroplasts to generate NADPH. The molecular oxygen is a by-product of photosynthesis, but it plays a key role in bioenergetics of higher organisms and aerobic microorganisms.

In heterotrophic organisms, the reaction of the conversion of water into dioxygen occurs in the opposite direction. In the respiratory electron transport chain of mitochondria, NADH or succinate are oxidized by complex I or complex II, producing the reduced ubiquinone (ubiquinol), which then transfers its electrons via complex III to cytochrome *c*, the ultimate substrate for cytochrome *c* oxidase (COX, also known as complex IV). COX belongs to heme-copper oxidases which together with *bd*-type cytochromes compose a large group of terminal respiratory oxidases. These widespread membrane-bound enzymes constitute the last component of the respiratory electron transfer chains in eukaryotes and aerobic prokaryotes. They catalyze reduction of dioxygen into water by cytochrome *c* or ubiquinol coupled to the transfer of electrons and protons across the membrane and formation of $\Delta\mu H^+$. The latter is a source of energy for cell's biosynthesis reactions, membrane transport, mechanical movement of bacterial cells, etc. In this review, we describe some similar and distinctive features of these important energy-converting molecular machines.

3. OVERALL CHARACTERIZATION OF CATALYTIC FUNCTION AND SYSTEMATIC CLASSIFICATION

During catalysis both molecular machines (PSII and TRO) are faced with the need to couple the four-electronic conversion of water to dioxygen (or vice versa) with redox transformation of one-electron and two-electron carriers. To perform the catalytic function of the reduction of molecular oxygen or the oxidation of water, TRO and PSII use specific catalytic sites which are located in the hydrophobic core of the enzyme, and several multivalent metal atoms which are specifically arranged in cooperation with each other and with protein amino acid residues.

The presence of these centers enables enzymes to carry out catalytic reactions in one stage that avoids the release of the intermediate products of dioxygen evolution and simultaneously prevents uncontrolled solvent participation in the catalytic reaction. However, localization of the catalytic center within the membrane protein requires the specific arrangement of the pathways to deliver and release all substrates and products including electrons, protons, dioxygen and water molecules.

The implementation of the catalytic functions by these membrane proteins is accompanied by the conversion of free energy into membrane potential gradient. A significant difference between the enzymes is due to the fact that in the case of PSII, a source of energy is the energy of the quantum of visible light, whereas in the case of TRO, it is the oxidation of substrates with a lower (more negative) redox potential (cytochrome *c* or quinol). In order to distinguish the energy-coupling membrane proteins, the two main mechanisms of the membrane potential generation are accepted: redox loop and proton pump ones. The first mechanism, Mitchell's chemiosmotic oxidoreduction (redox) loop, is based on the organization of oxidation and reduction half-reactions on different sides of the membrane, and uses an electrogenic charge transfer within the membrane in the form of an unpaired electron. This mechanism is utilized by

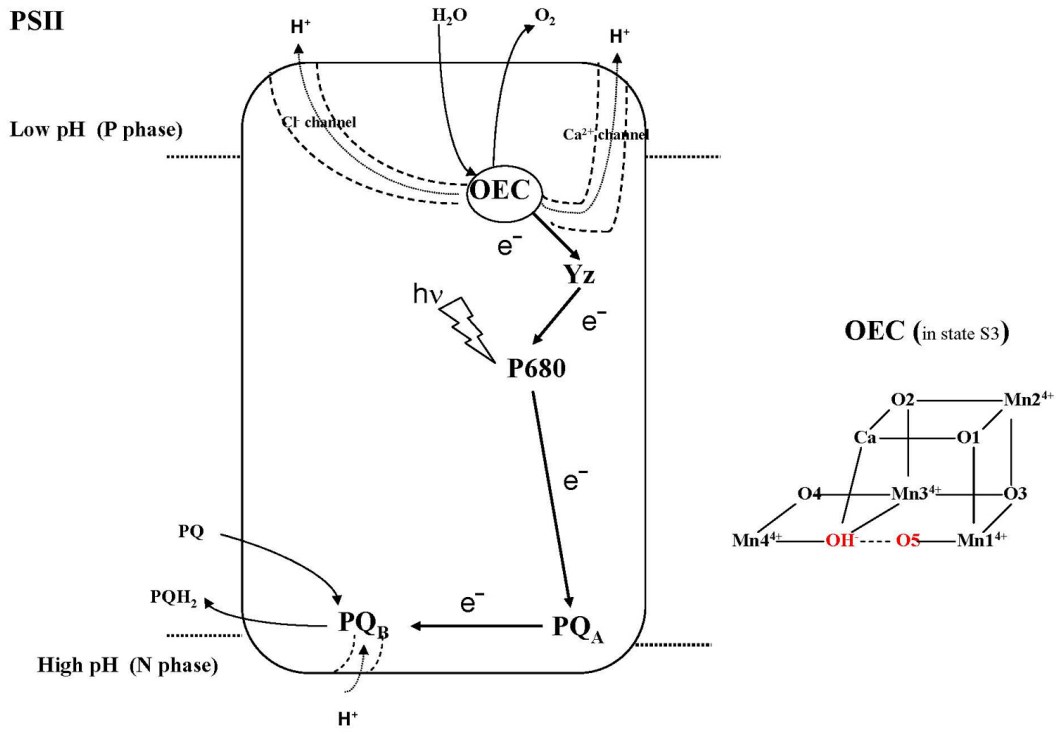

Figure 1. The overall structure of Photosystem II. The redox-active cofactors and the proton pathways (protonic "Ca^{2+} channel" and "Cl^- channel") are indicated. The structure of the catalytic OEC centre (Mn_4CaO_5 cluster) is shown in the S3 state, without protein ligands. The oxygen atoms, which form the oxygen molecule are shown in red color. During the catalytic cycle the cubane of Mn_4CaO_5 cluster is converted from the "open" to the "closed" state and vice versa. In the "open" state, the O5 atom is bound to the Mn4, Ca and Mn3. During formation of the S3 state, the cubane is converted from the "open" to the "closed" state and the O5 atom is shifted from the Mn4 and becomes to be bound to the Mn1. Besides, the vacant coordination site formed on Mn4 is filled with the second molecule of substrate water that binds as a hydroxide ligand.

both PSII and TRO. However, unlike PSII, the sites of oxidation and reduction of the redox reactions in TRO are located closer to one side of the membrane and a significant portion of the membrane potential is formed by electrogenic intraprotein proton transfer from the opposite side of the membrane. In addition, heme-copper TRO have a special mechanism for the $\Delta\mu H^+$ generation by using of a pumping device which transports protons from one side of the membrane to the other.

3.1. Photosystem II

In the thylakoid membrane(s) of higher plants, cyanobacteria and green algae, PSII is organized in the form of a homodimeric transmembrane protein complex, which consists of more than 40 subunits. The core of each PSII monomer, the so-called reaction center (RC) is formed by the two homologous proteins D1 and D2, which contain most of the cofactors involved in catalysis and electron transfer (Figure 1). The PSII core complex functions enzymatically as water:plastoquinone oxidoreductase. This enzyme uses light energy to transfer electrons from water to plastoquinone (energetically uphill without light energy) and to build the proton gradient in the manner that can be described in terms of Mitchell's chemiosmotic oxidoreduction loop. The water oxidation and generation of molecular oxygen occur in the catalytic water splitting center of PSII, also known as the oxygen-evolving center, OEC, which is located on the donor side of the thylakoid membrane, close to the lumen side. During oxidation of the water, the protons are released from the OEC into the lumen, which is a low-pH compartment. The process of the plastoquinone reduction is arranged on the opposite ("acceptor") side of the membrane and is coupled to the proton uptake from the stroma, the high-pH compartment. The donor and acceptor faces correspond to the P (positive) and N (negative) sides of the internal membrane of mitochondria, in which the $\Delta\mu H^+$ is stored mainly as a $\Delta\Psi$, whereas the ΔpH form is that in a chloroplast. It should be noted that the *in vivo* storage of $\Delta\mu H^+$ may differ from that observed *in vitro* or in electrode-impaled cells, where ionic balance may be disrupted. In accordance with this, experiments performed on isolated spinach thylakoids demonstrated that a significant fraction of transthylakoid proton motive force can be stored as $\Delta\Psi$ for long periods of time, provided that activities of ions permeable to the thylakoid membrane were kept low, consistent with earlier results (1).

PSII catalyzes the following reaction:

$2H_2O + 2PQ + 4$ photons $+ 4H^+$ (stroma) $\rightarrow$ $2PQH_2 + O_2 + 4H^+$ (lumen) $+ 4q$

where q is the amount of charge transferred across the membrane

The tunneling of electrons through a series of intermediate acceptors, across the protein from the electron donor on the P-side to the electron acceptor on the N-side makes a major contribution to the membrane potential generation. A quantum of solar light absorbed by antenna proteins is transmitted to chlorophyll P680, a special pigment located close to the P-side the membrane. Further oxidation of the excited P680 by pheophytin (~15 ps) and subsequent electron transfer to the primary quinone acceptor, PQ_A, (~250 ps) occur towards the N side of the membrane (2-3). Acting as one-electron carrier, the PQ_A is the electron donor (through the non-heme iron atom) for the secondary quinone acceptor, PQ_B. As a two-electron acceptor, PQ_B takes two protons from the stroma and then the completely reduced PQ (PQH_2) diffuses out of the PQ_B pocket into the membrane quinone pool. Though the protons are delivered to the buried PQ_B site electrogenically towards the P-side of the membrane to “meet” the electrons at the quinone reducing site, the distance of that movement is relatively small as compared to the primary charge separation due to the photoinduced electron transfer.

Oxidized P680 is reduced by a redox-active tyrosine (Y_Z), which serves as one-electron carrier between the OEC and P680. Y_Z is re-reduced through the oxidation of the OEC which consists of a cluster of four manganese and one calcium ions (the Mn_4CaO_5 cluster) (Figure 1). In the OEC, bridging oxide ions connect the metal ions. In addition, the water molecules and the surrounding amino acid residues provide further carboxylic acid (oxygen) and histidine (nitrogen) ligation of the metals in the first coordination sphere. The release of protons onto the P side of the membrane induced by oxidation of water in the OEC occurs at a distance of ~ 30 Å through a ‘protein-cap’ that protrudes greatly from the membrane into the lumen. As a result, it makes a relatively small contribution to the $\Delta\mu H^+$ generation and, thus, the charge movement by PSII across the membrane is mainly contributed by the electron transfer from the P- to the N-side of the membrane and only partially by the proton transferred in the opposite direction.

Thus, PSII is a complex and unique molecular machine which combines the light-induced charge separation due to one-electron transfer across the membrane, four-electron oxidation of water to dioxygen associated with proton release to the lumen side and the two-electron reduction and protonation of the PQ_B molecule on the acceptor side of the membrane, thus producing and maintaining the ΔpH across the thylakoid membrane.

Chloroplast genomes typically contain 100–150 genes and encode proteins important for photosynthesis and other functions of chloroplasts. A chloroplast has its own nucleus where all the major subunits (*PsbA, PsbB, PsbC, PsbD, PsbE, PsbF* and several others) (but not all) are encoded.

3.2. Terminal respiratory oxidases

Terminal respiratory oxidases comprise a superfamily of heme-copper oxidases and a very important distinct group of *bd*-type oxidases. The most important differences between these two groups are: a different structure of the catalytic dioxygen-reducing centre, an unprecedented resistance of the catalytic center of cytochrome *bd* to inhibitors, the lack of redox-active copper ions in cytochrome *bd*, the ability of heme-copper oxidases to pump protons across the membrane.

3.2.1. Heme-copper oxidases

The superfamily of heme-copper terminal oxidases includes cytochrome *c* oxidase (COX) of mitochondria of higher and lower eukaryotes, heme-copper oxidases of most aerobic prokaryotes and structurally related NO-reductases (4-6). Heme-copper oxidases catalyze the transfer of electrons from either cytochrome *c* or quinol to dioxygen to form water, coupled to the generation of a proton-motive force (7-9). All these oxidases contain two heme redox centers (the low-spin and the high-spin) buried in the membrane (Figure 2). The heme groups can be presented by different heme types: *a* or *b* for the low-spin heme, and a_3, o_3, or b_3 for the high-spin heme. The high-spin heme participates in the organization of the catalytic binuclear centre (BNC) which consists of a closely located iron ion of the heme and a copper ion (in the NO-reductase - an ion of the non-heme iron) (10-12). The BNC is a distinctive feature of the superfamily.

As one-electron mediator, the low-spin heme accepts electrons from cytochrome *c* (or quinol) oxidizing site located near the P-side of the membrane and passes them into the dioxygen-reducing BNC. If the electron donor is cytochrome *c*, as in cytochrome *c* oxidase of mitochondria, the electron transfer to the low-spin heme occurs through an additional copper center, Cu_A.

During the catalysis, electrons enter step-by-step the BNC from the outside of the membrane (P-side) at the distance of ~1/3 of the membrane thickness, while protons involved in the reduction of dioxygen and

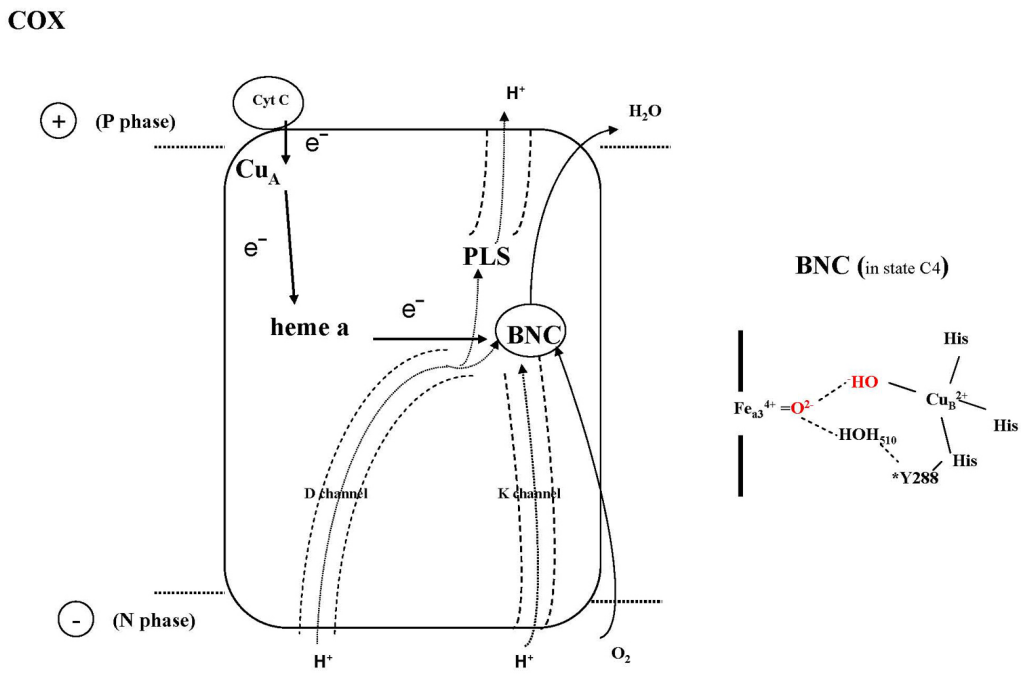

Figure 2. The overall structure of cytochrome *c* oxidase. The redox-active cofactors and the D and K proton pathways are indicated. The likely structure of the catalytic BNC center including the redox-active tyrosine residue and the water molecule 510 is shown in the C4 state. The oxygen atoms which form the oxygen molecule are shown in red color.

formation of water molecules (the so-called "substrate" protons) are transferred electrogenically into the BNC from the inner aqueous phase (N-side) (Figure 2). Two molecules of water are produced from one molecule of oxygen. This spatial organization of the transfer of the charged substrates to the BNC can be considered as a modified Mitchell's redox loop mechanism of the $\Delta\Psi$ generation in which both redox reactions are located close to the P-side of the membrane, and the uncompensated charged proton passes through the largest part of the membrane thickness (13). In addition, heme-copper oxidases are the redox-linked proton pumps (14-15). I.e., the enzyme transfers additionally four protons (the so-called "pumped" protons) from the N-side to the P-side of the membrane on average per a molecule of oxygen, by using of a special mechanism of an active unidirectional proton translocation against a proton gradient. Structurally similar to the heme-copper oxidases, NO-reductases reduce N_2O to NO. However, those are not capable of pumping protons through the membrane (16).

Similarly to PSII, a heme-copper terminal oxidase can be characterized as a complex and unique molecular machine which combines one-electron oxidation of cytochrome *c* (or two-electron oxidation in case of a quinol oxidase), four-electron reduction and protonation of the oxygen molecule to form water and redox-linked unidirectional transfer of protons across the membrane (13-14, 17-19). Due to a unique proton pump mechanism, the chemical reaction catalyzed by COX involves the charge separation corresponding to the directed translocation of eight charges across the membrane per each molecule of the reduced dioxygen that is two times greater than in case of PSII.

A heme-copper terminal oxidase catalyzes the following reaction:

$$4c^{2+} + O_2 + 8H^+_{in} \rightarrow 4c^{3+} + 2H_2O + 4H^+_{out} + 8q$$

(when the electron donor is cytochrome *c*)

or

$$2QH_2 + O_2 + 8H^+_{in} \rightarrow 2Q + 2H_2O + 8H^+_{out} + 8q$$

(when the electron donor is quinol)

where q is the amount of charge transferred across the membrane

The superfamily of the heme-copper oxidases can be divided into three main families (A, B, C), the differences between them are mainly based on the structure of the proton-conducting pathways (6, 20-21). The most studied members of the A family include the eukaryotic cytochrome *c* oxidase from bovine heart mitochondria, the aa_3 oxidases from *Paracoccus denitrificans* and *Rhodobacter sphaeroides*, and the bo_3-type quinol oxidase from *Escherichia coli* (6, 22-32). All these enzymes are characterized by a high degree of homology between primary structures of three major subunits forming a catalytic core. Prokaryotic oxidases usually contain 1-2 additional

subunits. A core subunit of the eukaryotic oxidase is mitochondrial genome-encoded, while additional subunits (up to 11 in mammals (33)) are encoded by the nuclear genome.

A typical member of the B family of the heme-copper terminal oxidases is ba_3 from *Thermus thermophilus*. It has a low primary sequence homology with those of the A family and, in addition, is characterized by a number of functional features (34-37). The C family is the most remote family from an evolutionary point of view and consists of the cbb_3 oxidases from various prokaryotic organisms (38-40).

3.2.2. bd-type oxidases

Cytochromes *bd* constitute a separate family of TRO. The *bd* enzymes reveal no sequence homology to the heme-copper oxidases (5, 41-43). They have been found only in bacteria and archaea (44-48). Cytochromes *bd* are solely quinol oxidases and cannot use cytochrome *c* as an electron donor. It is of interest to note that a bacterial cytochrome *bd* can tightly bind to the bovine heart mitochondrial membrane and operate as an intrinsic component of the chimeric myxothiazol-inhibited respiratory chain thereby supporting cytochrome bc_1 bypassed respiration (45). Some *bd*-type enzymes (e.g. from *Escherichia coli* and *Azotobacter vinelandii*) form uniquely stable oxy-complexes (49-52) because of high O_2 affinity (53-54). Cytochromes *bd* are reported to protect bacteria against a variety of stresses (46, 48, 55-56) induced by such agents as peroxynitrite (48, 57), nitric oxide (46-48, 55, 58-62), sulfide (63-64), carbon monoxide (65), hydrogen peroxide (47-48, 66-74). A *bd*-type oxidase has been detected in a number of pathogens and there is a positive correlation between its expression level and virulence (see (48) and references therein). Thus, like the mitochondrial cytochrome *c* oxidase (75-76), a prokaryotic cytochrome *bd* has a role in human physiology and pathophysiology.

Cytochrome *bd* is composed of two large (CydA and CydB), and one small subunits. The CydA subunit carries a quinol binding site and three hemes, b_{558}, b_{595} and *d* (77). Heme b_{558} serves as the immediate electron acceptor from the quinol. It is low-spin (78) and seems to be functionally homologous to heme *a* in the mitochondrial cytochrome *c* oxidase. Hemes b_{595} and *d* are in the high-spin state (78). The chemistry of O_2 reduction takes place at heme *d*. The precise role of heme b_{595} is still unclear. A hydrophilic connection between transmembrane helices 6 and 7 in CydA that is part of the quinol binding site is called 'Q-loop' (77, 79-84). Based on the size of the Q-loop, the *bd*-type oxidases can be divided into two subfamilies, L ('long Q-loop' that comes from the fact that they have an insert in the C-terminal portion of the Q-loop) and S ('short Q-loop') (43, 85-87). Some of the S subfamily members are referred to as cyanide-insensitive oxidases (CIO) (43). CIOs are able to support respiration even in the presence of 1 mM cyanide (88). Their heme content is not entirely clear; however, it was shown that at least in some CIO members heme *d* is replaced with heme *b* (88-90).

The first atomic structure of cytochrome *bd* (77) does not support a linear sequence of electron transfer accepted so far (quinol $\rightarrow b_{558} \rightarrow b_{595} \rightarrow d$). The distance between hemes b_{558} and b_{595} appeared to be larger than that between b_{558} and *d* (77). Therefore, the three hemes appeared to be in a triangular arrangement: an electron transferred from quinol to heme b_{558} moves directly to heme *d*, and then possibly equilibrates with heme b_{595} (77). The highly conserved Trp374 located between heme b_{558} and heme *d* is probably needed for efficient electron transfer from b_{558} and *d* (77).

Cytochrome *bd* catalyzes the following reaction:

$$2QH_2 + O_2 + 4H^+_{in} \rightarrow 2Q + 2H_2O + 4H^+_{out} + 4q$$

where q is the amount of charge transferred across the membrane

The mechanism of the $\Delta\mu H^+$ generation by cytochrome *bd* is supposed to represent a variation of a redox loop mechanism and formally resembles that of the heme-copper oxidases which is based on the vectorial redox chemistry. As with the heme-copper oxidases, the two half-reactions, quinol oxidation and O_2 reduction to water, occur at the same side of the membrane, closer to its P-side. The voltage ($\Delta\psi$) is generated mainly by protons coming from the N-side and crossing the "bulk" of the membrane to "meet" electrons at the O_2 reducing site. A much smaller part of $\Delta\psi$ is generated due to release of protons from the site of quinol oxidation to the P-side of the membrane and due to the electron transfer in the opposite direction from the site of quinol oxidation to the O_2 reducing site. Also, as in the case of PSII, each electron transfer through the *bd* enzyme is coupled to the transfer of one charge across the membrane.

4. THREE-DIMENSIONAL STRUCTURE. SUBUNIT COMPOSITION AND REDOX COFACTORS. DELIVERY OF SUBSTRATES

For all the above mentioned enzymes (photosystem II, heme-copper oxidases, cytochrome *bd*), three-dimensional structures were established by the X-ray structural analysis in recent decades. This has promoted the study of the mechanism at the molecular level. General topography, relative positioning of subunits to each other and within the membrane were elucidated. All redox cofactors, putative channels for

supply of the substrates into the active centre, and proton and electron transfer pathways were localized. Considerable changes in the structure were clarified for a number of mutants and intermediates of the catalytic center, which indicates the importance of key amino acid residues and the mechanism of change of conformation and a way of delivery of the substrates of the reaction.

In recent years, significant progress has been made due to the emergence of new femtosecond X-ray lasers, the use of which prevents radiation damage and reduction of metal atoms in active centers of enzymes during X-ray structure analysis. It gives more accurate information about the catalytic centre of enzymes and imposes restrictions that are important in the breakdown of the mechanism of mutual conversion of dioxygen and water at the atomic level (in particular, the clarification of the exact native "undamaged" distances between the metal ions in the OEC is essential to establish the mechanism for O-O bond formation in the PSII).

It should be noted that in both types of enzymes the reaction of the conversion between water and dioxygen occurs in the highly organized active centers. These centers are located in the hydrophobic core of the protein and contain several atoms of polyvalent metals. In both enzymes, there is a redox-active tyrosine residue located near the catalytic center and, as one-electron carrier, directly involved in the exchange of electrons and (in some cases) protons with an active catalytic center. Both enzymes reveal a histidine residue in the neighborhood of the tyrosine residue. It forms the covalent or hydrogen bond with the tyrosine, thereby modulating the redox-active and proton-acceptor properties of that tyrosine. In both cases, the delivery of substrates (O_2, H_2O, electrons and protons) to the active center inside the protein is believed to occur via specific pathways that are arranged and adjusted in a special way.

4.1. Photosystem II

4.1.1. Subunits composition, redox-centers

The structure of PSII core complexes from cyanobacteria has been solved by X-ray diffraction with a resolution up to the 1.9 Å (91-95). PSII is a 700 kD homodimeric membrane protein complex (95), which has dimensions of 105 Å depth (45 Å in membrane), 205 Å length, and 110 Å width (92). The PSII complex from cyanobacteria (*Thermosynechococcus elongatus or Thermosynechococcus vulcanus),* contains 16 integral membrane subunits composed of 35 transmembrane helices and 3 lumenal subunits (92-93).

The reaction center (RC) of each PS-II monomer includes two subunits, D1 and D2, each comprising five transmembrane helices. Flanking the opposite sides of the D1/D2 heterodimer are the core antenna proteins: CP43 (PsbC) and CP47 (PsbB) subunits, each having six transmembrane helices (I to VI) arranged in a circular manner (92). The overall reaction centre (CP43/D1–D2/CP47 core) is characterized by pseudo-twofold symmetry (92). In addition to the protein subunits, 35 chlorophylls, two pheophytins, 11 β-carotenes, more than 20 lipids, two plastoquinones (PQ), two heme irons, one non-heme iron, four manganese atoms, three or four calcium atoms, three Cl ions, one bicarbonate ion and more than 15 detergents per a monomer were resolved (93). One of the calcium ion and all Mn ions are included into the Mn_4CaO_5 cluster of the OEC (the oxygen evolving centre), and two of the Cl ions are in the vicinity of the Mn_4CaO_5 cluster.

Outside the CP43/D1–D2/CP47 core, there are 13 transmembrane helices, which are assigned to specific low-molecular-weight subunits (92). The two of these helices (PsbE and PsbF) are assigned to subunits of cytochrome b559 (Cyt *b*559). The remaining 11 transmembrane helices are assigned to 10 low-molecular weight subunits, including PsbZ, which has two transmembrane helices (I and II). The functions of most of these small subunits are unclear. They are supposed to be involved in dimer formation, in stabilization of the peripheral chlorophylls of the D1 and D2 proteins, in facilitation of the carotenoid binding, in participation of the formation of the a "cap" over the OEC at the lumenal surface.

CP47 and CP43 bind 16 and 13 antenna chlorophylls, respectively, which are arranged as double layers connected by a special chlorophyll at the middle of the two layers (93). In response to the illumination, excitation energy is transferred from the antenna system to the P680, formed by chlorophyll a (Chl) molecules, located toward the lumenal surface. The P680 excited state (P680*) is delocalized over the four chlorophylls (ref. in (92)). An electron is ejected from the excited primary electron donor P680 toward the stromal surface to the final electron acceptor, plastoquinone PQ_B. The intermediate electron transfer sites are the ones of the chlorophylls of P680 (ChlD1), which is the chlorophyll closest to the pheophytin (PheoD1), the pheophytin (PheoD1) and is a firmly bound plastoquinone PQ_A (ref. in (92)).

The cationic radical $P680^{*+}$ is reduced by a redox-active tyrosine (Tyr161 of D1 subunit), known as Yz, to generate a neutral tyrosine radical Yz*, which acts as an oxidant for the water oxidation process at the OEC. The redox-active Tyr is located on the 7 Å distance from the OEC. It should be noted that unlike the heme-copper oxidase, Yz is included in neither the first nor the second sphere atoms surrounding the OEC, however, is associated with the OEC

through a network of hydrogen bonds formed by water molecules. With the exception of PQ_A, all the redox-active cofactors involved in the electron transfer processes are located on the D1 subunit of the RC. The PQ_A is hydrogen bonded to the main-chain amide group of D2 Phe261 and D2 His214, where the latter also serves as a ligand to the nonheme Fe. The quinone ring is accommodated within a hydrophobic cavity composed of residues, including D2 Ile213, D2 Thr217, D2 Met246, D2 Ala249, D2 Trp253, D2 Ala260, and D2 Leu267.

The nonheme Fe mediates electron transfer from the primary (Q_A) to the secondary (Q_B) plastoquinone molecules and it has four histidine ligands: D1 His215, D1 His272, D2 His214, and D2 His268 and fifth bidentate ligand, bicarbonate (93). The PSII PQ_B is hydrogen bonded to D1 Ser264 and D1 His215, which is also a ligand for the nonheme Fe, and possibly to the main-chain amide group of D1 Phe265. The PQ_B binding pocket is composed of the residues including D1 Met214, D1 Leu218, D1 Ala251, D1 Phe255, and D1 Leu271. The D1 His252 residue, which is within hydrogen-bonding distance of D1 Ser264, could facilitate protonation of PQ_B molecule (92).

4.1.2. Structure of the oxygen-evolving complex (OEC)

The active centre of the OEC contains pentamethalic cluster, which consists of the four manganese atoms and the single calcium atom (92-93). Five oxygen atoms were found to serve as oxo bridges linking the five metal atoms whereby the whole structure is organized in a shape of "distorted chair". Three manganese (Mn1, Mn2, Mn3), one calcium and four oxygen atoms (O1, O2, O3, O5) form a cubane-like structure in which the calcium and manganese atoms occupy four corners and the oxygen atoms occupy the other four (Figure 1). Every two adjacent manganese ions are linked by di-μ-oxo bridges (i.e. deprotonated water molecules). Mn1 and Mn2 are linked by a di-μ-oxo bridges via O1 and O3, Mn2 and Mn3 are linked via O2 and O3. The calcium is linked to manganese ions in a cubane by oxo bridges: to Mn1 via the di-μ-oxo bridge formed by O1 and O5, to Mn2 via O1 and O2, to Mn3 via O2 and O5 (93).

The fourth manganese (Mn4), which is referred to as a "dangling" Mn, and the O4 oxygen are located outside the cubane. They form the backrest of the chair, which consists of the Mn4–O4 linkage and the connection of the Mn4 and O4 to one of the oxo bridges (O5) and one of the Mn atom (Mn3) of the cubane, correspondingly. Two of the three Mn in the cubane (Mn1 and Mn3) and "dangling" Mn4 are redox active. They can exist in the +3 or +4 state. Mn2 is the most distant from "dangling" Mn4 and is redox-inactive being in the oxidation state +4 for the entire catalytic cycle.

The asymmetry of cubane is explained by the different bond lengths between atoms, caused in particularly by the presence of Ca ion and O5. While the bond length between the oxygens and manganese ions are in the range of 1.8–2.1 Å, those between O5 and the manganeses (Mn4 and Mn1) are in the range of 2.4–2.6 Å (93). Besides, the bond lengths between the oxygens and the calcium in the cubane are generally in the range of 2.4–2.5 Å (for O1 and O2), and the bond length between O5 and the calcium is 2.7 Å. The unusual long distance of the Mn-O5 and Ca-O5 bond resolved in the three-dimensional structure of the S1 state was explained by that the O5 is not μ-oxo, but hydroxide (93).

The employed X-ray doses resulted in radiation damage in the form of partial reduction of the Mn ions. Most recently, 'radiation-damage-free' three-dimensional structure of the pentametallic cluster in the S1 state was obtained by employing X-ray Free Electron Laser (XFEL) pulses (95). This structure of PSII constrains the net oxidation state (III, IV, IV, III) of the manganese cofactor in the resting S1 state (96). It was found that the Mn4-O5 distance is about 2.3 Å and O5-Mn1 distance is about 2.7 Å. The unusual distance between the Mn1 and O5 state was eventually interpreted as the ability of O5 to be shifted along the axis Mn4-Mn1 to Mn4 atom, which may be accompanied by a transition of cubane from the open state to the closed one, change of the spin state and joining of the molecule of substrate water to the Mn1 atom at the next intermediate of the catalytic cycle (S2) (95-96).

In addition to the five oxygens, four water molecules (W1 to W4), or water derived ligands, are directly ligated to metal ions of the Mn_4CaO_5 cluster. Two of which (W1 and W2) are coordinated to Mn4 with respective distances of 2.1 and 2.3 Å, and W3 and W4 are coordinated to the calcium with a distance of 2.5-2.6 Å (95). The formation of the O-O bond in the oxygen molecule is suggested to occur between the two oxygen atoms located most probably on the axis between Mn4 and Mn1. One of these atoms is apparently O5 formed in the OEC at the initial stage of the catalytic cycle from the first substrate molecule of water (97). As suggested, W2 and/or W3 can be exchanged with water molecules from the water supplying channels and in turn to be molecules of the substrate water involved in the subsequent catalytic cycle, replacing O5 and moving onto the one axis between the atoms Mn1 and Mn4 during the catalytic cycle (95, 97). It is interesting to note that functionally active atoms Mn1 and Mn4 forming a connection with the oxygen atoms of the two substrate water molecules

are approximately located at the same distance from each other as the atoms of iron and copper in the oxygen-reducing binuclear center of heme-copper oxidases.

There are usual coordination numbers of high-valent Mn (5 or 6 coordinate) and Ca ions (typically 6-8 coordinate). Therefore, in addition to links to the di-μ-oxo bridge, the first coordination sphere of the Mn_4CaO_5 cluster contains the oxygen atoms of carboxylate residues Asp342, Glu333, Ala344 Asp170 of the D1, which bridge Mn1–Mn2, Mn3-Mn4, Ca^{2+}-Mn2 and Ca^{2+}-Mn4, correspondingly. Mn2-Mn3 is bridged by the CP43-Glu354. Only one N-donor, His332, coordinates to Mn1, which is also mono-coordinated by Glu189. The D1-His 337 and CP43-Arg 357, which are hydrogen-bonded to both O2, O3 and O4 of the Mn_4CaO_5 cluster may function to stabilize the cubane structure of the metal cluster as well as to provide partial positive charges to compensate for the negative charges induced by the oxo bridges and carboxylate ligands of the metal cluster (93).

In addition to the direct ligands of the Mn_4CaO_5 cluster, the residues and water molecules in the second coordination sphere may play important roles in maintaining the structure of the metal cluster and the dioxygen-evolving activity. These include for example the carboxylate oxygen of D1-Asp 61, which is hydrogen-bonded to W1 and also to O4 indirectly through another water molecule, is located at the entrance of a proposed proton exit channel and may function in facilitating proton exit from the Mn_4CaO_5 cluster (93). Another example is the network of the water molecules, which binds the W4, W3 W2 (and possibly O5), Tyr161–His190 couple and the WA water molecule located near the His with the WA–WD water molecules by which the proton could be transferred to the lumen (98). Thus, this network of water molecules forms a second path for proton transport into the lumen.

4.1.3. Substrate-transfer pathways: protons, O_2, H_2O

Several water-filled channels in PSII proteins structures have been identified by X-ray crystallography, which can form long-range hydrogen-bonded networks, connecting the Mn_4CaO_5 cluster with the lumen (99). They can be divided in general to the three or four sets of channels and they were named the “back channel”, “narrow and broad channels” and the “large channel system” (100-102). Substrate specificity (i.e., the role of these channels in the transfer of water, dioxygen and protons) remains unclear. Moreover, different ways can be used for transfer of substrates at different stages of the catalytic cycle, since the output of four protons as well as the binding of two molecules of water does not occur during one stage of the catalytic cycle but at different stages.

Of these channels, the “back channel” includes the nearest environment of the redox-active Yz and leads to Ca^{2+} and to water molecules W3 and W4 associated with it (99, 103). Initially proposed to function as a water channel, it has been shown through study of molecular dynamics to be impermeable for water, However, the hydrophobic water block in the middle of this channel may be permeable to dioxygen (104). The “large channel” was suggested to be a possible route to delivering of substrate water to the OEC (102, 105-106).

There are many indications that water-filled channels “narrow” and “broad”, starting from the D61 residue can participate in the transfer of protons into the lumen (101, 107-108). The “narrow” channel starts from the O4 oxo ligand of the OEC and goes to the D61 residue and further through the D1-N338, D2-N350 to the lumen at the interface of PsbO and PsbU in cyanobacteria (102). The ‘broad’ channel passes D61, E65, R334 residues of D1and E312 of D2, exiting to the lumen at the interface of the D2 and PsbO subunits. On the way to residues on the lumenal surface, this water-filled channel passes close a chloride Cl^- site and D2-K317, the amino group of which is a direct ligand of the Cl-1 site. Mutating D1-D61, D1-E65, D2-E312, and D1-R334, which interact with the chloride Cl^- site through a hydrogen bond network, to Ala decreased substantially one of the transitions (S3→S0) in the catalytic cycle (105, 109).

It is interesting to note the direct and stable salt-bridging interactions between D1–E65, D1–R334 and D2–E312. According to (101) this triad may represent a proton release group/proton loading site. As suggested, the part of the releasing pathways for the pumped protons in cytochrome *c* oxidase (110) and in bacteriorhodopsin (111) can be arranged in a similar way (including the electrostatic and structural effects). It should be noted that the study of the NH_3 binding to the OEC suggests that one of two substrate water molecules can be transferred along one path with protons releasing, the “narrow” channel (perhaps they are together only part of the way) (112). In accordance with this, a novel low-energy water binding mode was suggested through the path passing through D61 and reaching W1 (associated with “dangling” Mn4 molecule of water) (113).

Unlike S3→S0, the efficiency of other transitions in the catalytic cycle was not affected significantly by the D1-D61 and D2-K317 mutants (114-115). In this connection, it is assumed that another proton-conductive path can be used for proton excretion into the lumen from the OEC at several other stages of the catalytic cycle. In addition, a distinct isotope effect found for different stages of the catalytic cycle of PSII points to the participation of the alternative path (116).

This pathway is postulated on the basis of the structural data (93), as well as FTIR observation and QM/MM (quantum-mechanics/molecular-mechanics) data (98, 117). It includes an extensive hydrogen-bonding network between Yz and the Mn_4CaO_5 cluster and from Yz to the lumenal bulk phase. Yz is hydrogen-bonded to the two waters coordinated to the calcium either directly (to the W4) or indirectly through another water molecule to the W3 (93). This additional water also mediates the hydrogen bond between the two waters bound to Mn4 and Y_Z. The network of water molecules (WA-WD) starts from W4 and passes close to the D1-H190, which is further hydrogen-bonded to D1-N298 and to several waters and residues including CP43-A411, D1-N322 and PsbV-Y137, leading to an exit pathway to the lumenal bulk solution.

For this path, a novel proton transfer mechanism was proposed (98, 117), which suggests that a proton hopping from the Nτ-H of D1-His190 in the state of Y_Z*-HisH$^+$ to the WA water molecule. This proton hopping is the rate-limiting step that triggers rapid proton transfer from the water ligands, W4, W3 and W2 (and possibly O5 of the OEC) to the Y_Z oxygen. The proton accepted by WA is transferred to the lumen via the network of the water molecules (WA–WD) (98, 117). This mechanism is suggested to be driven by the electrostatic repulsion and its use can be connected to those catalytic states of the OEC, in which it holds an additional positive charge (116).

It remains unclear whether there is a dedicated route to facilitate the transport of O_2 away from the OEC (102). The oxidative damage of the residues caused probably by the reactive oxygen species (ROS) chemistry is shown in the “narrow channel” (118). Derivatization of enzyme with Kr suggests the participation of the “large channel” in the release of dioxygen (103), while computer simulation of the diffusion of dioxygen and the results of studying mutants indicate that the molecular oxygen may use the same transfer path as that of the water molecules in the broad channel (119).

On the electron acceptor side, upon accepting two electrons, PQ_B is converted into a plastoquinol molecule by the uptake of two protons, and is then exchanged with oxidized plastoquinones in the plastoquinone pool in the thylakoid membrane. PQ_B is reduced by the electron transfer from PQ_A mediated by a non-heme iron, which is coordinated by D1–H215, D1–H272, D2–H214, D2–H268 histidines and a bidentate bicarbonate ligand. Key residues H215, E244, Y246, H252, S264 from the D1 have been variously considered to participate in the proton transfer to PQ_B (101, 120).

The D1-His252/Ser264 residues in PSII are analogous to Asp-L213/Ser-L223 in one of the proton pathways of the bacterial reaction centre (BRC) (101). It is presumed to be at the end of the proton channel through which the proton is transferred to the PQ_B^-. The Glu-L212 residue in another proton channel, which provides a proton for Q_BH^- in the BRC is replaced by an alanine in the corresponding position of PSII. Instead, the D1–H215 residue that is ligated to the non-heme iron has been proposed to provide this proton to PQ_BH^- (121). It is suggested that the water molecule should entry between bicarbonate and D1–H215 to complete a hydrogen bonding network from the bulk via D1–Y246 and the bicarbonate to D1–H215, providing proton delivery to PQ_BH^- (101)

4.2. Terminal oxidases

This section discusses the structural data obtained basically during X-ray analysis of the heme-copper oxidases and the *bd*-type oxidase. Despite the similarity of the catalyzed reactions, in the three-dimensional structures of the heme-copper oxidases and cytochrome *bd*, a number of intimate features and important structural differences were identified, pointing to the peculiarities of the mechanism of dioxygen reduction and the membrane potential generation.

4.2.1. Heme-copper oxidases

4.2.1.1. Subunit composition, redox-centres and catalytic sites

The three-dimensional crystal structures of several members of the A type family were determined by the X-ray crystallography. These are COX from bovine mitochondria (122-125), the bacterial aa_3-type cytochrome oxidases from *Paracoccus denitrificans* (126-128) and *Rhodobacter sphaeroides* (129-130), the bo_3-type quinol oxidase from *Esherichia coli* (31), cytochrome caa_3 from *Thermus thermophilus* (131). Besides, the atomic structures of the B and C family members, cytochrome ba_3 from *Thermus thermophilus* (37, 132) and cytochrome cbb_3 from *Pseudomonas shutzeri* (39), were resolved. Although high-resolution X-ray structures of the bovine cytochrome *c* oxidase reported so far were exclusively of its dimeric form, by using the electron crystallography of two-dimensional crystals it was shown recently that the monomeric form of the mammalian cytochrome *c* oxidase is physiologically relevant and not an artifact of its isolation from mitochondria (133).

All members of the heme-copper terminal oxidases share a central largest subunit I built up of 12 membrane-spanning helices. The monomer of the mitochondrial COX contains 11 and 14 subunits (in yeast and mammals respectively) (33, 134), while the bacterial enzymes are usually made up of no more than four peptides. Three largest subunits form

a core of the enzyme. The subunit I contains three redox-active cofactors: the low-spin heme *a*, the high-spin heme a_3 and Cu_B. The center-to-center distance between heme *a* and heme a_3 is around 13 Å, whereas they are within Wan der Waals contact at the edges that provides a basis for rapid electron transfer (135). A distance between constituents of the catalytic BNC, the Fe atom of the high-spin heme and the copper atom Cu_B, is about ~ 4.5-5 Å (37, 39, 122, 126).

The low-spin heme and the binuclear centre are located at a depth of about one third of the membrane thickness from the P-side (122, 126) (Figure 2). The hemes are oriented perpendicular to the membrane plane, so that their propionate moieties are pointing to the P-side. Two other substituents of the hemes *a* and a_3 (the formyl group and the hydroxyethylfarnesyl side chain) are pointing to the N-side of the membrane. Cu_B is retained in the protein by the ligation with three histidines (H284, H333 and H334; amino acid numbering from *R. sphaeroides* is used). There is a crosslink between one of the Cu_B histidine ligands (H284) and a tyrosine residue (Y288) (123, 136-137), which is suggested to supply a proton to promote scission of the O-O bond and may be included as part of the catalytic site (17, 138-139) (Figure 2).

The low-spin heme *a* is an immediate electron donor for the heme a_3/Cu_B site. It is re-reduced by Cu_A, a redox-active center composed of two copper ions. Cu_A is held by subunit II of COX, which has two membrane spanning α-helices and provides a docking surface for cytochrome *c* at the P-side of the membrane. The distance between Cu_A and the hemes are 20.6 and 23.2 Å, respectively, when measured from the central point of the two coppers to the iron atoms (122). The third subunit composed of seven transmembrane helices does not hold any redox-active metal sites, but it is highly conserved. In the absence of this subunit, the turnover rate of cytochrome *c* oxidase becomes 100-1000-fold lower and the enzyme undergoes suicide inactivation (140).

In the bo_3-type ubiquinol oxidase from *E. coli*, hemes *a* and a_3 are replaced with hemes *b* and o_3 respectively. Subunit I is very similar to that of other members of the A family. The ubiquinone-binding site is proposed to be at the surface between transmembrane helices I and II of subunit I, near the P-side surface (141). This site is located close to heme *b* at a position analogous to Cu_A in e.g. cytochrome *c* oxidase. Q101, H98, D75 and R71 were proposed to interact with ubiquinone.

Experimental evidence suggests the existence of two ubiquinone binding sites in cytochrome bo_3: the low-affinity site (Q_L), at which the substrate is oxidized from ubiquinol to ubiquinone, and the high-affinity site, Q_H, which is proposed to mediate (as a bound semiquinone) the electron transfer from Q_L to the metal centers (142). EPR studies of site-directed mutants provided evidence that the quinone binding site derived from X-ray structure is the Q_H-site which stabilizes the observed semiquinone (143). It is suggested that the two quinone binding sites may be adjacent to each other or partially overlap (142).

4.2.1.2. Substrate-transfer pathways: protons, O_2, H_2O

Two conserved structures (the so-called D- and K-channels) were identified in the three-dimensional structures of the mammalian mitochondrial and prokaryotic cytochrome *c* oxidases of the A family, leading from the inner aqueous phase into the hydrophobic region of the protein to the binculear center (37, 122, 126, 129). The proton-conductive D-pathway (D-channel (144-146)) leads from a conserved aspartate residue, D132, through a chain of 10-12 water molecules linked by the hydrogen bonds (128-130) to a conserved glutamate residue, E286, located at a distance of 10-12 Å from the BNC and 24-26 Å from D132 (129). Water molecules in the D-channel are stabilized by hydrogen bonds with a number of highly conserved hydrophilic amino acid residues: N139, N121, N207, S142, S200, S201 and S197 (147).

The proton-conductive K-pathway (K-channel (145-146)) is located directly under the BNC and leads from the surface of the protein from the N-side of the membrane to a conserved tyrosine residue, Y288, that is located near the BNC and is an electron donor for the formation of the P_M state. The entrance to the K-channel is located near the E101 residue of subunit II (128, 148). In addition to the lysine residue (K362) the channel includes conserved threonine residues (T352 and T359), a serine residue (S299) and a few firmly bound water molecules (128-129).

On the basis of kinetic studies of the mutant forms of cytochrome *c* oxidase from *R. sphaerodies* and *P. denitrificans* it is assumed that all pumped and the two (or three) substrate protons in the bacterial cytochrome *c* oxidases of the A family are transported through the D-channel (145). At the same time, in the D-channel, the proton path above the E286 residue is not revealed crystallographically. Molecular dynamics showed that the cavity between E286 and the BNC can be filled with several weakly bound water molecules (up to 4), which are capable of spontaneously forming a short-lived chain of hydrogen bonds. These chains can be stretched in the direction of the BNC or to the external aqueous phase (149-151). It is assumed that in a prokaryotic cytochrome *c* oxidase of the A family, the pumped protons are released into outside of the membrane through a hydrophilic domain located above

the heme group and Cu_B (152). This domain comprises a cluster of negatively charged groups of the protein (including conserved residues D399 and D404), several arginine residues, propionate substituents of hemes, molecules of water and a redox-inactive metal atom - Mg^{2+}, that can be partially replaced with Mn^{2+} (128). It should be noted that the two propionates of hemes *a* and a_3 are salt-bridged with guanidino groups of R439 and R438 respectively that, as in the case of PSII, can play a key role in the gating of proton release.

In addition to the D- and K-channels, the third proton-conductive pathway, H-channel, was discovered in the structure of the mammalian mitochondrial cytochrome *c* oxidase (124, 153). The H-channel begins at the N-side of the membrane near the H413 residue. This proton-conductive pathway includes series of cavities filled with water molecules. The cavities are connected by the serine, threonine and farnesyl group of heme *a*. The H-channel leads from the inner aqueous phase to the Y371 and R38 residues, which form a connection with formyl and propionate groups of heme *a*, respectively. Further, the H-channel passes through the peptide bond between Y440 and S441, which, presumably, plays the role of a valve or “gate” that determines the direction of the proton in the H-channel through the S205 residue and then to the D51 residue which is located near the P-side of the membrane (124).

In the structure of the ba_3-type cytochrome oxidase from *T. thermophilus* belonging to the evolutionary distant B family, three potential proton-conducting pathways can be distinguished (37). Two of them have a weak homology with the D- and K-proton channels of the A family oxidases. They lead from the internal aqueous phase to the BNC of the enzyme. The third proton-conductive pathway (the Q-channel) does not contain conserved amino acid residues, while the overall structure of the Q-channel is similar to the H-channel of the mitochondrial cytochrome *c* oxidase (37). Based on the site-direct mutagenesis it is concluded that in the B type cytochrome oxidases, there is only one functioning entry channel for the uptake of both scalar and vectorial protons, the K-channel (154). For the proton transfer above the BNC of the ba_3 oxidase from *T. thermophilus*, a potential mechanism is proposed which involves the A propionate of heme a_3, and the D372, H376, and E126 residues (155).

Delivery of molecular oxygen into the BNC is provided by several hydrophobic channels which contain conserved tryptophan and phenylalanine residues and lead from the middle part of membrane lipid bilayer towards the active center (122, 129, 156-158). The release of water molecules from the BNC to the P-side of the membrane occurs, as suggested, via a path lying over the heme groups in the contact area between the subunits I and II, in close proximity to the Mg^{2+}/Mn^{2+} site (the redox-inactive metal center) (159). In mammals, Mg^{2+} bridges between E198 of subunit II and H368 of subunit I (122). There are indications that the path of the release of water molecules is composed of two channel-like structures which can also participate in conducting pumped protons to the outside of the membrane (155, 159-160).

4.2.2. bd-type oxidases

4.2.2.1. Subunit composition, redox centres and catalytic sites

Very recently, the first crystal structure of cytochrome *bd* (from *Geobacillus thermodenitrificans*) at 3.1 - 4 Å resolution has been reported (77). The protein consists of the two large subunits, CydA and CydB, and the newly discovered small subunit (66, 161-164). The latter may be needed for maintenance of the catalytic activity and stabilization of the hemes (161-162, 164). CydA and CydB were reported to possess the same fold that could be due to gene duplication of a single ancestral gene that coded for a homodimeric enzyme and subsequent mutations (77). As redox cofactors, cytochrome *bd* carries three different hemes located on CydA, one low-spin, b_{558}, and the two high-spin, b_{595} and *d*. Heme b_{558} is stabilized by the small subunit (77). This heme is in close proximity to the Q-loop and thus is directly involved in quinol oxidation. Its axial ligands are His186 and Met325 (Met393 in *E. coli*) (165). Heme *d* is the site at which O_2 binds and undergoes reduction to $2H_2O$. It is thought to have Glu378 (Glu445 in *E. coli*) as the axial ligand (77). The axial ligands of heme b_{595} are His21 and Glu101 (His19 and Glu99 in *E. coli*) (77). The vertical distances from the central Fe atoms of the hemes b_{558}, b_{595} and *d* to the P side of the membrane are ca. 18, 22.5 and 13.5 Å respectively (77). The precise role of heme b_{595} is not quite clear. The distance between the central Fe atoms of hemes b_{595} and *d* (11.6 Å) is too large for the formation of a *structural* binuclear site analogous to that in heme-copper oxidases (77). At the same time, edge-to-edge distances between these hemes are ca. 3.5 Å, i.e. they are in van der Waals contacts (77). This implies a possibility of a very rapid electron transfer between the hemes that indeed obtained experimental support (166). Thus, although heme b_{595} and heme *d* do not compose a *structural* binuclear site, one can speak of a *functional* di-heme site. The latter idea received support from spectroscopic and electrometric studies on cytochromes *bd* from *E. coli* and *A. vinelandii* (78, 166-180). Of interest, unlike cytochrome *bd*-I from *E. coli* (177), a *bd*-type oxidase from *G. thermodenitrificans* does not show any substantial excitonic interaction between heme b_{595} and heme *d* (87). Thus there may be differences in the organization of the active site for O_2 reduction between cytochromes *bd* from different prokaryotes.

There are also data that heme b_{595} might be a second site in the *bd* enzyme that reacts with O_2 (181-182) and H_2O_2 (72).

Which of the quinols is utilized by cytochrome *bd* depends on a particular bacterial species. It is known that the *bd* enzyme in *A. vinelandii* oxidizes ubiquinol, cytochrome *bd* in *G. thermodenitrificans* deals with menaquinol, whereas cytochrome *bd*-I in *E. coli* seems to be able to oxidize both ubiquinol and menaquinol (183-184). There are data that cytochrome *bd* in cyanobacteria can oxidize plastoquinol (185-190), though some doubts still remain (191-193). Some studies report that the isolated cytochrome *bd*-I from *E. coli* contains a bound quinol (167-168, 194) while others do not show that (83-84, 195-199). Whether a bound quinol is present in the enzyme is probably defined by a method for protein isolation and purification (43). A stable semiquinone radical in cytochrome *bd*-I from *E. coli* was reported (200-201).

As said above, the CydA subunit of cytochrome *bd* comprises the Q-loop, the hydrophilic domain exposed at the extracellular space that links transmembrane helices 6 and 7 (77). This structural domain is necessary for quinol oxidation (79-84) and underlies protein classification (43, 85-87). The Q-loop has a largely irregular protein fold apart from a short helical stretch that leads to an antiparallel β sheet (77). A potential quinol binding pocket seems to be near Glu257 and Lys252 in the short helix of the Q-loop (77). Lys252 can form a polar contact with the O1/2A propionate group of heme b_{558} (77). If cytochrome *bd* has the only site for the quinol binding and oxidation (77, 83-84, 199), what is the role of other quinol molecule(s) likely bound to the protein (167-168, 194)? The question remains unanswered. Of interest, Kusumoto *et al*. reported a second quinol-binding site essential for the activity of the *bd*-oxidase from *Corynebacterium glutamicum* (202).

4.2.2.2. Substrate transfer pathways: protons, O_2, H_2O

The existence of an intraprotein proton-conducting pathway in cytochrome *bd* that goes from the cytoplasm to the O_2-reducing site was predicted based on the time-resolved electrometric and optical studies (167-168, 194, 197, 203). The crystal structure by Safarian *et al*. (77) indeed indicates that there are two potential proton transfer pathways, one in CydA and the second one in CydB. Accordingly, those were called the CydA and CydB pathways. Both pathways leading from the cytoplasm converge on heme b_{595} located within the bilayer - ca. 22.5 Å away from the periplasmic side of the membrane (77). Whether both pathways or only one of them are functional is not known. A proton transfer route from heme b_{595} to heme *d* has not been identified. It is proposed that such a transfer is facilitated by connecting unresolved water molecules (77). The location of the highly conserved Glu108 (Glu107 in *E. coli*) within the CydA pathway of the *G. thermodenitrificans bd* structure is in line with earlier proposal (168) for the key role of this residue in the intraprotein proton transfer. Another conserved glutamate, Glu378 (Glu445 in *E. coli*), the heme *d* axial ligand (77), was suggested to be a key residue to compensate for the negative charge of an electron used to reduce the high-spin hemes (167).

The structure suggests (77) that O_2 can reach the heme *d* site laterally from the alkyl chain interface with the membrane over a short distance. Thus, O_2 does not need to go through any tunnel-like protein cavity (77) that enables it to bind heme *d* very rapidly (54, 204). A water channel of cytochrome *bd* remains to be identified.

5. SEQUENCE OF CATALYTIC INTERMEDIATES AND MECHANISM OF $\Delta\mu H^+$ GENERATION

When comparing the catalytic cycles of PSII and TRO, the following similarities and distinctive features have to be noted. In both cases, the catalytic cycle consists of the same number (five) of primary intermediates which are connected by one-electron transitions. In both enzymes, the four-electron cycle of the $O_2/2H_2O$ transformation in the active centre is coupled to one-electron change of the reduction state of the primary electron acceptor or donor. In TRO the primary electron donor is the low-spin heme whereas in PSII the primary electron acceptor is the redox-acitve tyrosine (Yz) of the D1 subunit. During the catalytic cycle, the active site of the enzyme successively receives either four reducing (TRO) or four oxidizing (PSII) redox equivalents, followed by a key phase of the reaction. During the latter phase, there is a simultaneous exchange of four electrons between the atoms of polyvalent metals and two oxygen atoms in the active center of the enzymes. This process is accompanied by breaking or formation of the O-O bond. As a result, it becomes possible to avoid the release of highly reactive intermediates of dioxygen reduction.

During the catalytic cycle of PSII, the $P680^{*+}$ radical that occurs every time under light-induced charge separation, takes sequentially one electron from the OEC. The electron transfer from the OEC is mediated by the redox-active tyrosine, Yz. In the course of the four consecutive one-electron stages the OEC is oxidized from the S0 state to the S4 state, reaching sequentially the most oxidized state (S4) from the most reduced state (S0) through the S0→S1→S2→S3→S4 transitions (Figure 3). Two water molecules are bound and deprotonated through these transitions. The most reduced S0 state is formed again upon the release of the product, O_2, by the most oxidized S4 state. The

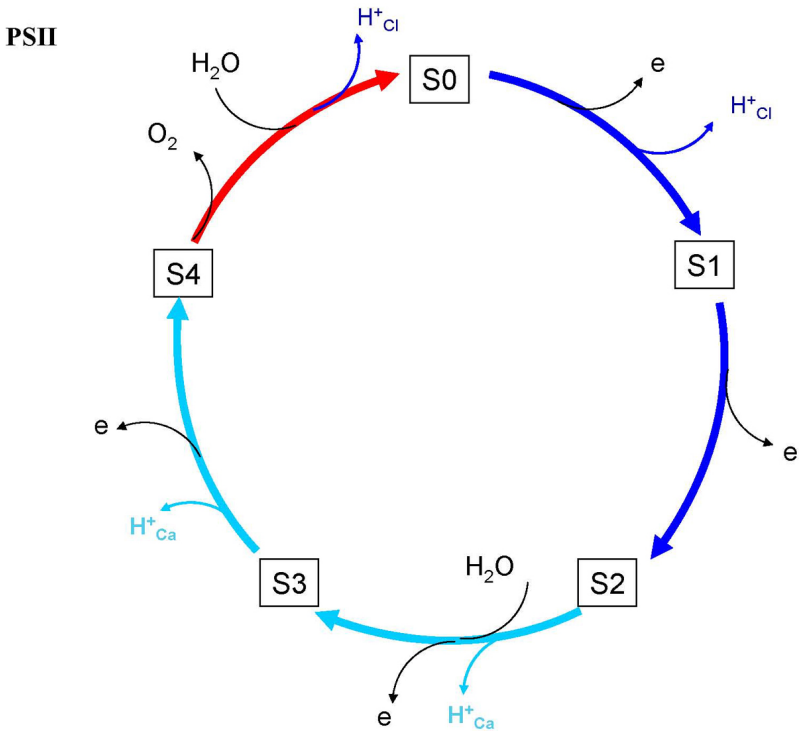

Figure 3. Scheme of the catalytic cycle of Photosystem II. S0→S1→S2 transitions form the "low-spin" part of the catalytic cycle (dominantly antiferromagnetic coupling between adjacent Mn sites; shown in blue color), while S2→S3→S4 transitions form the "high-spin" part (dominantly ferromagnetic coupling between adjacent Mn sites; shown in cyan color) of the cycle. The main catalytic step (S4→S0) is shown in red color. Protons released during the catalytic cycle via the protonic pathways ("Ca^{2+} channel" and "Cl^- channel") are indicated as H^+_{Ca} and H_{Cl}^+, respectively.

catalytic cycle of TRO can be similarly represented as a series of the five states (205). The most reduced state, C0 (R) is formed from the most oxidized state, C4 (P_M) through the four stages of one-electron reduction (C4→C3→C2→C1→C0). The C4 state is formed from C0 in one step as a result of the binding and simultaneous four-electron reduction of molecular oxygen (Figure 4). In the C4 state formed, the O-O bond is split, the oxygen atoms are coordinated to the metal atoms of the BNC and are reduced to the degree of reduction that corresponds to that of the water molecule.

The conversion of dioxygen into water takes place in PSII and TRO in specially organized sites which contain polyvalent metals and are located deep in the membrane part of the enzyme. In the case of the heme-copper oxidases, the active center (BNC) is composed of the Cu atom and the Fe atom of the heme, while the OEC of PSII contains 4 atoms of Mn and Ca. The Fe and Cu atoms of the BNC change their oxidation state in the range from 2+ to 4+ and 1+ to 2+, respectively; in the case of the OEC, the oxidation state of Mn varies between 3+ and 4+. In the active site of PSII, three metals (not two, like in the BNC) change the oxidation state and accumulate oxidizing equivalents during catalysis. These are Mn1, Mn3, and Mn4, while Mn2 and Ca remain to be redox inactive. As suggested, the choice of metal atoms to build an active center may be due to the chemical properties of compounds of these metals with oxygen in different degrees of valence and their proton-acceptor properties (206-207). Mn4 and Mn1 are assumed to be associated with oxygen atoms that are on the same axis and can form a connection between them at the end of the catalytic cycle. It is interesting to note that the distance between Mn4 and Mn1 in the OEC is close to that between copper and iron atoms in the BNC. These atoms of manganese can be compared in some ways with the atoms of Fe and Cu in the BNC, also taking into account the fact that the spin state and the coordination sphere of these atoms are expected to be changed during the catalytic cycle.

In addition to the dioxygen/water conversion, the function of both enzymes is to transform the energy of redox reactions into the electrochemical form, performing work against the difference of electrochemical potentials of hydrogen ions across the membrane. To create an effective, relatively simple and, therefore, the maximum uniform mechanism of energy conversion based on the coupling of electron transfer with proton transport, it would be logical to use the free energy of redox reaction, dividing it into 4 roughly equal portions. However, the standard Gibbs free energy gap, ΔG^0, is quite different for the

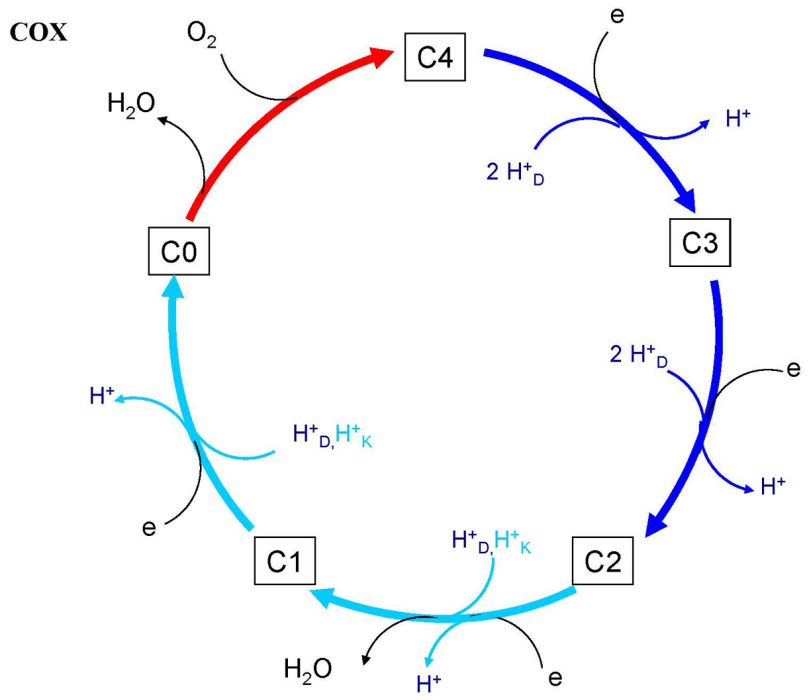

Figure 4. Scheme of the catalytic cycle of cytochrome *c* oxidase. Transitions from R to O_H (C0→C4→C3→C2) form the oxidative part, while transitions from O_H to R (C2→C1→C0) form the reductive part of the cycle. Transitions in which the Fe of heme a_3 of the BNC is in the "low-spin" state are shown in blue color, while "high-spin" transitions are shown in cyan color. The main catalytic step (C0→C4) is shown in red color. Protons supplied during the catalytic cycle via the D and K pathways are indicated as H_D^+ and H_K^+, respectively.

individual one-electron transfer steps of the dioxygen/water transformation in non-catalytic reduction system (208-209). In particular the first one-electron redox step of oxidative water splitting is highly endergonic and cannot be driven by the energy of a photon in the red wavelength region (210). This is also true for the first step of the opposite reaction during reduction of dioxygen (208). Nature has not only evolved two entirely different devices to catalyze the reaction in the forward and backward direction but also has endowed these enzymes with the ability to function in a unidirectional manner (210). Besides, the four step sequence comprises reactive oxygen species (ROS) which are harmful to biological systems and therefore the population of these species has to be prevented (210). To solve these problems, the catalytic process is encapsulated into a protein bound transition metal clusters. In addition, the redox-active tyrosine residues play the important role in both enzymes.

In case of the heme-copper oxidases, the redox active tyrosine residue (Y288 in aa_3 oxidase from *R. sphaeroides*) is part of the active center. The tyrosine residue is located in direct vicinity (~5 Å) of the BNC (126, 129, 211). It is considered to be not only the electron donor but also the proton donor (used as a Lewis acid cofactor) at the stage of the O-O bond splitting. The *bd*-type oxidases seem to be an exception. In the *bd*-enzymes, a porphyrin radical presumably plays a role of the tyrosine, while the proton donor has not been identified. By the way, a direct proton acceptor that in the OEC performs a similar function in the O−O bond formation has not yet been identified (94). The covalent bond between the tyrosine and a histidine ligand of Cu_B lowers the pK of tyrosine that facilitates its functioning as a proton donor (212-214). In the recent years, it is assumed that the redox-active tyrosine can participate in all four single-electron transitions of the catalytic cycle of the heme-copper oxidases, thereby contributing to leveling of the values of the redox potentials of the BNC during these transitions (214-215).

Though the redox-active tyrosine (Yz) in the PSII is located at a distance of 7 Å from the Mn_4CaO_5 cluster, it is not part of the OEC, in contrast to that in the heme-copper oxidases. Yz is an electron carrier that is oxidized by the $P680^{*+}$ radical and then is reduced by the Mn_4CaO_5 cluster during each transition of the catalytic cycle. Though it is not covalently bound to the histidine residue, it shares the proton with His190 through the hydrogen bond. The proton is believed to perform a catalytic function in the activation of dioxygen and redox transformation of the tyrosine (the so-called "proton-rocking" mechanism (216)). The proton migrates between Yz and His190 that is linked to the redox transformations of the tyrosine. However, according to the latest data, the tyrosine-

histidine pair can participate in the proton transfer over long distances in the course of the proton release into the lumen at some stages of the catalytic cycle. It should be noted that the interaction between Yz and His190 slightly increases the redox potential of Yz that facilitates its functioning as an electron carrier between the OEC and the $P680^+$ radical (the value of the redox-potential of the latter is ~+1.25 V) (217).

While the net oxidation state of the Mn_4CaO_5 cluster increases by four, from the S0 to the S4 state, the redox states of the atoms in these states are $Mn(III)_3Mn(IV)$/Yz-OH and $Mn(IV)_4$/Yz-O* respectively. Similarly, the most reduced (C0) and the most oxidized (C4) states in the heme-copper oxidases are Fe^{2+} Cu^{1+} Y-OH and Fe^{4+}=O^{2-} Cu^{2+}-OH Y-O* respectively. Since Yz is not directly involved in the formation of the O-O bond, a more detailed study is needed to identify the fourth oxidizing equivalent, which is located directly in the OEC. In particular, as suggested, the Yz-O* radical in the S4 state can be re-reduced by a fully deprotonated substrate water bound to Mn4 (or Mn1), yielding the oxyl radical, Mn(IV)-O* /Yz-OH or Mn(V)=O /Yz-OH, depending on where the radical is localized (on the Mn atom or on the oxygen ligand) (218-220).

In order to study the mechanism of partial events that comprise every one-electron stage of the catalytic cycle in both enzyme systems, it is necessary to use approaches which could convert all the enzyme population into the distinct states of the cycle. It is much simpler in case of PSII, because the dark-adapted state of the enzyme (S1) is almost homogeneous and due to a high quantum yield each of the short laser flashes converts PSII to the next state of the cycle almost entirely. Nevertheless, the S4 cannot be isolated since it is apparently converted to the next state faster than it is formed. There are two basic approaches to study the terminal oxidase reactions in a single turnover of the enzyme. It is the reaction of the reduced enzyme with molecular oxygen started by the photolysis of the complex of the BNC with CO in presence of dioxygen (oxidative “pulse”) ((7, 221-227)) and single-electron injection into the enzyme with different degrees of reduction (reductive “pulse”) (27, 228-237).

The approximate stoichiometry of the reaction of the coupled transfer of protons into individual one-electron stages of the catalytic cycle of the PSII and the TRO is considered to be established; however the mechanism of individual proton transport events requires further study. All S-state transitions of PSII except S1-to-S2 involve a single proton release to the lumen. In the heme-copper oxidases, each of the one-electron stages of the catalytic cycle is considered to include on average the transfer of one pumped proton across the membrane and the transfer of one substrate proton into the BNC. For both types of the enzymes, separate one-electron stages of the catalytic cycle may have a different set of the coupled events of electron and proton transfers that differ in temporal parameters, the order of the transfer of an electron and a proton, and the proton-conductive channels used.

It is suggested that at some stages of the catalytic cycle of PSII, extraction of the electron from the OEC happens earlier than the release of the proton to the lumen, whereas at other stages it is vise versa. These might correlate with different mechanisms of proton release into the lumen. Similarly, the two different mechanisms of the coupled proton pumping are discussed in case of the heme-copper oxidases, which differ in the sequence of events of electron transfer into the BNC and translocation of the pumped protons through the membrane. The rates of proton transfer and coupled electron transfer reactions in the catalytic centers of both enzymes vary from a few tens of microseconds to milliseconds. The slowest stage occurs in the millisecond time range and controlled by the proton reactions, probably associated with conformational changes between substates of the protein. In the study of these features, the use of specific mutant forms of the residues in the proton-conducting pathways, and kinetic isotope effect is of great importance.

It is interesting to note that the release of protons formed during the oxidation of water into the lumen in PSII and the delivery of substrate protons into the BNC of TRO is assumed to occur via two separate proton-conducting pathways (Figures 1-4). In both systems, the role of these pathways during the catalytic cycle is strictly regulated in a complex manner and most likely is mediated by a change in charge and/or spin state of the catalytic center. As with PSII, it can be assumed that multiple pathways can be used in the heme-copper oxidases for the release of the pumped protons, which can vary depending on the mechanism and the stage of the catalytic cycle in which they participate. Electrostatic interactions, ionic interactions (salt bridges) in both enzymes are equally important. So, at least at some of the catalytic transitions in PSII, excess positive charge in the OEC is used for the release of a proton by a different mechanism through another putative protonic channel due to the electrostatic repulsion with the proton located between Yz and His190. At the same time, the release of the pumped proton to the P-side of the membrane in the heme-copper oxidases is provided by electrostatic repulsion from the proton coming into the BNC.

5.1. Catalytic cycle of the OEC. Proton and electron transfer steps coupled to single-electron transitions

5.1.1. S0→S1 transition

The degrees of oxidation of Mn ions and Yz in the S0 state are $Mn(III)_3Mn(IV)$/Yz-OH state. Mn1,

Mn3 and Mn4 ions are in the oxidation state of +3, and only redox-inactive ion Mn2 is in the oxidation state +4. In the S0 state, the OEC already has a molecule of substrate water in the form of hydroxyl groups, whose oxygen atom occupies the position O5 and forms a connection with Ca^{2+}, Mn4 and Mn1 (96, 219). It is assumed that O5 is not coordinated with Mn1 in the S0 state that results in the "open" form of the cubane of the Mn_4CaO_5 cofactor with a gape between O5 and Mn1, while the "backrest" is in the fully closed form. It is worth noting that in the course of the cycle O5 never communicates only with a redox-inactive ion Mn2.

The S0→S1 transition is accompanied by electron transfer from the OEC to Yz-O*. The degree of oxidation of the manganese ions decreases by one, when it is believed the Mn3 ion is oxidized to the oxidation state +4. The state of S0 and S1 are characterized as low-spin and have values of spin, respectively S=1/2 and S=0. The form of "open" cubane of Mn_4CaO_5 cofactor is maintained during the transition. The S0→S1 transition is accompanied by the release of a proton from the OEC into the lumen, leaving the hydroxyl group O5. It is assumed that the electron is transferred before the proton (with rates of ~40 μs and ~100 μs, respectively) at this stage of the catalytic cycle (Figure 3). This was concluded from the data recorded with the use of X-ray absorption and from the time-resolved photothermal beam deflection experiments (116, 238). Either the proton transfer is concomitant with the electron transfer with a rate of ~ 130 μs, as suggested from the time-resolved infrared spectroscopy (TRIR) data (117). This proton transfer step is characterized by a high activation energy (Ea ~ 33 kJ/mol) and strong H/D kinetic isotope effect (approximately 3) (116). The TRIR data show that the main proton-coupled electron transfer reaction in the S0→S1 transition seems to be followed by a slow conformational change of the protein (τ = 1–4 ms), relaxing to the dark stable S1 state (117).

The electrogenic reactions associated with the electron and proton transfer in thylakoids and in PSII core particles during S-state transitions of the OEC were identified on the basis of their kinetic properties using electrochromic absorption changes of carotenoids (239) and electrometrical technique (239-240), respectively. The data derived from PSII core particles reconstituted into liposomes using direct electrometrical technique revealed that the S0→S1 transition was not included to a significant extent (less than 1% of $Y_Z^*PQ_A^-$ formation) in the electrogenic components that occurred with the half-rise times of the other transitions.

5.1.2. S1→S2 transition

S1 is a stable resting (dark-adapted) state of PSII. In the S1 state the Mn oxidation states of Mn1,Mn2,Mn3 and Mn4 is III,IV,IV,III, respectively. S1 is converted to S2 upon the loss of one electron. The efficiency of the S1→S2 transition is independent of pH values within the range 3.5–9.5, whereas the other three transitions were all inhibited at acidic pHs with pKa values of 3.6, 4.2 and 4.7 for the S2→S3, S3→S0 and S0→S1 transitions, respectively (241). That is, unlike other transitions, the S1→S2 transition is not accompanied by the release of protons into the lumen. As a result, in the S2 state, the OEC acquires an additional positive charge. This accumulated charge is not released until the S0 state is reformed after the O_2 release (116).

During the S1→S2 transition, the time constant of the electron transfer from the Mn_4CaO_5 cluster to Y_Z-O* is 50–70 μs (238). Despite the fact that there is no proton release to the lumen, the results of TRIR measurements indicate that the electron transfer is concerted with rearrangement of protons in the hydrogen bond networks of protein (117). It is proposed that the S1→S2 transition is a simple process of concerted PCET between Y_Z and the Mn_4CaO_5 cluster with the time constant of ~60 μs; and the proton on D1-His190, which was shifted from the Yz upon its oxidation by the $P680^+$, returns to Y_Z-O* upon its rereduction by the Mn_4CaO_5 cluster (117), in agreement with the so-called "proton-rocking" mechanism (216). A minor activation energy (Ea ~ 5 kJ/mol) and H/D kinetic isotope effect (KIE) of 1.3 were determined (116, 209).

Mn2 and Mn3 are in the highest oxidation state +4 in the S1 state and do not change their oxidation state to the end of the catalytic cycle. At the same time, the two Mn centers most often invoked as participating in the O–O bond-forming reaction in the OEC (Mn4, the "dangler" manganese, and Mn1, ligated by H332, the only histidine ligand in the first coordination sphere) undergo further oxidation and the change of coordination state. In the S1 state they are in the oxidation state 3+, while with further oxidation to the S2 state, there is only a single Mn(III).

A feature of the S2 state is that S2 is present as two spin isomers with oxidation states (III,IV,IV,IV) or (IV,IV,IV,III) and a spin 1/2 and 5/2, respectively (242). It is assumed that in the low-spin form in which the Mn1 and Mn4 atoms have the oxidation number III and IV, respectively, a Mn_4O_5Ca cofactor retains the "open" form of cubane with a five-coordinate Mn1 of tetragonal symmetry; the backrest has the "closed" form. In the high-spin form of the S2 state where the Mn1 and Mn4 atoms have the oxidation number IV and III, correspondingly (243), the O5 center is shifted to the Mn1, and the distance between Mn4 and O5 is increased (Figure 1). That is, it is assumed that in step S2, it becomes possible for the OEC to interconvert between low-spin and high-spin states, accompanied

by changes from the opened conformation into the closed one (96). On the contrary, the backrest becomes to be open in the high-spin form of Mn_4CaO_5 cofactor (Figure 3).

Based on the direct electrometrical results derived from proteoliposomes containing PSII core complexes, S1→S2 transition was estimated to be less than 3.5% of Y_Z*PQ_A^- formation and ascribed to the electron transport from the Mn_4CaO_5 to Yz (239-240).

5.1.3. S2→S3 transition

The next oxidation event results in the loss of one proton and one electron from the OEC to form S3, in which all four Mn ions are in the +4 oxidation state (242). During the S2→ S3 transition, the oxidation state of Mn4 is advanced from +3 to +4. As it was suggested, a high-spin S2 intermediate (with closed cubane) is active in the subsequent transition and in the S3 state, the system has spin S=3 (244). Because the S1-to-S2 transition does not involve proton release, the abstraction of a single electron by Y_Z-O* along with the proton release pattern implies that in the S2 and S3 states, the Mn_4CaO_5 cluster accumulates an excess positive charge. This excess positive charge might play a key role in the mechanism of proton-coupled electron transfer at the S2 and S3 states.

Unlike S0→S1, for the S2→S3 transition, the TRIR and photothermal beam deflection results suggest that proton transfer precedes electron transfer (116-117) (Figure 3). While the electron transfer during the S2→S3 transition proceeds with a rate constant of ~300 μs (238), the rapid proton release before electron transfer was proposed recently in the ~30 μs component by photothermal beam deflection (116). Similarly, by using the TRIR, the two processes with fast (τ ~70 μs) and slow (τ ~350-460 μs) time constants were shown. The 70 μs phase was interpreted as reflecting the rearrangement of protons in the hydrogen bonds in proteins or proton release to the bulk, whereas this slow phase at 300–500 μs was consistent with the rate of electron transfer during this transition (117). The ~30-μs component has a high value of the activation energy (Ea ~ 48 kJ/mol) and a large H/D kinetic isotope effect (5.6), that is significantly larger that of the ~300 μs component (1.7) (116).

The S3 state has recently been characterized by multidimensional EPR spectroscopy measurements with each Mn center having octahedral coordination sphere, implying that an additional ligand is incorporated during the S2→S3 transition to convert five-coordinate Mn(III) to six-coordinate Mn(IV) (244). During conversion of the cubane of Mn_4CaO_5 cluster from the “open” to the “closed” state the O5 atom becomes to be bound to the Mn1 (96). Therefore, it is suggested that during the formation of the S3 state the previously vacant coordination site on Mn4 to be filled with a new molecule of substrate water that binds as a hydroxide ligand (Figure 1). As a result, at the S3 state, all Mn ions within the OEC have tetragonal symmetry.

Site-directed mutations of residues in the proposed proton-conducting path starting from D61 and passing through the chlorine ion (protonic “Cl^- channel”; Figures 1, 3), do not inhibit (or not so effective) the S2→S3 transition, while the next transition is suppressed strongly (114). It is assumed that at this stage the output of the proton is carried out by a special mechanism in two stages using different proton path from what is used in the subsequent transition. This proton path (protonic “Ca^{2+} channel”, Figure 1, 3) is believed to begin from the water molecules W4 associated with the Ca ion, and it passes by Yz to the surface of the protein into the lumen (98). It is possible that the redox state (the positive charge in the OEC) controls the exit of a proton through the channel. According to the proposed mechanism, the first stage (~30 μs) is the output of a proton from $HisH^+$-O*-Yz pairs into the lumen, caused by electrostatic repulsion with the positive charge in the OEC. During the second stage (~300 μs), reprotonation of Yz* from the OEC simultaneously with the transfer of an electron from the OEC and reduction of Yz-O* into the Yz-OH occur (116-117). Of interest, it is assumed for cytochrome oxidase that during its catalytic cycle, the change in the redox state of the BNC (or its spin state) can control opening/closing of proton-conducting path (the K-channel) in a similar way.

Noticeably, in proteoliposomes with the PSII core particles, electrogenic reaction during the S2→S3 transition of the OEC (~6.5.% of Y_Z*PQ_A^- formation) is related to proton transfer from unknown amino acid in the vicinity of Mn cluster into the lumen (239-240, 245).

5.1.4. S3→S4→S0 transitions

Oxidation of Y_Z following the next charge separation causes release of a proton from S3 to form a modified S3’ state (116), which then forms the S4 state by the 4-th electron transfer from the OEC to the Yz-O* (242). S4 spontaneously produces O_2, binds substrate water molecule, and releases another proton to form S0, thus resetting the catalytic cycle (Figure 3). The S4 state decays faster than it is formed and, therefore, cannot be observed as a kinetic intermediate and its structure is poorly understood. The electron transfer from the Mn_4CaO_5 cluster to the Yz-O* through the S4→S0 transition occurs with τ ~ 1–2 ms and is generally agreed to be the rate-limiting step of the OEC turnover (102).

The presence of a distinct intermediate, S3′ (distinguished from the S4 state having an oxidized

catalytic center), and a "lag phase" (S3→S3′, ~200 μs) before the electron transfer from the Mn_4CaO_5 cluster to Yz-O* was proposed from time-resolved UV and X-ray absorption measurements (238, 246). The S3' state of the OEC is uncharged as compared to the S3 state, which, like the S2 state, has an additional positive charge. In other words, in the S3-to-S0 transition the first proton is released into the lumen before the set of the events, including: the electron transfer from the OEC, formation of the O-O bond, inclusion of a new water molecule into the position of O5 and release of the second proton from the OEC. In a recent paper, using the method of photothermal beam deflection, in addition to the 200-μs phase of the proton transfer, in the S3→S3' transition, an additional phase of proton displacement in PSII with a rate constant of 25 μs was discovered (247). The TRIR measurements confirm these results and indicate that during the "lag phase" before electron transfer the release of a proton from the substrate water to the lumen most provably occurs (117).

While the proton transfer reactions through the S3→S3′ transition slow down considerably in D_2O buffer, at lower temperatures (247), the measured value for the electron transfer step during this transition demonstrates moderate activation energy (Ea ~ 18 kJ/mol) and small KIE (1.3) (116), which is in accord with the assumption that the S3'-to-S0 transition includes several events in the catalytic cycle and is rate-limited by another event than in the S2→S3 transition. Besides, as opposed to the S2→S3 transition, the proton removal step(s) in the S3→S0 transition likely exploit another proton path to the lumen, which involves D1–D61 and the channel passing through the chlorine ion (Figure 3).

In the transition from the S3 state to the S0 state, the Mn_4CaO_5 cluster is returned from the high-spin state to the low-spin state, while the form of cubane is changing from closed to open. It is interesting to note that the change in the spin state of the Mn_4CaO_5 cluster correlates with the change in the charge and the mechanism of sequencing (articulation) of the events of proton and electron transfer, components of the individual one-electron transitions (Figure 3). If during the S0→S1→S2 the electron transfer preceded the proton transfer (or occurred simultaneously), then the course of events S2→S3→S0 opposite the exit of the proton was preceded by the stage of the electron transfer (96). The early deprotonation process observed during the S3→S0 transition, and the S2→S3 transition, is a crucial step for lowering the redox potential of the Mn_4CaO_5 cluster, which possesses an excess positive charge in the S2 and S3 states, to facilitate its oxidation (117).

Unlike the S2→S3 transition, the total S3→S0 transition is slowing down by the mutations in the so-called protonic "Cl^- channel" (96). However, because the total transition S3→S0 is accompanied with release of the two protons, it is possible that the slowdown is due to the effect on the output of one of the protons, whereas the second proton is transferred via a different mechanism, which it is assumed in the S2→S3 transition (by using of a protonic "Ca^{2+} channel"). The roles of the two proton pathways in the release of protons into the lumen during the catalytic cycle of PSII, the mechanism of their switching in connection with a change in spin and redox state of the OEC is reminiscent of the articulation of the input proton channels in cytochrome oxidase (Figures 3, 4), but remains very interesting, intriguing and mysterious to the end.

Using direct electrometrical technique in the PSII core particles, the proton release upon the third photon-induced final oxygen evolving S4→S0 step revealed relative electrogenic component of ~5% of Y_Z*PQ_A^- formation (pH 6.5) (239-240).

The mechanism of O-O bond formation. The Mn oxidation states in S3 are (IV,IV,IV,IV). The S4 state is one electron more oxidized and it is equipped to pull four electrons to synthesize the molecule of oxygen. Since the S4 state decays faster than it is formed, no direct experimental evidence for the nature of O–O bond formation in S4 has been produced. However, insights from inorganic and computational chemistry have produced two competing mechanisms: water-nucleophile attack and oxo–oxyl radical coupling. (242), depending on where the fourth oxidizing equivalent is localized: on the manganese atom (MnV –oxo species) or on the oxygen ligand (MnIV–oxyl radical). The first mechanism would involve a terminal water-nucleophile attack to a formally Mn(V)–oxo electrophile. Under this mechanism it is assumed that the 4th oxidation equivalent is located on the Mn4 atom, which then must be oxidized to the +5 oxidation state in the S4 state, and the role of the water-nucleophile could be performed by the molecule W3, the ligand of Ca ion. A water-nucleophile attack mechanism is most consistent with synthetic water oxidation catalysts (220, 242).

Recently, a lot of data were obtained in favor of another mechanism, the oxo–oxyl radical coupling mechanism, which involves the placement of the fourth oxidizing equivalent in the form of a terminal oxyl radical (Mn(IV)-O*) of the Mn4 (or Mn1) ions (an oxidized form of a substrate water molecule, deprotonated and ligated to Mn) (96, 219, 244). The oxyl radical is produced from one of the substrate waters, which binds presumably to the Mn4 during the S2→S3 transition. In this mechanism, O_2 is produced in the reaction between a Mn(IV)–oxyl radical and a Mn-bridging oxo atom. The source of the second oxygen atom is the O5 atom, another Mn-bridging oxo

atom, which becomes to be bound to the Mn1 in the S3 state during the transition of the cubane of Mn_4CaO_5 cluster from the open to the closed state (96). It is interesting to note that the switch of the protonic channels from the "Ca^{2+} channel" to the "Cl^- channel" for proton transfer(s) during the S3→S0 transition may somehow be related to the change of the spin state of the OEC in the S2 state, and to the incorporation of the substrate water molecule into the Mn_4CaO_5 cluster during the S2→S3 transition (Figure 3). The expected way to deliver this molecule of substrate water to the Mn_4CaO_5 cluster may partially or completely overlap with protonic "Cl^- channel" (96), which leads through the D61 residue to the water ligands (W1 and W2) of Mn4.

5.2. Catalytic cycle of terminal oxidases. Proton and electron transfer steps coupled to single-electron transitions

This section discusses the data obtained basically in measurements of single-electron injection into the separate states of the catalytic cycle of the heme-copper oxidases and the single-turnover data obtained by flow-flash method with *bd*-type cytochromes. The results of the measurements on heme-copper oxidases obtained by the use of flow-flash method bring to a close (or complementary) conclusions (for review see, for example (7)). For more analogy with the corresponding transitions in PSII caused by the injection of a quantum of light, a nomenclature, similar to that for S states in the PSII catalytic cycle, is used. The greatest attention is paid to the results obtained by the time-resolved electrometric method (or capacitive potentiometry) (27-28, 233-237, 248-250) .

5.2.1. Heme-copper oxidases

5.2.1.1. C0→C4 transition *(R→A and A→P_M transitions)*

If the BNC of the heme-copper oxidase is reduced by two electrons, dioxygen can bind to the BNC and react. The corresponding state of the BNC, the R state (C0, Figure 4), is characterized by the ferro-cuprous ($Fe^{2+}Cu^{1+}$) state of the heme a_3 and Cu_B redox centres. The C0→C4 transition includes formally two main subsequent events which can be resolved kinetically. The first one is binding of dioxygen to heme a_3 in the BNC (R→A transition). If the concentration of O_2 is 1 mM, the first spectroscopically detectable intermediate, the A state (251-252), is formed within 10 μs (222). The resonance Raman Fe-O_2 stretch spectrum of the A intermediate is similar to that found in oxyhemoglobin and oxymyoglobin (253-254). It is believed that the A intermediate to a great extent is a form in which the iron atom is oxidized, and oxygen is a superoxide anion, Fe^{3+}-O_2^- (255).

The generation of the A compound is followed by the second event that consists of the simultaneous transfer of electrons and a proton to dioxygen and the O-O bond cleavage (A→P_M transition). Three out of four electrons required for dioxygen reduction at this stage are taken from the BNC, whereas the fourth electron and a proton are provided by the tyrosine Y288 (213) which is cross-linked to the histidine ligand of Cu_B. Since both an electron and a proton move in the same direction and distance, the A→P_M transition does not generate a transmembrane voltage and virtually no phase of potential generation during R→A→P_M steps has been obtained using the electrometric technique (224).

Based on the X-ray structural analysis of the mitochondrial cytochrome *c* oxidase in the complex with cyanide, it is suggested that dioxygen binding to Cu_B on the way to heme a_3 induces translational movement of the heme a_3 plane to form a hydrogen-bond connection with Y288-OH via a water molecule, Water 510 (255) (Figure 2). This water is not the product of the enzymatic reaction, but a cofactor stored in a water storage site near the O_2-reduction site. Due to migration of Water 510 to the BNC, the negatively charged Fe^{3+}−O_2^- induces change of coordination in the BNC, to form three possible electron-transfer pathways, each transferring one electron equivalent, for the nonsequential synchronous reduction of the bound O_2^- (255).

In the P_M (C4) intermediate, the redox centers of the BNC are characterized by the following redox state: Fe^{4+} = O^{2-} Cu_B^{2+}- OH^- Y-O*, i.e., the catalytic center is in the most oxidized state (4 oxidizing equivalents higher than in the R(C0) intermediate), and the oxygen atoms are reduced to the water redox state. Due to the fact that the disruption of the O-O bond and reduction of the oxygen atoms occur in a single step, reactive intermediate forms of dioxygen reduction are not produced and released. The rate-limiting step through the O-O bond scission is suggested to be the formation of the hydroperoxy intermediate initiated by the simultaneous transfer of a proton (from Y288) and an electron (from Y288 or Cu_B) to the distal oxygen atom of the A compound (208, 256). The small value of KIE (~1.5) for the A→P_M transition is in accord with this rate-limiting internal proton transfer (257).

5.2.1.2. C4→C3 transition *(P_M→F transition)*

C4→C3 transition (P_M→F transition) corresponds to one-electron reduction of the P_M state (Figure 4). It can be observed during the single-electron injection into the cytochrome *c* oxidase converted initially into the P_M state by the special pre-treatment with the use of CO (28, 234). In the P_M→F transition, the electron acceptor in the BNC is a radical of the redox-active tyrosine, Y-O* (with E_m ~ 0.82 V (208)).

The transition to the F state results in the change of the α-band spectrum of the ferryl compound of heme a_3 (a shift of the peak from 607 to 580 nm), that can be explained by the proton transfer from the N-phase to the vicinity of heme a_3, most likely to the Cu_B bound hydroxyl (258-260).

In the F intermediate formed, the BNC is in a state of Fe^{4+} = O^{2-} Cu_B^{2+}-H_2O Y-O^- . However, according to recent results of computer simulation, the electron acceptor in this transition may be Cu_B, thus the tyrosine is stored in the form of a radical in this and the subsequent stages of the catalytic cycle, and the structure of the F intermediate would be then as Fe^{4+} = O^{2-} Cu_B^{1+}-H_2O Y-O* (215). The general role of the tyrosine radical during the catalytic cycles of cytochrome *c* oxidase and PSII has to be noted. Hence, the tyrosine has a functional importance beyond the P_M state providing leveling of a high redox potential of the intermediates through the catalytic cycle that began to emerge in details in recent years for cytochrome *c* oxidase (215, 261).

By direct measurements of pH and by the electrometric measurements, it was shown that the formation of the F state is linked to proton pumping across the membrane (28, 225, 234, 262-264) (Figure 4). It is associated with uptake of two protons from the inside solution of the COX incorporated proteoliposomes and release of one proton to the outer bulk phase. The value of driving force for this transition of ~0.52 eV is well enough to transfer two charges across the membrane against the membrane electric potential of ~0.2 eV.

The kinetics of voltage generation across the membrane consists of several kinetic phases. The first electrogenic phase of the mitochondrial enzyme with the rate constant of ~ 40-50 μs and relative amplitude of about 20% reflects the electrogenic transfer of an electron from Cu_A to heme *a,* which is reoxidized by the BNC in the subsequent phases. The role of heme *a* can be compared with the function of Yz in PSII, which receives electrons from the OEC and transfers them to $P680^+$. The subsequent voltage generation during the P_M→F transition is formed by two components of the proton movement with time-constants of approximately 0.3 ms and 1.3 ms (with a ratio of about 1:2.4) coupled to the electron transfer from heme *a* to the BNC (28, 234). The electron transfer between the hemes itself does not contribute to the membrane potential generation, since it is directed in parallel to the membrane surface. The pattern of the electrogenic components is similar to the subsequent transition; therefore, the features of the generation component of the membrane potential will be discussed in the next section.

As for PSII, in case of the terminal oxidases striking examples of the influence of the electrostatic charge in the catalytic centre on the rate measured and the mechanism of the coupled transfer of electrons and protons can be noted. As described above, in the S2 and S3 states obtained, the OEC has an additional positive charge, whereby PSII uses a different (two-step) mechanism of proton release, consisting of the fast (~30 μs) phase of the proton transfer from the His190-Yz* pair (or their surroundings) through the protonic "Ca^{2+} channel" into the lumen followed by the slow (~ 300 μs) phase of electron and proton transfer from the OEC to the His190-Yz* pair (116). In the terminal oxidases, a similar situation is observed in the case of rapid reaction of the fully reduced enzyme with dioxygen in a single-turnover regime. Instead of P_M, P_R intermediate is observed with an additional negative charge in the BNC as a result of the electron transfer from heme *a* to the tyrosil radical during the A→P_R transition (7). The rate of the P_R→F transition is significantly faster as compared to the P_M→F transition (~80 μs phase in the mitochondrial enzyme (224)) and is a single-step reaction (instead of the two-step reaction for the P_M→F transition). While the P_M→F transition is induced and limited by the proton-coupled electron reduction of the BNC from heme *a* (208, 265), the P_R→F transition is rate-limited by the pure internal proton transfer step, presumably by the deprotonation of the conserved glutamate residue (E286) at the top of the D-channel (266-268).

In addition, as an example of the influence of an additional positive charge at the BNC on the measured rate and the sequence of the transfer of protons and electrons into the BNC is the injection of an electron into the C2 state (the O_H state, see further) of the ba_3 oxidase from *T. thermophilus*. In this case, the electron transfer into the BNC occurs at a rate of 20 μs, that is about 10-times faster and is due to the presence of an additional proton in close proximity to the BNC (269).

5.2.1.3. C3→C2 transition *(F→O_H transition)*

The BNC of cytochrome *c* oxidase can be fully converted into the F state (C3) by the peroxide pre-treatment (270). If bovine COX poised at the ferryl-oxo F state, the photoinjection of a single electron from RuBpy gives rise to 3 major electrogenic phases ("rapid", "middle" and "slow") coupled to the conversion of the enzyme to the oxidized O_H (C2) form (248, 271) (Figure 4). As with the P_M→F transition, the "rapid" electrogenic phase in the F→O_H transition of the mitochondrial enzyme (τ_1 ~ 40-50 μs, 20% of the total amplitude) reflects the electron transfer from Cu_A to heme *a* due to pure tunneling. It shows a very weak temperature dependence (E_a~ 3.6 kcal/mol**)** (19), does not depend on pH, is not affected by the H_2O/D_2O-replacement that most probably points out that neither bond making nor bond breaking occurs. Meanwhile,

there are data obtained in the parallel time-resolved pH measurements that indicate the interaction of protons with surface groups (the binding of protons in response to the reduction of Cu_A and the removal of protons parallel to the electron transfer to heme *a*, respectively) (272).

The following "intermediate" (τ_2 ~ 1.2 ms, r.a. ~ 20%) and "slow" (τ_3 ~ 4.5 ms, r.a. ~ 60%) electrogenic components demonstrate the high values of the energy activation (~ 17 and ~ 19 kcal/mol, correspondingly (19)), that should be attributed to structural changes in the proteins, which are accompanying and controlling the intraprotein proton translocation (249, 273). These electrogenic steps are sensitive to the inhibitors of the BNC and originate in the vectorial proton transfer coupled to reoxidation of heme *a* by the ferryl-oxo complex of heme a_3. In agreement with this, they demonstrate significant H_2O/D_2O kinetic solvent isotope effect: KIE~1.5-1.7 for the "intermediate" and KIE ~2.1-3.5 for the "slow" electrogenic phase, somewhat varied depending on the mitochondrial or prokaryotic enzyme (19, 27). The electron acceptor during the $F \rightarrow O_H$ transition is a ferryl state of heme a_3 (with E_m ~0.76 V (208)). As a result of the electron transfer to heme a_3, the C2 intermediate is formed, in which Fe^{3+} is associated with the hydroxyl: Fe^{3+}-OH^-.

The very similar magnitude ratio of the "apparent" amplitudes of two main protonic phases ("intermediate" and "slow") is observed for both $F \rightarrow O$ and $P_M \rightarrow F$ transitions. The ratio can be approximated as ~1:3 and ~1:2.4 correspondingly (27). But if the two protonic phases occur in series, rather than in parallel (which is likely to be the case), the true magnitude values need to be recalculated, according to refs. (28, 274). The recalculated amplitudes of the two consecutive protonic phases are similar in magnitudes (A_2/A_3 ~ 1:1.25) for both of the single-electron steps $P_M \rightarrow F$ and $F \rightarrow O$ in the mitochondrial oxidase.

The contribution of the electron transfer to heme *a* is in close agreement with the value obtained for the electrogenic distance of the Fe ion of heme *a* from the P-side of the membrane by theoretical calculations (around 40% in (275)) and slightly more than it can be assumed from the geometrical position of heme *a* (around 33% in (126, 276)). Each of the two protonic electrogenic phases ("intermediate" and "slow") similar in amplitude and resolved during the $F \rightarrow O$ transition corresponds to the H^+ transfer across ~ 0.7-0.9 of the dielectric thickness (19). Uptake of the substrate proton from the N-phase into the BNC accounts for the transfer across about 0.6-0.7 fraction of the membrane, while the resting charge transfer is due to proton pumping. In accord with this, it has been found that the total voltage generated during the $F \rightarrow O$ transition in the uncoupled N139D mutant, where the pumping of a proton across the membrane is absent, corresponds to about half of that observed with the wild type oxidase (27).

The fact that both protonic phases coupled to the transfer of the electron into the P_M state are 3-4-fold faster than observed for the transfer of the electron into the F state (234) can be reasonably explained by the higher midpoint redox potential of the electron acceptor, the tyrosine radical in the $P_M \rightarrow F$ transition, as compared to the oxoferryl heme a_3 (the $F \rightarrow O$ transition) (208). Accordingly, the value of driving force for the $F \rightarrow O$ transition of ~0.46 eV is slightly less than for the $P_M \rightarrow F$ transition but sufficient to transfer two charges across the membrane against the membrane electric potential of ~0.2 eV. The overall number of charges translocated across the membrane during the $P_M \rightarrow F$ and $F \rightarrow O$ single-electron steps is shown to be equal (19). The total amplitude of the proton electrogenic phases includes the translocation of the substrate proton into the BNC from the internal aqueous phase and pumping of one proton across the membrane (249).

Based on the comparative study of the H/D kinetic isotope effects (KIE) of the wild type enzyme and the N139D mutant, the "intermediate" electrogenic phase in the wild type oxidase was assigned to the translocation of the pumped proton to the proton-loading site (PLS) located above the hemes. Accordingly, the "slow" protonic phase was attributed to the transfer of the proton required for oxygen chemistry from the inner water phase to the BNC (27) and to the extrusion of the pumped H^+ from the PLS to the outside. In accord with this, the "slow" electrogenic phase is decelerated 6-7-fold by zinc ions added from the outside of proteoliposomes that shows that the addition of zinc ions may inhibit release of the protons due to competition of zinc ions and protons for a binding site on the external surfaces of the H^+ transfer pathways (277).

For the prokaryotic aa_3 oxidases from *R. sphaeroides* and *P. denitrificans*, the corresponding charge transfer steps coupled to the $C4 \rightarrow C3$ ($F \rightarrow O$) transition are characterized by the 3-4 fold faster rate constants (ca. 15 μs, 0.4 ms and 1.5 ms (30, 145)) and have a very similar relative contribution, except of the noticeably higher relative amplitude of the "rapid" electrogenic phase. This is due to the "rapid" electrogenic component in the bacterial COX that may include an internal proton transfer step (with τ ~ 40 μs) in addition to pure vectorial electron transfer from Cu_A to heme *a* (with τ ~ 10 μs) (236). Among other possibilities (236), the phase with τ ~ 40 μs might be explained by a shift of a proton in the output pathway near the Mg^{2+}-binding site, which may be triggered by the electron transfer through Cu_A to heme *a* (278).

The electrogenic uptake of both pumped and chemical protons coupled to the F→O transition occurs via the protonic D-channel, while blocking the K-channel does not affect the electrogenic response any significantly (27, 145). It is suggested that the D-channel provides all four pumped protons during the catalytic cycle of the prokaryotic oxidases. The direct internal donor of proton to the BNC (and possibly the PLS) in the D-channel of the prokaryotic oxidases is assumed to be the E286 residue, which is situated at the intramembrane end of the D-channel at ca. 15% of the membrane dielectric thickness from the BNC (236). If the D-channel is blocked at the entrance, in addition to E286, other residue (Y33 in the aa_3 oxidase from *P. denitrificans*) can be deprotonatable, which is located in the middle part of the D-channel (263).

The K-channel was concluded to conduct only the substrate protons during the stages of reductive phase of the catalytic cycle (C2→C1 and/or C1→C0), since mutating the K-channel residues does not affect significantly the oxidative phase (C4→C3 and C3→C2) and blocks the reductive halve of the catalytic cycle (27, 145, 279-282) (Figure 4). As found recently by X-ray structure analysis, the strong hydrogen bonding between the hydroxyl of Y288 and the hydroxyethyl farnesyl side chain of heme a_3 may function as a closed gate of the K pathway (130). This bond is present in the oxidized form of COX, prohibiting proton transport via that path to the active site (278), while it is absent in the reduced COX structure in parallel with the appearance of resolved water molecules leading from the top of the K pathway into the BNC (130).

For the mitochondrial enzyme there are a number of indications on the possible involvement of the H-channel in conducting the pumped protons. This channel passes close to heme *a* and, as suggested, can be controlled by changing its redox state, whereas the role of the D- and K-channels is only the delivery of substrate protons (124, 153). It is interesting to note that the indication of the possible difference in the mechanisms of coupling of electron transport and proton pumping between the prokaryotic and the eukaryotic oxidases was obtained (19). While the two protonic phases in the *R. sphaeroides* oxidase coupled to the electron transfer from heme *a* match two phases of heme *a* reoxidation by heme a_3, the electrogenic proton transfer in the F→O as well as in the P_M→F transition in the mitochondrial COX lags behind the electron transfer. It is tempting to propose that the part of redox-energy derived from the electron transfer into the BNC of the mitochondrial COX is stored in the stretched conformation of the protein matrix (19, 249), although the more profound study is probably required to clarify the phenomenon and its relation to possible differences in the use of proton-conducting H- and D-channels.

5.2.1.4. C2→C1 transition (O_H→E_H transition)

The initial oxidized resting state of the mitochondrial COX and the bacterial COX from *P. denitrificans* (the O state) is competent neither in the rapid electron transfer into the BNC nor in the coupled proton pumping (234-235). The single electron injection into the O state gives rise to a single microsecond electrogenic phase matching the electron transfer from Cu_A to heme *a* and there is no electron transfer into the BNC during the millisecond time range (234-235, 272, 283). For the typical cytochrome *c* oxidases, the C2→C1 transition (Figure 4) can be resolved only by the single-electron injection method, since the kinetics of oxidation of the fully (four-electron) reduced COX in a single-turnover regime is terminated at the fully oxidized state (C2 or O). However, for the caa_3-type cytochrome oxidase, it is possible to trace this transition because the enzyme has an additional redox center, cytochrome *c* (9, 284).

In contrast to the O resting state, injection of the electron into the just oxidized state (the so-called high-energy C2 state (O_H)) of the aa_3 cytochrome oxidase from *P. denitrificans,* which is generated upon oxidation of the fully reduced COX by O_2, results in the rapid electron transfer into the BNC, to Cu_B. Besides, the electron injection into the O_H intermediate of the COX from *P. denitrificans* is coupled to pumping of a proton (29, 281). The measurements on the ba_3- and caa_3-type cytochrome oxidases from *T. themrophilus* confirmed the properties of the O_H intermediate (9, 269, 284).

The four electrogenic phases have been resolved during the O_H→E_H transition (29, 205). The first resolved phase (τ ~ 10 μs) has been assigned to the electron transfer from Cu_A to heme *a*. The rate constants of the second (~0.2 ms) and the third (~0.8 ms) electrogenic components (29) resemble those of the “intermediate” and “slow” phases, associated with the F→O transition of the COXs from *P. denitrificans* and *R. sphaeroides* (27, 30). The net amplitude of the protonic electrogenic steps, associated with the O_H→E_H transition was close to that coupled to the P_M→F and F→O. The relative amplitudes of these phases are in agreement with their attribution to uptake of a pumped proton from the N-phase to the PLS and a chemical proton to the BNC, correspondingly. The forth electrogenic component (τ ~ 2.6-5.3 ms) was attributed to the slow release of the proton from the PLS. During the O_H→E_H transition only the pumped proton is transferred through the D-pathway, whereas the substrate proton is taken from the protonic K-channel (281). The K-pathway is opened in the reductive halve of the catalytic cycle, while it is proposed to be closed during the oxidative half by the hydrogen bonding between the hydroxyl of Y288 and the hydroxyethyl farnesyl side chain of heme a_3, functioning as a proton gate (130).

In the O_H state, Y288 is suggested to be in the radical form. Cu_B is reduced by the electron from the tyrosine and the molecule of water formed in the previous stages loses communication with Cu_B, but remains near the BNC. Cu_B is weakly ligated by the hydroxy ligand of heme a_3 in a strained fashion (214-215). Such a μ-hydroxo bridge between iron and copper (261) remains the μ-oxo bridge in the OEC of PSII (see above), while the removal of water molecule from the axis between Cu_B and Fe of the BNC remains the binding of the second substrate water molecule into the OEC in the middle of the catalytic cycle of PSII.

The structural rearrangement of the water molecule is suggested to convert the O_H into the relaxed O state, in which the ferric heme iron is ligated by a water molecule, which in turn is strongly hydrogen bonded to the OH^- ligand of Cu_B, and Y288 remains as tyrosinate (214). According to another point of view, transition of O_H into the relaxed O state occurs due to proton transfer to the tyrosine radical from the internal aqueous phase coupled to the return of an electron from Cu_B and to the formation of a neutral form of tyrosine (215). A change of the spin-state from the low-spin to the high-spin state or vice versa is an additional interesting similarity between COX and PSII (261). The ferric high-spin heme–hydroxide complex in the oxidized state of COX is the one of very few cases (261), which is made possible only by considerable interaction by strong H-bonding to the aqua ligand of Cu_B or directly with Cu_B (214, 285). So, in the heme-copper oxidases, the iron in the BNC is high-spin through the C2→C1→C0 transition, while through the C4→C3→C2 transition the ferric superoxo complex and the ferryl Fe(IV)=O^{2-} complexes have the low-spin iron (Figure 4).

The value of driving force for the O→E (and for the E→R) transition is less than ~0.1 eV that is absolutely not enough to transfer two charges across the membrane and is in agreement with uncoupling of this transition with proton pumping. With the use of quantum mechanical study it was shown that the change in free energy during the $O_H \rightarrow E_H$ transition (which is the genuine C2→C1 transition in the catalytic cycle) is much higher than it follows from the stationary redox titrations and can provide enough energy for the coupled pumping of protons in these transitions (286). As suggested (214), a radical character of the cross-linked tyrosine in the O_H state apparently provides part of the driving force required for proton pumping upon arrival of the next electron, which does not occur upon electron transfer to the "relaxed" O state. On the other hand, the Cu_B potential calculated with the use of quantum mechanics was found to be at least as high as the proton coupled potentials of both the tyrosyl radical and the heme a_3 ferryl (286). Hence, the final electron acceptor during the $O_H \rightarrow E_H$ transition of the BNC is most probably to be Cu_B, Y* or Y*/Cu_B mixing pair.

5.2.1.5. C1→C0 transition *(E_H→R transition)*

Addition of a second electron to the E state or to the E_H state creates a two-electron reduced form of the enzyme (C0 or R) (Figure 4). Analysis of multiple electron injection into the resting O state shows that single-electron reduction of the E state of the enzyme is not competent in proton pumping and is accompanied only by uptake of a substrate proton, through the K-channel (235). At the same time, in the time-resolved measurement of the membrane potential, the oxidative (C4→C3→C2) and reductive (C2→C1→C0) halves of the catalytic cycle of cytochrome *c* oxidase were indirectly estimated to be approximately equivalent in relative to the transmembrane potential generation, which means that the E_H state is not equvivalent to the E state (287).

The $E_H \rightarrow R$ transition is the least explored with a time resolution and consequently less understood step of the catalytic cycle due to technical difficulties with stabilization of the COX in this state. Assuming that $O_H \rightarrow E_H$, F→O and $P_M \rightarrow F$ (or C4→C3→C2→C1) are coupled to pumping of approximately one proton, the resting forth pumped proton should be associated with the $E_H \rightarrow R$ transition (C1→C0) (287) (Figure 4). A state of the enzyme bearing under special conditions about one, on the average, electron equivalent was checked by the single-electron injection technique and the kinetics of membrane potential generation was similar to that of the F→O transition (30). However, in this case the electron equivalent was distributed among heme *a*, heme a_3 and Cu_B (30), whereas in the E_H state formed by electron injection into the O_H state the electron is located exclusively on Cu_B (29, 269, 284). Further experiments are necessary to shed light on these discrepancies.

The computer modeling suggests that the substrate proton that was taken up through the $O_H \rightarrow E_H$ transition is inside the BNC and the tyrosine remains unprotonated and is in a radical form (215). The electron is shifted from the tyrosine anion to the heme a_3 iron that corresponds to reduction of Fe(III)−OH^- to Fe(II)−OH_2. The tyrosyl radical has a significantly larger reduction potential than Fe (III)−OH^-. The relatively high reduction energy of the tyrosyl radical in the E_H state, as in the O_H state, allows both reduction steps in the reductive part of the cycle become exergonic enough for both electrogenic chemistry and proton pumping at a high gradient. The prerequisite for this is protonation of the BNC on each stage during the transfer of the substrate proton in the previous stage of the catalytic cycle and leaving the tyrosine unprotonated (215). The presence of an additional proton in the BNC increases its affinity for the electron, and averages its Em value

in the course of the cycle, despite the fact that the equilibrium redox potential of Fe and Cu is much lower than that of the tyrosine. The formation of the low-energy E form from E_H (like the $O_H \rightarrow O$ transition) corresponds to the proton coupled reduction of the tyrosyl radical by returning of the electron from heme a_3 and uptake of an additional proton from the N-phase (215).

During the final step, $E_H \rightarrow R$, yielding the R state, the tyrosyl becomes fully reduced and protonated, to make the BNC ready for binding and cleavage of the next oxygen molecule. Y288 is located at the top of the K-channel, which for a long time was suggested to supply one or two substrate protons during the reductive phase (145). It is believed that protonation of the tyrosine through the K-channel does not occur due to the low value of the pK of the tyrosine anion, resulting in a kinetic barrier for proton transfer through the K-channel in the oxidative phase (214). I.e., the K-channel is effectively gated by the protonation state of Y288. Accordingly, a substrate proton can be supplied through the K-channel only in the transitions of the reductive phase when Cu_B is cuprous ($O_H \rightarrow E_H \rightarrow R$), and the pKa of Y288 is high (214). The protonated side chain of tyrosine most likely dissociates from the hydroxy group of the farnesyl chain of heme a_3, thereby allowing proton transfer to the oxygenous ligands of the BNC, in accord with the X-ray structure data (130). Another model using molecular dynamics simulation assigns a key role to K362 for proton gating of the K-channel through the reductive phase of the catalytic cycle. It is based on the increasing protonation probability of K362 with the reduction of the BNC during the $O_H \rightarrow E_H \rightarrow R$ transitions and moving of the protonated K362 upwards to bridge the gap to Y288 via an H-bond chain (288). At the same time, in accordance with prerequisite of the unprotonated state of the tyrosine for the efficient pumping through both of the $O_H \rightarrow E_H \rightarrow R$ transitions (215), it is suggested that all substrate protons are transferred through the D-channel, but only one (on the stage of reduction of the E_H state) is transferred via the K-channel.

5.2.2. bd-type oxidases

Cytochrome *bd* catalyzes the four-electron reduction of O_2 to $2H_2O$ with reducing equivalents extracted from a quinol (5, 43, 46-48, 289). According to the modern point of view, the catalytic cycle of cytochrome *bd* comprises the following steps: $\mathbf{A}^1 \rightarrow \mathbf{A}^3 \rightarrow$ **'P'** $\rightarrow \mathbf{F} \rightarrow \mathbf{O}^1 \rightarrow \mathbf{A}^1$, where: $\mathbf{A}^1$ is a species in which heme *d* is reduced and O_2-bound while both hemes *b* are oxidized ($b_{558}^{3+}b_{595}^{3+}d^{2+}$–$O_2$); $\mathbf{A}^3$ is a three-electron-reduced short-lived species in which heme *d* is O_2-bound ($b_{558}^{2+}b_{595}^{2+}d^{2+}$–$O_2$) (167, 194, 197, 204); **'P'** is a short-lived species discovered by Belevich *et al*. (194). To date it is thought to be a ferryl species with a π-cation radical on the porphyrin ring of heme *d* and one electron on heme b_{558} ($b_{558}^{2+}b_{595}^{3+}d^{*4+}$=$O^{2-}$) (290). **F** is a ferryl species with no radical ($b_{558}^{3+}b_{595}^{3+}d^{4+}$=$O^{2-}$); $\mathbf{O}^1$ is one-electron-reduced species in which the electron is probably located on heme b_{558} ($b_{558}^{2+}b_{595}^{3+}d^{3+}$–OH). $\mathbf{A}^1$ and **F** are reported to be the dominant species at steady-state (52). Under steady-state conditions, a small amount of the $\mathbf{O}^1$ species can also be observed (52). The fully oxidized (**O**, $b_{558}^{3+}b_{595}^{3+}d^{3+}$–OH) and fully reduced ($\mathbf{R}^3$, $b_{558}^{2+}b_{595}^{2+}d^{2+}$) species, although may be produced *in vitro* (51, 291), do not participate in the catalytic cycle (52, 292). The **F** species can be generated *in vitro* by addition of H_2O_2 to the isolated cytochrome *bd* (59, 172-173, 197).

5.2.2.1. Membrane potential generation by cytochrome bd

It was reported that the *bd*-type oxidases from *E. coli* generate a transmembrane voltage difference (167-168, 194, 196-197, 203, 293-294), reaching a value of 160-180 mV at steady-state (196, 294). At variance with the heme-copper oxidases (9, 249, 260) cytochromes *bd* function with a lower efficiency with the H^+/e^- ratio = 1 (203, 295-296), and without true proton pumping (167-168, 194, 197, 203, 296-298). The proton motive force in cytochrome *bd* is thought to develop as a sum of the two major events: (i) the release of the quinol protons into the periplasmic space during the quinol oxidation at the quinol oxidizing site located on the periplasmic side of the membrane (within the Q-loop) and (ii) the vectorial movement of 'chemical' protons (needed to form a water molecule) via one or two (77) proposed proton-conducting pathways leading from the cytoplasm to the dioxygen-reducing site located closer to the extracellular membrane surface (77). On oxidation of one quinol molecule, the two protons are released into the periplasmic space, and the two electrons move through heme b_{558} to hemes *d* and b_{595}. The four protons required to reduce O_2 at the heme *d* site are likely taken up from the cytoplasm. In view of the relative vertical distances between the quinol binding site, heme b_{558} and heme *d* (77), the contribution of the electron transfer from the quinol binding site to heme *d* (via heme b_{558}) to the $\Delta\psi$ generation is not expected to be large.

5.2.2.2. Single-turnover electrogenic reactions of cytochrome bd

The use of a combination of microsecond time-resolved spectrophotometric and electrometric techniques allowed to resolve the sequence of the catalytic intermediates and an electrogenicity for each transition in the reaction of the fully reduced ($\mathbf{R}^3$) cytochrome *bd* of *E. coli* with O_2 (167-168, 194, 197, 203). The photolysis of the complex of the *bd* enzyme in the $\mathbf{R}^3$ state with CO ($\mathbf{R}^3$**-CO**) in the presence of O_2 results in the immediate unresolved formation of the

unliganded $\mathbf{R}^3$ cytochrome *bd*. $\mathbf{R}^3$ binds O_2 quickly producing the $\mathbf{A}^3$ species. The $\mathbf{R}^3 \rightarrow \mathbf{A}^3$ transition is nonelectrogenic; its rate is proportional to the O_2 concentration (k_{on} = 1.9 × 10^9 $M^{-1} \times s^{-1}$ (194, 204)). The $\mathbf{A}^3$ formation is followed by the electron transfer from heme b_{595} yielding the '**P'** species. The $\mathbf{A}^3 \rightarrow$'**P'** transition has τ of 4.5 μs and is not electrogenic (194). Then '**P'** is converted into **F** with τ = 48 μs synchronously to the electron transfer from heme b_{558}. The '**P'**→**F** transition is coupled to membrane potential generation (167-168, 194, 197). This electrogenesis is thought to be induced by the proton movement along a proton transfer pathway. If cytochrome *bd* contains a bound quinol, the reaction goes further and possibly gives rise to the formation of the $\mathbf{A}^1$ species. The last transition occurs with τ = 1.1 ms and is electrogenic (167-168, 194). The electrogenesis is likely due to the fact that the electron transfer from heme b_{558} to the dioxygen-reducing site occurring on that step is accompanied by the vectorial proton movement.

The electron transfer between the two catalytically relevant heme groups (heme b_{595} and heme *d*) of cytochrome *bd*-I from *E. coli* cannot itself limit or control the rate constant of the time-resolved transitions in single-turnover catalytic cycle. This is deduced from the flash photolysis of CO from the "mixed-valence" form of the enzyme that is a method by which heme-to-heme electron transfer can be measured for TRO under conditions in which this electron transfer is not limited by the coupled proton transfer or protein conformational changes.

In the "mixed-valence" form of cytochrome *c* oxidase, the heme a_3/Cu_B binuclear site initially is trapped in its reduced ferrous/cuprous state and stabilized by CO binding to the heme iron whereas the two other redox sites, heme *a* and Cu_A, are oxidized. Flash photolysis of CO results in ultrafast displacement of CO from heme a_3 (within a fraction of a picosecond) to bind Cu_B which in turn gives rise to the three phases of the reverse electron transport (the so-called ''electron backflow'') at neutral pH. It should be noted that the sequence of light-induced ''electron backflow'' in TRO is formally reminiscent of the light-dependent oxidation of the OEC in PSII.

The electron re-equilibration should occur first by the electron transfer to heme *a* (in two steps with τ ~1.4 ns and ~3 μs) and then from both hemes to Cu_A (~35 μs). The 3-μs phase was reported to be rate-limited by CO dissociation from Cu_B (299), whereas the 1.4-ns and 35-μs phases are rate-limited by the electron tunneling between heme a_3 and heme *a* and between heme *a* and Cu_A, respectively (135). Recently, evidence for the existence of a fast electron backflow component, on a submicrosecond time range, induced by photodissociation of CO from the ferrous heme *d* in one-electron-reduced state of cytochrome *bd*-I was provided (166, 180). The electron from heme *d* first moves to heme b_{595} and then reaches heme b_{558} with the rate constant of ~16 μs (180). Thus, the mechanism of nanosecond interheme electron transfer may be universal not only in the family of heme-copper oxidases but also in the *bd*-type oxidases.

6. MODELS OF PROTON-PUMPING MECHANISM IN HEME-COPPER OXIDASES

The feature of the molecular mechanism of the $\Delta\mu H^+$ generation by the heme-copper oxidases is that these enzymes use both the oxidoreductive loop principle and a proton pump mechanism. All models of the redox-coupled proton pump suggest the presence in the structure of the so-called "gating", a special mechanism that ensures the irreversibility of proton transfer across the membrane against the membrane potential. Parts of the proton-conducting paths that are responsible for "gating" should be directly linked with a redox reaction or with a concomitant change in the conformation of the protein. The gate mechanism of the proton-conducting path is connected with reversed phase to the aqueous protein surfaces through the proton-conductive "channels" which transport protons in the passive mode. (300).

To date, a relatively large amount of information in study of the proton pump mechanism of the A family bacterial cytochrome oxidases was received. According to one of the most mentioned schemes, each of the one-electron transitions starts from the transfer of the pumped proton from the E286 residue in the protonic D-channel into the "trap" (the proton-loading site, PLS), which is located above the BNC (301-304). The uptake of a proton to be pumped into the PLS is triggered by the electron transfer from Cu_A to heme *a* or from heme *a* to the BNC. In the latter case, it is a synchronous proton/electron transfer event, which results in stabilization of the proton in the PLS, being electrically neutralized by the appearance of a negative charge in the BNC due to the electron transfer from the low-spin heme. Subsequent uptake of a substrate proton from the inner water phase removes electrostatic stabilization resulting in the expulsion of the proton from the PLS to the outside of the membrane.

The exact localization of the proton-loading sites is unknown. One of the likely candidates which is now considered by most authors as a possible PLS is the A-propionate of heme a_3 and/or one of the histidine ligands of Cu_B (208, 302-305). According to the other researchers, the PLS may be localized in the hydrophilic domain, which is located above the hemes closer to heme *a* (306). The computational study suggests that the PLS is a cluster rather than a single residue (307) consisting of the A and D propionates of heme a_3 and nearby residues (e.g. Asp 52 and Lys171

in the bovine COX) (155). For the B family member, the ba_3-type cytochrome oxidase, theoretical analysis suggests that the proton transfer above the BNC involves the A-propionate of heme a_3 and D372, H376 and E126 residues, with the H376 residue acting as the PLS (155)

The exact path of the pumped proton above the E286 residue is not known. The proton pathway from E286 towards the BNC and to the PLS is believed to be formed by a chain of temporary water molecules (302-303, 308). The E286 residue can presumably act as a valve or switch that blocks proton back-flow from the PLS which is located between E286 and the P-phase (25). However, there are indications that neither E286 nor water chains constitutes a possible gating element, which were obtained using a multifaceted set of computational analysis (309). According to the recent improved results of the computational simulation of the E286 properties, there is remaining uncertainty regarding the valve model (310).

According to another scheme, protonation of the BNC occurs before protonation of the PLC and is accompanied by creation of the transient conformation, which stores a portion of the free energy provided by the chemical reaction, and then uses this energy for the proton transfer (301). It is suggested that conformational changes, including the PLC and the path between E286 and the PLS can play a key role. This is indicated by several changes in protein conformation, which are observed in the three-dimensional structure of the reduced enzyme compared with the oxidized one, namely, changes in the conformation of E286, the propionate substituents of heme a_3, and the conserved residue W172. These changes are believed to influence on the proton transfer from E286 to the PLS (129).

A fundamentally different model of the proton pump in the bacterial oxidases were recently proposed based on experimental observations of tryptophan W272* radical (W280 in COX from *R. sphaeroides*) during the F→O transition (311-312). This model also assumes that the pumped proton is transferred after the substrate proton. The tryptophan residue W272, which is located at a distance of 10 Å from heme a_3 in the direction to the P-side of the membrane, is assumed to be a working element of the proton pump ensuring the unidirectionality of the proton pumping. The change of the redox state of this residue is supposed to be linked to the uptake and release of the pumped proton. In the first step, W272 releases a proton onto the outside of the membrane and donates an electron to heme a_3 forming a W272* radical; besides at this stage, the proton is transferred from the N-phase into the BNC. In the next step, the electron and proton are transferred to the W272* radical from heme *a* and from the internal aqueous phase, respectively. Given the proposed role of W272 and its location in the structure, this residue might function as a PLS in the oxidative (C4→C3→C2) phase of the catalytic cycle, while the redox-linked activity of W272 seems less likely in the reductive (C2→C1→C0) phase (313). If so, one could suggest that different PLSs and proton release pathways might be used through the catalytic cycle of cytochrome oxidase that is similar to the above-mentioned use of the proton release pathways at different stages of the catalytic cycle of PSII.

The similar model has been suggested earlier for the mitochondrial cytochrome *c* oxidase, in which the role of a redox-dependent pump element is assigned to heme *a*. The protonic D- and K-channels of the mitochondrial oxidase are suggested to be involved in the transfer of substrate protons only (124), whereas the translocation of protons to be pumped can occur by a mechanism that is different from that in the bacterial cytochrome oxidase. The key role in the mechanism is assigned to the protonic H-channel, which passes near heme *a* (124-125, 153). In this case, a gating mechanism is directly linked to the redox conversion of heme *a* and to the conformational changes away from the BNC, arising from changes in the redox state of heme *a*. The role of redox coupled stage of the proton transfer, which is similar to the proton translocation between E286 and the PLS, is assigned to the proton translocation from the Y54 residue via a peptide bond between Y440 and S441, during its tautomerization, through the S205 residue to the D51 residue, near the P-side of the protein.

In accord with this, the most noticeable structural changes between the reduced and oxidized forms of cytochrome oxidase can be observed in the area of the D51 residue, as well as the structural changes affect the area below heme *a*, including changes in the S382 residue and the relative positions of the cavities of the water molecules (300). In the hypothetical model of proton translocation in the mitochondrial cytochrome oxidase, during the R→A transition, four protons are loaded from the internal N-phase in the aqueous cavity of the H-channel. (18, 314-315). After closing the channel, the protons are released in each of the subsequent transitions P→F→O→E→R (C4→C3→C2→C1→C0 on the Figure 4) that are associated with the electron transfer via heme *a* to the BNC (316). Reduction of heme *a* leads to exhibiting of D51 into the external aqueous phase and to the deprotonation of D51 (124). The reoxidation of heme *a* is accompanied by the return of the original conformation of D51 and by the reprotonation of D51, in which the proton transfer via a peptide bond between the Y440 and S441 residues plays a key role.

According to another point of view, only the upper part of the H-channel is involved in the

translocation of the pumped protons. Besides, the proton pumping occurs by different mechanisms in different stages of the catalytic cycle of the mitochondrial enzyme (306). It is assumed that the transfer of two pumped protons in the reductive (C2→C1→C0) part of the catalytic cycle is controlled by the redox transformations of heme *a* and Cu_A (306). The pumped protons are transported through the D-channel to the E286 residue, and then are transferred to the chain of water molecules in the upper part of the H-channel to the R38 residue and formyl/propionate groups of heme *a*. Two other pumped protons are transferred during the oxidative (C4→C3→C2) part of the catalytic cycle via the D-channel by using the mechanism and a trajectory similar to those of the A family bacterial cytochrome oxidase (306).

A possibility that the H-channel does not function as a path for proton pumping but serves as the so-called dielectric "well" has to be mentioned (300). These "wells" are different from full proton-conducting pathways in the protein because they have interruptions or deadlock. Their role is possibly to modulate the redox potential of the electron transferring redox-center located nearby. In this case, it is assumed that the hydrophilic residues within the H-channel contribute to movement of protons or change their orientation in the direction to heme *a*. As a result, the negative charge arising on heme *a* during its reduction is partially neutralized that may be important for the mild regulation of the cytochrome oxidase activity (300).

7. PERSPECTIVES

Biological systems that harvest free energy from light are of major interest for biotechnology. They may serve as prototypes for gadgets harvesting electric free energy directly from solar illumination. In this respect, the pigment–protein complex of PSII is a key component of the most successful solar energy converting machinery on Earth. The study of the proton pump mechanism of the heme-copper oxidases is extremely important to clarify the features of the device and the design of artificial membranes and nanosystems that are able to efficiently convert different forms of energy. The study of TRO is extremely important and promising from a medical point of view. In particular, a comparative study of the heme-copper oxidases and the *bd*-type oxidases may contribute to the development of new generation antibiotics.

8. ACKNOWLEDGMENTS

The work has been supported by the grants from the Russian Foundation for Basic Research (15-04-06266-a to S.A.S.; 14-04-00153-a to V.B.B.; 14-04-00519 to M.D.M.).

9. REFERENCES

1. J. A. Cruz, C. A. Sacksteder, A. Kanazawa and D. M. Kramer: Contribution of electric field (Delta psi) to steady-state transthylakoid proton motive force (pmf) *in vitro* and *in vivo*. control of pmf parsing into Delta psi and Delta pH by ionic strength. *Biochemistry* 40(5), 1226-1237 (2001) DOI: 10.1021/bi0018741

2. I. V. Shelaev, F. E. Gostev, M. I. Vishnev, A. Y. Shkuropatov, V. V. Ptushenko, M. D. Mamedov, O. M. Sarkisov, V. A. Nadtochenko, A. Y. Semenov and V. A. Shuvalov: P680 (P(D1) P(D2)) and Chl(D1) as alternative electron donors in photosystem II core complexes and isolated reaction centers. *J Photochem Photobiol B* 104(1-2), 44-50 (2011) DOI: 10.1016/j.jphotobiol.2011.02.003

3. M. D. Mamedov, I. O. Petrova, D. V. Yanykin, A. A. Zaspa and A. Y. Semenov: Effect of trehalose on oxygen evolution and electron transfer in photosystem 2 complexes. *Biochemistry (Mosc)* 80(1), 61-66 (2015) DOI: 10.1134/S0006297915010071

4. S. Ferguson-Miller and G. T. Babcock: Heme/copper terminal oxidases. *Chem Rev* 7(96), 2889-2907 (1996) DOI: 10.1021/cr950051s

5. R. K. Poole and G. M. Cook: Redundancy of aerobic respiratory chains in bacteria? Routes, reasons and regulation. *Adv Microbiol Physiol* 43, 165-224 (2000) DOI: 10.1016/S0065-2911(00)43005-5

6. J. Hemp and R. B. Gennis: Diversity of the heme-copper superfamily in archaea: insights from genomics and structural modeling. *Results Probl Cell Differ* 45, 1-31 (2008) DOI: 10.1007/400_2007_046

7. I. Belevich and M. I. Verkhovsky: Molecular mechanism of proton translocation by cytochrome *c* oxidase. *Antioxidants and Redox Signaling* 10, 1-29 (2008) DOI: 10.1089/ars.2007.1705

8. P. Brzezinski and R. B. Gennis: Cytochrome c oxidase: exciting progress and remaining mysteries. *J Bioenerg Biomembr* 40, 521-531 (2008) DOI: 10.1007/s10863-008-9181-7

9. S. A. Siletsky, I. Belevich, T. Soulimane, M. I. Verkhovsky and M. Wikstrom: The

fifth electron in the fully reduced caa(3) from Thermus thermophilus is competent in proton pumping. *Biochim Biophys Acta* 1827(1), 1-9 (2013)
DOI: 10.1016/j.bbabio.2012.09.013

10. G. T. Babcock and M. Wikstrom: Oxygen Activation and the conservation of energy in cell respiration. *Nature* 356, 301-309 (1992)
DOI: 10.1038/356301a0

11. N. J. Watmough, S. J. Field, R. J. Hughes and D. J. Richardson: The bacterial respiratory nitric oxide reductase. *Biochem Soc Trans* 37(Pt 2), 392-399 (2009)
DOI: 10.1042/BST0370392

12. V. Sharma and M. Wikstrom: A structural and functional perspective on the evolution of the heme-copper oxidases. *FEBS Lett* 588(21), 3787-3792 (2014)
DOI: 10.1016/j.febslet.2014.09.020

13. P. Mitchell: Chemiosmotic coupling and energy transduction. Glynn Research Ltd., Bodmin (1968)

14. M. Wikstrom: Proton pump coupled to cytochrome *c* oxidase in mitochondria. *Nature* 266, 271-273 (1977)
DOI: 10.1038/266271a0

15. M. Wikstrom: Cytochrome c oxidase: 25 years of the elusive proton pump. *Biochim Biophys Acta* 1655, 241-247 (2004)
DOI: 10.1016/j.bbabio.2003.07.013

16. K. Kakishima, A. Shiratsuchi, A. Taoka, Y. Nakanishi and Y. Fukumori: Participation of nitric oxide reductase in survival of *Pseudomonas aeruginosa* in LPS-activated macrophages. *Biochem Biophys Res Commun* 355(2), 587-591 (2007)
DOI: 10.1016/j.bbrc.2007.02.017

17. R. B. Gennis: Coupled proton and electron transfer reactions in cytochrome oxidase. *Front Biosci* 9, 581-591 (2004)
DOI: 10.2741/1237

18. S. Yoshikawa, K. Muramoto and K. Shinzawa-Itoh: Proton-pumping mechanism of cytochrome *c* oxidase. *Annu Rev Biophys* 40, 205-223 (2011)
DOI: 10.1146/annurev-biophys-042910-155341

19. S. A. Siletsky and A. A. Konstantinov: Cytochrome c oxidase: charge translocation coupled to single-electron partial steps of the catalytic cycle. *Biochim Biophys Acta* 1817(4), 476-488 (2012)
DOI: 10.1016/j.bbabio.2011.08.003

20. M. M. Pereira, M. Santana and M. Teixeira: A novel scenario for the evolution of haem-copper oxygen reductases**.** *Biochim Biophys Acta* 1505(2-3), 185-208 (2001)
DOI: 10.1016/S0005-2728(01)00169-4

21. M. M. Pereira and M. Teixeira: Proton pathways, ligand binding and dynamics of the catalytic site in haem-copper oxygen reductases: a comparison between the three families. *Biochim Biophys Acta* 1655, 340-346 (2004)
DOI: 10.1016/j.bbabio.2003.06.003

22. J. Hemp, H. Han, J. H. Roh, S. Kaplan, T. J. Martinez and R. B. Gennis: Comparative genomics and site-directed mutagenesis support the existence of only one channel for protons in the C-family (cbb_3 oxidase) of heme-copper oxygen reductases. *Biochemistry* 46, 9963-9972 (2007)
DOI: 10.1021/bi700659y

23. S. Yoshikawa: Structural chemical studies on the reaction mechanism of cytochrome *c* oxidase. In: *Biophysical and structural aspects of bioenergetics*. Ed W. M. RSC Publishing, Norfolk (2005)

24. G. Capitanio, P. L. Martino, N. Capitanio, E. De Nitto and S. Papa: pH dependence of proton translocation in the oxidative and reductive phase of the catalytic cycle of cytochrome *c* oxidase. The role of H_2O produced at the oxygen-reduction site. *Biochemistry* 45, 1930-1937 (2006)
DOI: 10.1021/bi052080v

25. V. R. Kaila, M. I. Verkhovsky, G. Hummer and M. Wikstrom: Glutamic acid 242 is a valve in the proton pump of cytochrome *c* oxidase. *Proc Natl Acad Sci U S A* 105(17), 6255-6259 (2008)
DOI: 10.1073/pnas.0800770105

26. A. Namslauer, H. Lepp, M. Branden, A. Jasaitis, M. I. Verkhovsky and P. Brzezinski: Plasticity of proton pathway structure and water coordination in cytochrome c oxidase. *J Biol Chem* 282(20), 15148-15158 (2007)
DOI: 10.1074/jbc.M700348200

27. S. A. Siletsky, A. S. Pawate, K. Weiss, R. B. Gennis and A. A. Konstantinov: Transmembrane charge separation during

the ferryl-oxo -> oxidized transition in a non-pumping mutant of cytochrome *c* oxidase. *J Biol Chem* 279, 52558-52565 (2004)
DOI: 10.1074/jbc.M407549200

28. S. A. Siletsky, D. Han, S. Brand, J. E. Morgan, M. Fabian, L. Geren, F. Millett, B. Durham, A. A. Konstantinov and R. B. Gennis: Single-electron photoreduction of the P_M intermediate of cytochrome *c* oxidase. *Biochim Biophys Acta* 1757(9-10), 1122-1132 (2006)
DOI: 10.1016/j.bbabio.2006.07.003

29. I. Belevich, D. A. Bloch, M. Wikstrom and M. I. Verkhovsky: Exploring the proton pump mechanism of cytochrome *c* oxidase in real time. *Proc Natl Acad Sci U S A* 104, 2685-2690 (2007)
DOI: 10.1073/pnas.0608794104

30. M. Ruitenberg, A. Kannt, E. Bamberg, K. Fendler and H. Michel: Reduction of cytochrome c oxidase by a second electron leads to proton translocation. *Nature* 417(6884), 99-102 (2002)
DOI: 10.1038/417099a

31. J. Abramson, S. Riistama, G. Larsson, A. Jasaitis, M. Svensson-Ek, L. Laakkonen, A. Puuustinen, S. Iwata and M. Wikstrom: The structure of the ubiquinol oxidase from *Escherichia coli* and its ubiquinone binding site. *Nat Struct Biol* 7, 910-917 (2000)
DOI: 10.1038/82824

32. G. F. White, S. Field, S. Marritt, V. S. Oganesyan, R. B. Gennis, L. L. Yap, A. Katsonouri and A. J. Thomson: An EPR spin label study of the quinol oxidase, *E. coli* cytochrome bo_3: A search for redox induced conformational changes. *Biochemistry* 46, 2355-2366 (2007)
DOI: 10.1021/bi062265h

33. E. Balsa, R. Marco, E. Perales-Clemente, R. Szklarczyk, E. Calvo, M. O. Landazuri and J. A. Enriquez: NDUFA4 is a subunit of complex IV of the mammalian electron transport chain. *Cell Metab* 16(3), 378-386 (2012)
DOI: 10.1016/j.cmet.2012.07.015

34. B. H. Zimmermann, C. I. Nitsche, J. A. Fee, F. Rusnak and E. Munck: Properties of a copper-containing cytochrome ba_3: a second terminal oxidase from the extreme thermophile *Thermus Thermophilus*. *Proc Natl Acad Sci USA* 85, 5779-5783 (1988)
DOI: 10.1073/pnas.85.16.5779

35. J. A. Fee, D. Sanders, C. E. Slutter, P. E. Doan, R. Aasa, M. Karpefors and T. Vдnngerd: Multi-frequency EPR Evidence for a Binuclear Cu_A Center in Cytochrome *c* Oxidase: Studies with a ^{63}Cu- and ^{65}Cu-enriched, Soluble Domain of the Cytochrome ba_3, Subunit II from *Thermus Thermophilus*. *Biochem Biophys Res Commun* 212(1), 77-83 (1995)
DOI: 10.1006/bbrc.1995.1938

36. T. Soulimane, M. von Walter, P. Hof, M. E. Than, R. Huber and G. Buse: Cytochrome *c*-552 from *Thermus thermophilus*: a functional and crystallographic investigation. *Biochem Biophys Res Commun* 237, 572-576 (1997)
DOI: 10.1006/bbrc.1997.7041

37. T. Soulimane, G. Buse, G. B. Bourenkov, H. D. Bartunik, R. Huber and M. E. Than: Structure and mechanism of the aberrant ba_3-cytochrome *c* oxidase from *Thermus thermophilus*. *EMBO J* 19(8), 1766-1776 (2000)
DOI: 10.1093/emboj/19.8.1766

38. V. Rauhamaki, D. A. Bloch, M. I. Verkhovsky and M. Wikstrom: Active site of cytochrome cbb_3. *J Biol Chem* 284, 11301-11308 (2009)
DOI: 10.1074/jbc.M808839200

39. S. Buschmann, E. Warkentin, H. Xie, J. D. Langer, U. Ermler and H. Michel: The structure of cbb_3 cytochrome oxidase provides insights into proton pumping. *Science* 329(5989), 327-330 (2010)
DOI: 10.1126/science.1187303

40. H. Xie, S. Buschmann, J. D. Langer, B. Ludwig and H. Michel: Biochemical and biophysical characterization of the two isoforms of cbb3-type cytochrome c oxidase from Pseudomonas stutzeri. *J Bacteriol* 196(2), 472-482 (2014)
DOI: 10.1128/JB.01072-13

41. J. van der Oost, A. P. N. deBoer, J.-W. L. deGier, W. G. Zumft, A. H. Stouthamer and R. J. M. van Spanning: The Heme-copper Oxidase Family Consists of Three Distinct Types of Terminal Oxidases and is Related to Nitric Oxide Reductase. *FEMS Microbiol Lett* 121(1), 1-9 (1994)
DOI: 10.1111/j.1574-6968.1994.tb07067.x

42. G. N. Green, H. Fang, R.-J. Lin, G. Newton, M. Mather, C. D. Georgiou and R. B. Gennis: The nucleotide sequence of the *cyd* locus

encoding the two subunits of the cytochrome *d* terminal oxidase complex of *Escherichia coli*. *J Biol Chem* 263(26), 13138-13143 (1988)

43. V. B. Borisov, R. B. Gennis, J. Hemp and M. I. Verkhovsky: The cytochrome bd respiratory oxygen reductases. *Biochim Biophys Acta* 1807(11), 1398-1413 (2011) DOI: 10.1016/j.bbabio.2011.06.016

44. V. B. Borisov: Cytochrome bd: structure and properties. *Biokhimiia (Biochemistry-Moscow)* 61(5), 786-799 (1996)

45. E. V. Gavrikova, V. G. Grivennikova, V. B. Borisov, G. Cecchini and A. D. Vinogradov: Assembly of a chimeric respiratory chain from bovine heart submitochondrial particles and cytochrome bd terminal oxidase of Escherichia coli. *FEBS Lett* 583(8), 1287-1291 (2009) DOI: 10.1016/j.febslet.2009.03.022

46. A. Giuffre, V. B. Borisov, D. Mastronicola, P. Sarti and E. Forte: Cytochrome bd oxidase and nitric oxide: from reaction mechanisms to bacterial physiology. *FEBS Lett* 586(5), 622-629 (2012) DOI: 10.1016/j.febslet.2011.07.035

47. A. Giuffre, V. B. Borisov, M. Arese, P. Sarti and E. Forte: Cytochrome bd oxidase and bacterial tolerance to oxidative and nitrosative stress. *Biochim Biophys Acta* 1837(7), 1178-1187 (2014) DOI: 10.1016/j.bbabio.2014.01.016

48. V. B. Borisov, E. Forte, S. A. Siletsky, M. Arese, A. I. Davletshin, P. Sarti and A. Giuffre: Cytochrome bd Protects Bacteria against Oxidative and Nitrosative Stress: A Potential Target for Next-Generation Antimicrobial Agents. *Biochemistry (Mosc)* 80(5), 565-575 (2015) DOI: 10.1134/S0006297915050077

49. R. K. Poole, C. Kumar, I. Salmon and B. Chance: The 650 nm chromophore in *Escherichia coli* is an 'Oxy-' or oxygenated compound, not the oxidized form of cytochrome oxidase *d*: A hypothesis. *J Gen Microbiol* 129, 1335-1344 (1983) DOI: 10.1099/00221287-129-5-1335

50. M. A. Kahlow, T. M. Loehr, T. M. Zuberi and R. B. Gennis: The Oxygenated Complex of Cytochrome *d* Terminal Oxidase: Direct Evidence for Fe-O_2 Coordination in a Chlorin-Containing Enzyme by Resonance Raman Spectroscopy. *J Am Chem Soc* 115, 5845-5846 (1993) DOI: 10.1021/ja00066a071

51. V. B. Borisov, I. A. Smirnova, I. A. Krasnosel'skaia and A. A. Konstantinov: Oxygenated cytochrome bd from Escherichia coli could be transformed into an oxidized form by lipophilic electron acceptors. *Biokhimiia (Biochemistry-Moscow)* 59(4), 598-606 (1994)

52. V. B. Borisov, E. Forte, P. Sarti and A. Giuffre: Catalytic intermediates of cytochrome bd terminal oxidase at steady-state: ferryl and oxy-ferrous species dominate. *Biochim Biophys Acta* 1807(5), 503-509 (2011) DOI: 10.1016/j.bbabio.2011.02.007

53. I. Belevich, V. B. Borisov, A. A. Konstantinov and M. I. Verkhovsky: Oxygenated complex of cytochrome bd from Escherichia coli: stability and photolability. *FEBS Lett* 579(21), 4567-4570 (2005) DOI: 10.1016/j.febslet.2005.07.011

54. I. Belevich, V. B. Borisov, D. A. Bloch, A. A. Konstantinov and M. I. Verkhovsky: Cytochrome bd from Azotobacter vinelandii: evidence for high-affinity oxygen binding. *Biochemistry* 46(39), 11177-11184 (2007) DOI: 10.1021/bi700862u

55. E. Forte, V. B. Borisov, A. A. Konstantinov, M. Brunori, A. Giuffre and P. Sarti: Cytochrome bd, a key oxidase in bacterial survival and tolerance to nitrosative stress. *Ital J Biochem* 56(4), 265-269 (2007)

56. V. B. Borisov and M. I. Verkhovsky: Oxygen as Acceptor. *EcoSal Plus* 6(2) (2015) DOI: 10.1128/ecosalplus.ESP-0012-2015

57. V. B. Borisov, E. Forte, S. A. Siletsky, P. Sarti and A. Giuffre: Cytochrome bd from Escherichia coli catalyzes peroxynitrite decomposition. *Biochim Biophys Acta* 1847(2), 182-188 (2015) DOI: 10.1016/j.bbabio.2014.10.006

58. V. B. Borisov, E. Forte, A. A. Konstantinov, R. K. Poole, P. Sarti and A. Giuffre: Interaction of the bacterial terminal oxidase cytochrome bd with nitric oxide. *FEBS Lett* 576(1-2), 201-204 (2004) DOI: 10.1016/j.febslet.2004.09.013

59. V. B. Borisov, E. Forte, P. Sarti, M. Brunori, A. A. Konstantinov and A. Giuffre: Nitric oxide reacts with the ferryl-oxo catalytic intermediate of the CuB-lacking cytochrome bd terminal oxidase. *FEBS Lett* 580(20), 4823-4826 (2006)
DOI: 10.1016/j.febslet.2006.07.072

60. V. B. Borisov, E. Forte, P. Sarti, M. Brunori, A. A. Konstantinov and A. Giuffre: Redox control of fast ligand dissociation from Escherichia coli cytochrome bd. *Biochem Biophys Res Commun* 355(1), 97-102 (2007)
DOI: 10.1016/j.bbrc.2007.01.118

61. M. G. Mason, M. Shepherd, P. Nicholls, P. S. Dobbin, K. S. Dodsworth, R. K. Poole and C. E. Cooper: Cytochrome *bd* confers nitric oxide resistance to *Escherichia coli*. *Nature Chemical Biology* 5, 94-96 (2009)
DOI: 10.1038/nchembio.135

62. V. B. Borisov, E. Forte, A. Giuffre, A. Konstantinov and P. Sarti: Reaction of nitric oxide with the oxidized di-heme and heme-copper oxygen-reducing centers of terminal oxidases: Different reaction pathways and end-products. *J Inorg Biochem* 103(8), 1185-1187 (2009)
DOI: 10.1016/j.jinorgbio.2009.06.002

63. E. Forte, V. B. Borisov, M. Falabella, H. G. Colaco, M. Tinajero-Trejo, R. K. Poole, J. B. Vicente, P. Sarti and A. Giuffre: The Terminal Oxidase Cytochrome bd Promotes Sulfide-resistant Bacterial Respiration and Growth. *Sci Rep* 6, 23788 (2016)
DOI: 10.1038/srep23788

64. S. Korshunov, K. R. Imlay and J. A. Imlay: The cytochrome bd oxidase of Escherichia coli prevents respiratory inhibition by endogenous and exogenous hydrogen sulfide. *Mol Microbiol* 101(1), 62-77 (2016)
DOI: 10.1111/mmi.13372

65. H. E. Jesse, T. L. Nye, S. McLean, J. Green, B. E. Mann and R. K. Poole: Cytochrome *bd*-I in *Escherichia coli* is less sensitive than cytochromes *bd*-II or *bo"* to inhibition by the carbon monoxide-releasing molecule, CORM-3: N-acetylcysteine reduces CO-RM uptake and inhibition of respiration. *Biochim Biophys Acta* 1834, 1693–1703 (2013)
DOI: 10.1016/j.bbapap.2013.04.019

66. Y. H. Sun, M. F. de Jong, A. B. den Hartigh, C. M. Roux, H. G. Rolan and R. M. Tsolis: The small protein CydX is required for function of cytochrome *bd* oxidase in *Brucella abortus*. *Front Cell Infect Microbiol* 2, 47 (2012)
DOI: 10.3389/fcimb.2012.00047

67. D. Wall, J. M. Delaney, O. Fayet, B. Lipinska, T. Yamamoto and C. Georgopoulos: *arc*-Dependent Thermal Regulation and Extragenic Suppression of the *Escherichia coli* Cytochrome *d* Operon. *J Bacteriol* 174(20), 6554-6562 (1992)
DOI: 10.1128/jb.174.20.6554-6562.1992

68. A. Lindqvist, J. Membrillo-Hernandez, R. K. Poole and G. M. Cook: Roles of respiratory oxidases in protecting *Escherichia coli* K12 from oxidative stress. *Antonie Van Leeuwenhoek* 78(1), 23-31 (2000)
DOI: 10.1023/A:1002779201379

69. S. E. Edwards, C. S. Loder, G. Wu, H. Corker, B. W. Bainbridge, S. Hill and R. K. Poole: Mutation of cytochrome *bd* quinol oxidase results in reduced stationary phase survival, iron deprivation, metal toxicity and oxidative stress in *Azotobacter vinelandii*. *FEMS Microbiol Lett* 185(1), 71-77 (2000)
DOI: 10.1111/j.1574-6968.2000.tb09042.x

70. S. Korshunov and J. A. Imlay: Two sources of endogenous hydrogen peroxide in *Escherichia coli*. *Mol Microbiol* 75(6), 1389-1401 (2010)
DOI: 10.1111/j.1365-2958.2010.07059.x

71. V. B. Borisov, A. I. Davletshin and A. A. Konstantinov: Peroxidase activity of cytochrome bd from Escherichia coli. *Biochemistry (Mosc)* 75(4), 428-436 (2010)
DOI: 10.1134/S000629791004005X

72. V. B. Borisov, E. Forte, A. Davletshin, D. Mastronicola, P. Sarti and A. Giuffre: Cytochrome bd oxidase from Escherichia coli displays high catalase activity: an additional defense against oxidative stress. *FEBS Lett* 587(14), 2214-2218 (2013)
DOI: 10.1016/j.febslet.2013.05.047

73. E. Forte, V. B. Borisov, A. Davletshin, D. Mastronicola, P. Sarti and A. Giuffre: Cytochrome bd oxidase and hydrogen peroxide resistance in Mycobacterium tuberculosis. *MBio* 4(6), e01006-13 (2013)
DOI: 10.1128/mBio.01006-13

74. S. Al-Attar, Y. Yu, M. Pinkse, J. Hoeser, T. Friedrich, D. Bald and S. de Vries: Cytochrome bd Displays Significant Quinol

Peroxidase Activity. *Sci Rep* 6, 27631 (2016) DOI: 10.1038/srep27631

75. V. B. Borisov: Defects in mitochondrial respiratory complexes III and IV, and human pathologies. *Mol Aspects Med* 23(5), 385-412 (2002) DOI: 10.1016/S0098-2997(02)00013-4

76. V. B. Borisov: Mutations in respiratory chain complexes and human diseases. *Ital J Biochem* 53(1), 34-40 (2004)

77. S. Safarian, C. Rajendran, H. Muller, J. Preu, J. D. Langer, S. Ovchinnikov, T. Hirose, T. Kusumoto, J. Sakamoto and H. Michel: Structure of a bd oxidase indicates similar mechanisms for membrane-integrated oxygen reductases. *Science* 352(6285), 583-586 (2016) DOI: 10.1126/science.aaf2477

78. V. Borisov, A. M. Arutyunyan, J. P. Osborne, R. B. Gennis and A. A. Konstantinov: Magnetic circular dichroism used to examine the interaction of *Escherichia coli* cytochrome *bd* with ligands. *Biochemistry* 38(2), 740-750 (1999) DOI: 10.1021/bi981908t

79. R. G. Kranz and R. B. Gennis: Characterization of the Cytochrome *d* Terminal Oxidase Complex of *Escherichia coli* Using Polyclonal and Monoclonal Antibodies. *J Biol Chem* 259(12), 7998-8003 (1984)

80. R. M. Lorence, K. Carter, R. B. Gennis, K. Matsushita and H. R. Kaback: Trypsin Proteolysis of the Cytochrome *d* Complex of *Escherichia coli* Selectively Inhibits Ubiquinol Oxidase Activity While Not Affecting N,N,N',N"- Tetramethyl-p-phenylenediamine Oxidase Activity. *J Biol Chem* 11, 5271-5276 (1988)

81. T. J. Dueweke and R. B. Gennis: Epitopes of Monoclonal Antibodies Which Inhibit Ubiquinol Oxidase Activity of *Escherichia coli* Cytochrome *d* Complex Localize a Functional Domain. *J Biol Chem* 265, 4273-4277 (1990)

82. T. J. Dueweke and R. B. Gennis: Proteolysis of the Cytochrome *d* Complex with Trypsin and Chymotrypsin Localizes a Quinol Oxidase Domain. *Biochemistry* 30, 3401-3406 (1991) DOI: 10.1021/bi00228a007

83. Y. Matsumoto, M. Murai, D. Fujita, K. Sakamoto, H. Miyoshi, M. Yoshida and T. Mogi: Mass spectrometric analysis of the ubiquinol-binding site in cytochrome *bd* from *Escherichia coli*. *J Biol Chem* 281, 1905-1912 (2006) DOI: 10.1074/jbc.M508206200

84. T. Mogi, S. Akimoto, S. Endou, T. Watanabe-Nakayama, E. Mizuochi-Asai and H. Miyoshi: Probing the ubiquinol-binding site in cytochrome *bd* by site-directed mutagenesis. *Biochemistry* 45(25), 7924-7930 (2006) DOI: 10.1021/bi060192w

85. J. Sakamoto, E. Koga, T. Mizuta, C. Sato, S. Nogushi and N. Sone: Gene structure and quinol oxidase activity of a cytochrome *bd*-type oxidase from *Bacillus stearothermophilus*. *Biochim Biophys Acta* 1411, 147-158 (1999) DOI: 10.1016/S0005-2728(99)00012-2

86. J. P. Osborne and R. B. Gennis: Sequence analysis of cytochrome *bd* oxidase suggests a revised topology for subunits I. *Biochim Biophys Acta* 1410, 32-50 (1999) DOI: 10.1016/S0005-2728(98)00171-6

87. A. M. Arutyunyan, J. Sakamoto, M. Inadome, Y. Kabashima and V. B. Borisov: Optical and magneto-optical activity of cytochrome bd from Geobacillus thermodenitrificans. *Biochim Biophys Acta* 1817(11), 2087-2094 (2012) DOI: 10.1016/j.bbabio.2012.06.009

88. L. Cunningham and H. D. Williams: Isolation and characterization of mutants defective in the cyanide-insensitive respiratory pathway of *Pseudomonas aeruginosa*. *J Bacteriol* 177(2), 432-438 (1995) DOI: 10.1128/jb.177.2.432-438.1995

89. N. Azarkina, S. Siletsky, V. Borisov, C. von Wachenfeldt, L. Hederstedt and A. A. Konstantinov: A cytochrome *bb*'-type quinol oxidase in *Bacillus subtilis* strain 168. *J Biol Chem* 274(46), 32810-32817 (1999) DOI: 10.1074/jbc.274.46.32810

90. D. Zannoni: The respiratory chains of pathogenic pseudomonads. *Biochim Biophys Acta* 975(3), 299-316 (1989) DOI: 10.1016/S0005-2728(89)80337-8

91. A. Zouni, H. T. Witt, J. Kern, P. Fromme, N. Krauss, W. Saenger and P. Orth:

Crystal structure of photosystem II from Synechococcus elongatus at 3.8 A resolution. *Nature* 409(6821), 739-743 (2001)
DOI: 10.1038/35055589

92. K. N. Ferreira, T. M. Iverson, K. Maghlaoui, J. Barber and S. Iwata: Architecture of the photosynthetic oxygen-evolving center. *Science* 303(5665), 1831-1838 (2004)
DOI: 10.1126/science.1093087

93. Y. Umena, K. Kawakami, J. R. Shen and N. Kamiya: Crystal structure of oxygen-evolving photosystem II at a resolution of 1.9. A. *Nature* 473(7345), 55-60 (2011)
DOI: 10.1038/nature09913

94. I. Rivalta, G. W. Brudvig and V. S. Batista: Oxomanganese complexes for natural and artificial photosynthesis. *Curr Opin Chem Biol* 16(1-2), 11-18 (2012)
DOI: 10.1016/j.cbpa.2012.03.003

95. M. Suga, F. Akita, K. Hirata, G. Ueno, H. Murakami, Y. Nakajima, T. Shimizu, K. Yamashita, M. Yamamoto, H. Ago and J. R. Shen: Native structure of photosystem II at 1.95 A resolution viewed by femtosecond X-ray pulses. *Nature* 517(7532), 99-103 (2015)
DOI: 10.1038/nature13991

96. M. Perez-Navarro, F. Neese, W. Lubitz, D. A. Pantazis and N. Cox: Recent developments in biological water oxidation. *Curr Opin Chem Biol* 31, 113-119 (2016)
DOI: 10.1016/j.cbpa.2016.02.007

97. N. Cox and J. Messinger: Reflections on substrate water and dioxygen formation. *Biochim Biophys Acta* 1827(8-9), 1020-1030 (2013)
DOI: 10.1016/j.bbabio.2013.01.013

98. S. Nakamura, R. Nagao, R. Takahashi and T. Noguchi: Fourier transform infrared detection of a polarizable proton trapped between photooxidized tyrosine YZ and a coupled histidine in photosystem II: relevance to the proton transfer mechanism of water oxidation. *Biochemistry* 53(19), 3131-3144 (2014)
DOI: 10.1021/bi500237y

99. A. Guskov, J. Kern, A. Gabdulkhakov, M. Broser, A. Zouni and W. Saenger: Cyanobacterial photosystem II at 2.9-A resolution and the role of quinones, lipids, channels and chloride. *Nat Struct Mol Biol* 16(3), 334-342 (2009)
DOI: 10.1038/nsmb.1559

100. F. M. Ho: Structural and mechanistic investigations of photosystem II through computational methods. *Biochim Biophys Acta* 1817(1), 106-120 (2012)
DOI: 10.1016/j.bbabio.2011.04.009

101. K. Linke and F. M. Ho: Water in Photosystem II: structural, functional and mechanistic considerations. *Biochim Biophys Acta* 1837(1), 14-32 (2014)
DOI: 10.1016/j.bbabio.2013.08.003

102. L. Vogt, D. J. Vinyard, S. Khan and G. W. Brudvig: Oxygen-evolving complex of Photosystem II: an analysis of second-shell residues and hydrogen-bonding networks. *Curr Opin Chem Biol* 25, 152-158 (2015)
DOI: 10.1016/j.cbpa.2014.12.040

103. A. Gabdulkhakov, A. Guskov, M. Broser, J. Kern, F. Muh, W. Saenger and A. Zouni: Probing the accessibility of the Mn(4) Ca cluster in photosystem II: channels calculation, noble gas derivatization, and cocrystallization with DMSO. *Structure* 17(9), 1223-1234 (2009)
DOI: 10.1016/j.str.2009.07.010

104. S. Vassiliev, P. Comte, A. Mahboob and D. Bruce: Tracking the flow of water through photosystem II using molecular dynamics and streamline tracing. *Biochemistry* 49(9), 1873-1881 (2010)
DOI: 10.1021/bi901900s

105. R. J. Service, W. Hillier and R. J. Debus: Evidence from FTIR difference spectroscopy of an extensive network of hydrogen bonds near the oxygen-evolving Mn(4)Ca cluster of photosystem II involving D1-Glu65, D2-Glu312, and D1-Glu329. *Biochemistry* 49(31), 6655-6669 (2010)
DOI: 10.1021/bi100730d

106. S. Vassiliev, T. Zaraiskaya and D. Bruce: Exploring the energetics of water permeation in photosystem II by multiple steered molecular dynamics simulations. *Biochim Biophys Acta* 1817(9), 1671-1678 (2012)
DOI: 10.1016/j.bbabio.2012.05.016

107. A. N. Bondar and H. Dau: Extended protein/water H-bond networks in photosynthetic water oxidation. *Biochim Biophys Acta* 1817(8), 1177-1190 (2012)
DOI: 10.1016/j.bbabio.2012.03.031

108. A. N. Bondar and S. H. White: Hydrogen bond dynamics in membrane protein function. *Biochim Biophys Acta* 1818(4), 942-950 (2012)
DOI: 10.1016/j.bbamem.2011.11.035

109. R. J. Debus: Evidence from FTIR difference spectroscopy that D1-Asp61 influences the water reactions of the oxygen-evolving Mn4CaO5 cluster of photosystem II. *Biochemistry* 53(18), 2941-2955 (2014)
DOI: 10.1021/bi500309f

110. M. R. Blomberg and P. E. Siegbahn: The mechanism for proton pumping in cytochrome c oxidase from an electrostatic and quantum chemical perspective. *Biochim Biophys Acta* 1817(4), 495-505 (2012)
DOI: 10.1016/j.bbabio.2011.09.014

111. F. Garczarek, L. S. Brown, J. K. Lanyi and K. Gerwert: Proton binding within a membrane protein by a protonated water cluster. *Proc Natl Acad Sci U S A* 102(10), 3633-3638 (2005)
DOI: 10.1073/pnas.0500421102

112. P. H. Oyala, T. A. Stich, R. J. Debus and R. D. Britt: Ammonia Binds to the Dangler Manganese of the Photosystem II Oxygen-Evolving Complex. *J Am Chem Soc* 137(27), 8829-8837 (2015)
DOI: 10.1021/jacs.5b04768

113. M. Retegan, V. Krewald, F. Mamedov, F. Neese, W. Lubitz, N. Cox and P. D.A.: A five-coordinate Mn(IV) intermediate in biological water oxidation: spectroscopic signature and a pivot mechanism for water binding. *Chem Sci* 7, 72-84 (2016)

114. H. Suzuki, J. Yu, T. Kobayashi, H. Nakanishi, P. J. Nixon and T. Noguchi: Functional roles of D2-Lys317 and the interacting chloride ion in the water oxidation reaction of photosystem II as revealed by fourier transform infrared analysis. *Biochemistry* 52(28), 4748-4757 (2013)
DOI: 10.1021/bi301699h

115. P. L. Dilbeck, H. J. Hwang, I. Zaharieva, L. Gerencser, H. Dau and R. L. Burnap: The D1-D61N mutation in Synechocystis sp. PCC 6803 allows the observation of pH-sensitive intermediates in the formation and release of O(2) from photosystem II. *Biochemistry* 51(6), 1079-1091 (2012)
DOI: 10.1021/bi201659f

116. A. Klauss, M. Haumann and H. Dau: Alternating electron and proton transfer steps in photosynthetic water oxidation. *Proc Natl Acad Sci U S A* 109(40), 16035-16040 (2012)
DOI: 10.1073/pnas.1206266109

117. T. Noguchi: Fourier transform infrared difference and time-resolved infrared detection of the electron and proton transfer dynamics in photosynthetic water oxidation. *Biochim Biophys Acta* 1847(1), 35-45 (2015)
DOI: 10.1016/j.bbabio.2014.06.009

118. L. K. Frankel, L. Sallans, P. A. Limbach and T. M. Bricker: Identification of oxidized amino acid residues in the vicinity of the Mn(4)CaO(5) cluster of Photosystem II: implications for the identification of oxygen channels within the Photosystem. *Biochemistry* 51(32), 6371-6377 (2012)
DOI: 10.1021/bi300650n

119. S. Vassiliev, T. Zaraiskaya and D. Bruce: Molecular dynamics simulations reveal highly permeable oxygen exit channels shared with water uptake channels in photosystem II. *Biochim Biophys Acta* 1827(10), 1148-1155 (2013)
DOI: 10.1016/j.bbabio.2013.06.008

120. F. Muh, C. Glockner, J. Hellmich and A. Zouni: Light-induced quinone reduction in photosystem II. *Biochim Biophys Acta* 1817(1), 44-65 (2012)
DOI: 10.1016/j.bbabio.2011.05.021

121. K. Saito, A. W. Rutherford and H. Ishikita: Mechanism of proton-coupled quinone reduction in Photosystem II. *Proc Natl Acad Sci U S A* 110(3), 954-959 (2013)
DOI: 10.1073/pnas.1212957110

122. T. Tsukihara, H. Aoyama, E. Yamashita, T. Takashi, H. Yamaguichi, K. Shinzawa-Itoh, R. Nakashima, R. Yaono and S. Yoshikawa: The whole structure of the 13-subunit oxidized cytochrome c oxidase at 2.8 A. *Science* 272, 1136-1144 (1996)
DOI: 10.1126/science.272.5265.1136

123. S. Yoshikawa, K. Shinzawa-Itoh, R. Nakashima, R. Yaono, N. Inoue, M. Yao, M. J. Fei, C. P. Libeu, T. Mizushima, H. Yamaguchi, T. Tomizaki and T. Tsukihara: Redox-coupled crystal structural changes in bovine heart cytochrome *c* oxidase. *Science* 280, 1723-1729 (1998)
DOI: 10.1126/science.280.5370.1723

124. T. Tsukihara, K. Shimokata, Y. Katayama, H. Shimada, K. Muramoto, H. Aoyama, M. Mochizuki, K. Shinzawa-Itoh, E. Yamashita, M. Yao, Y. Ishimura and S. Yoshikawa: The low-spin heme of cytochrome *c* oxidase as the driving element of the proton-pumping process. *Proc Natl Acad Sci USA* 100(26), 15304-15309 (2003)
DOI: 10.1073/pnas.2635097100

125. K. Muramoto, K. Hirata, K. Shinzawa-Itoh, S. Yoko-o, E. Yamashita, H. Aoyama, T. Tsukihara and S. Yoshikawa: A histidine residue acting as a controlling site for dioxygen reduction and proton pumping by cytochrome *c* oxidase. *Proc Natl Acad Sci U S A* 104, 7881-7886 (2007)
DOI: 10.1073/pnas.0610031104

126. S. Iwata, C. Ostermeier, B. Ludwig and H. Michel: Structure at 2.8 A resolution of cytochrome *c* oxidase from *Paracoccus denitrificans*. *Nature* 376, 660-669 (1995)
DOI: 10.1038/376660a0

127. C. Ostermeier, S. Iwata, B. Ludwig and H. Michel: F_V fragment-mediated crystallization of the membrane protein bacterial cytochrome *c* oxidase. *Nat Struct Biol* 2, 842 (1995)
DOI: 10.1038/nsb1095-842

128. J. Koepke, E. Olkhova, H. Angerer, H. Muller, G. Peng and H. Michel: High resolution crystal structure of *Paracoccus denitrificans* cytochrome *c* oxidase: New insights into the active site and the proton transfer pathways. *Biochim Biophys Acta* 1787, 635-645 (2009)
DOI: 10.1016/j.bbabio.2009.04.003

129. M. Svensson-Ek, J. Abramson, G. Larsson, S. Tornroth, P. Brzezinski and S. Iwata: The X-ray crystal structures of wild-type and EQ(I-286) mutant cytochrome *c* oxidases from *Rhodobacter sphaeroides*. *J Mol Biol* 321, 329-339 (2002)
DOI: 10.1016/S0022-2836(02)00619-8

130. L. Qin, J. Liu, D. A. Mills, D. A. Proshlyakov, C. Hiser and S. Ferguson-Miller: Redox dependent conformational changes in cytochrome *c* oxidase suggest a gating mechanism for proton uptake. *Biochemistry* 48, 5121-5130 (2009)
DOI: 10.1021/bi9001387

131. J. A. Lyons, D. Aragao, O. Slattery, A. V. Pisliakov, T. Soulimane and M. Caffrey: Structural insights into electron transfer in caa3-type cytochrome oxidase. *Nature* 487(7408), 514-518 (2012)
DOI: 10.1038/nature11182

132. V. M. Luna, Y. Chen, J. A. Fee and C. D. Stout: Crystallographic studies of Xe and Kr binding within the large internal cavity of cytochrome ba_3 from *Thermus thermophilus*: Structural analysis and role of oxygen transport channels in the heme-Cu oxidases. *Biochemistry* 47, 4657-4665 (2008)
DOI: 10.1021/bi800045y

133. Y. Osuda, K. Shinzawa-Itoh, K. Tani, S. Maeda, S. Yoshikawa, T. Tsukihara and C. Gerle: Two-dimensional crystallization of monomeric bovine cytochrome c oxidase with bound cytochrome c in reconstituted lipid membranes. *Microscopy (Oxf)* 65(3), 263-267 (2016)
DOI: 10.1093/jmicro/dfv381

134. B. Meunier, A. Marechal and P. R. Rich: Construction of histidine-tagged yeast mitochondrial cytochrome c oxidase for facile purification of mutant forms. *Biochem J* 444(2), 199-204 (2012)
DOI: 10.1042/BJ20120116

135. E. Pilet, A. Jasaitis, U. Liebl and M. H. Vos: Electron transfer between hemes in mammalian cytochrome *c* oxidase. *Proc Natl Acad Sci USA* 101, 16196-16203 (2004)
DOI: 10.1073/pnas.0405032101

136. G. Buse, T. Soulimane, M. Dewor, H. E. Meyer and M. Bloggel: Evidence for a copper coordinated histidine-tyrosine crosslink in the active site of cytochrome oxidase. *Protein Sci* 8, 985-990 (1999)
DOI: 10.1110/ps.8.5.985

137. V. Rauhamaki, M. Baumann, R. Soliymani, A. Puustinen and M. Wikstrom: Identification of histidin-tyrosin cross-link in the active site of the cbb_3-type cytochrome *c* oxidase from *Rhodobacter sphaeroides*. *Proc Natl Acad Sci U S A* 103, 16135-16140 (2006)
DOI: 10.1073/pnas.0606254103

138. G. T. Babcock: How oxygen is activated and reduced in respiration. *Proc Natl Acad Sci U S A* 96, 12971-12973 (1999)
DOI: 10.1073/pnas.96.23.12971

139. D. A. Proshlyakov, M. A. Pressler, C. DeMaso, J. F. Leykam, D. L. DeWitt and G. L. Babcock: Oxygen activation and reduction in respiration: involvement of redox-active

tyrosine 244. *Science* 290, 1588-1591 (2000) DOI: 10.1126/science.290.5496.1588

140. D. A. Mills and J. P. Hosler: Slow proton transfer through the pathways for pumped protons in cytochrome *c* oxidase induces suicide inactivation of the enzyme. *Biochemistry* 44, 4556-4666 (2005) DOI: 10.1021/bi0475774

141. J. Abramson, S. Riistama, G. Larsson, A. Jasaitis, M. Svensson-Ek, L. Laakkonen, A. Puustinen, S. Iwata and M. Wikstrom: The structure of the ubiquinol oxidase from *Escherichia coli* and its ubiquinone binding site. *Nat Struct Biol* 7, 910-917 (2000) DOI: 10.1038/82824

142. L. L. Yap, M. T. Lin, H. Ouyang, R. I. Samoilova, S. A. Dikanov and R. B. Gennis: The quinone-binding sites of the cytochrome bo3 ubiquinol oxidase from Escherichia coli. *Biochim Biophys Acta* 1797(12), 1924-1932 (2010) DOI: 10.1016/j.bbabio.2010.04.011

143. P. Hellwig, T. Yano, T. Ohnishi and R. B. Gennis: Identification of the residues involved in stabilization of the semiquinone radical in the high-affinity ubiquinone binding site in cytochrome bo_3 from *Escherichia coli* by site-directed mutagenesis and EPR spectroscopy. *Biochemistry* 41(34), 10675-10679 (2002) DOI: 10.1021/bi012146w

144. J. R. Fetter, J. Qian, J. Shapleigh, J. W. Thomas, A. Garcia-Horsman, E. Schmidt, J. Hosler, G. T. Babcock, R. B. Gennis and S. Ferguson-Miller: Possible proton relay pathways in cytochrome *c* oxidase. *Proc Natl Acad Sci U S A* 92, 1604-1608 (1995) DOI: 10.1073/pnas.92.5.1604

145. A. A. Konstantinov, S. Siletsky, D. Mitchell, A. Kaulen and R. B. Gennis: The roles of the two proton input channels in cytochrome *c* oxidase from *Rhodobacter sphaeroides* probed by the effects of site-directed mutations on time resolved electrogenic intraprotein proton transfer. *Proc Natl Acad Sci U S A* 94, 9085-9090 (1997) DOI: 10.1073/pnas.94.17.9085

146. R. B. Gennis: Multiple proton-conducting pathways in cytochrome oxidase and a proposed role for the active-site tyrosine. *Biochim Biophys Acta* 1365, 241-248 (1998) DOI: 10.1016/S0005-2728(98)00075-9

147. L. Qin, C. Hiser, A. Mulichak, R. M. Garavito and S. Ferguson-Miller: Identification of conserved lipid/detergent-binding sites in a high-resolution structure of the membrane protein cytochrome *c* oxidase. *Proc Natl Acad Sci U S A* 103, 16117-16122 (2006) DOI: 10.1073/pnas.0606149103

148. M. Branden, F. Tomson, R. B. Gennis and P. Brzezinski: The entry point of the K-proton-transfer pathway in cytochrome *c* oxidase. *Biochemistry* 41, 10794-10798 (2002) DOI: 10.1021/bi026093+

149. M. Wikstrom, C. Ribacka, M. Molin, L. Laakkonen, M. I. Verkhovsky and A. Puustinen: Gating of proton and water transfer in the respiratory enzyme cytochrome *c* oxidase. *Proc Natl Acad Sci U S A* 102, 10478-10481 (2005) DOI: 10.1073/pnas.0502873102

150. X. Zheng, D. M. Medvedev, J. Swanson and A. A. Stuchebrukhov: Computer simulation of water in cytochrome *c* oxidase. *Biochim Biophys Acta* 1557, 99-107 (2003) DOI: 10.1016/S0005-2728(03)00002-1

151. M. Tashiro and A. A. Stuchebrukhov: Thermodynamic properties of internal water molecules in the hydrophobic cavity around the catalytic center of cytochrome *c* oxidase. *J Phys Chem B* 109(2), 1015-1022 (2005) DOI: 10.1021/jp0462456

152. D. M. Popovic and A. A. Stuchebrukhov: Proton exit channels in bovine cytochrome *c* oxidase. *J Phys Chem B* 109(5), 1999-2006 (2005) DOI: 10.1021/jp0464371

153. K. Shimokata, Y. Katayama, H. Murayama, M. Suematsu, T. Tsukihara, K. Muramoto, H. Aoyama, S. Yoshikawa and H. Shimada: The proton pumping pathway of bovine heart cytochrome *c* oxidase. *Proc Natl Acad Sci U S A* 104, 4200-4205 (2007) DOI: 10.1073/pnas.0611627104

154. H. Y. Chang, J. Hemp, Y. Chen, J. A. Fee and R. B. Gennis: The cytochrome ba_3 oxygen reductase from *Thermus thermophilus* uses a single input channel for proton delivery to the active site and for proton pumping. *Proc Natl Acad Sci U S A* 106(38), 16169-16173 (2009) DOI: 10.1073/pnas.0905264106

155. L. Yang, A. A. Skjevik, W. G. Han Du, L. Noodleman, R. C. Walker and A. W. Gotz: Water exit pathways and proton pumping mechanism in B-type cytochrome c oxidase from molecular dynamics simulations. *Biochim Biophys Acta* 1857(9), 1594-1606 (2016)
DOI: 10.1016/j.bbabio.2016.06.005

156. S. Riistama, A. Puustinen, M. I. Verkhovsky, J. E. Morgan and M. Wikstrom: Binding of O_2 and its reduction are both retarded by replacement of valine 279 by isoleucine in cytochrome *c* oxidase from Paracoccus denitrificans. *Biochemistry* 39(21), 6365-6372 (2000)
DOI: 10.1021/bi000123w

157. L. Salomonsson, A. Lee, R. B. Gennis and P. Brzezinski: A single-amino-acid lid renders a gas-tight compartment within a membrane-bound transporter. *Proc Natl Acad Sci U S A* 101(32), 11617-11621 (2004)
DOI: 10.1073/pnas.0402242101

158. O. Einarsdottir, C. Funatogawa, T. Soulimane and I. Szundi: Kinetic studies of the reactions of O_2 and NO with reduced *Thermus thermophilus* ba_3 and bovine aa_3 using photolabile carriers. *Biochim Biophys Acta* 1817(4), 672-679 (2012)
DOI: 10.1016/j.bbabio.2011.12.005

159. B. Schmidt, J. McCracken and S. Ferguson-Miller: A discrete water exit pathway in the membrane protein cytochrome *c* oxidase. *Proc Natl Acad Sci U S A* 100(26), 15539-15542 (2003)
DOI: 10.1073/pnas.2633243100

160. R. Sugitani and A. A. Stuchebrukhov: Molecular dynamics simulation of water in cytochrome c oxidase reveals two water exit pathways and the mechanism of transport. *Biochim Biophys Acta* 1787, 1140-1150 (2009)
DOI: 10.1016/j.bbabio.2009.04.004

161. C. E. VanOrsdel, S. Bhatt, R. J. Allen, E. P. Brenner, J. J. Hobson, A. Jamil, B. M. Haynes, A. M. Genson and M. R. Hemm: The *Escherichia coli* CydX protein is a member of the CydAB cytochrome *bd* oxidase complex and is required for cytochrome *bd* oxidase activity. *J Bacteriol* 195(16), 3640–3650 (2013)
DOI: 10.1128/JB.00324-13

162. J. Hoeser, S. Hong, G. Gehmann, R. B. Gennis and T. Friedrich: Subunit CydX of *Escherichia coli* cytochrome *bd* ubiquinol oxidase is essential for assembly and stability of the di-heme active site. *FEBS Lett* 588(9), 1537–1541 (2014)
DOI: 10.1016/j.febslet.2014.03.036

163. R. J. Allen, E. P. Brenner, C. E. VanOrsdel, J. J. Hobson, D. J. Hearn and M. R. Hemm: Conservation analysis of the CydX protein yields insights into small protein identification and evolution. *BMC Genomics* 15(1), 946 (2014)
DOI: 10.1186/1471-2164-15-946

164. H. Chen, Q. Luo, J. Yin, T. Gao and H. Gao: Evidence for requirement of CydX in function but not assembly of the cytochrome *bd* oxidase in *Shewanella oneidensis*. *Biochim Biophys Acta* 1850(2), 318-328 (2015)
DOI: 10.1016/j.bbagen.2014.10.005

165. F. Spinner, M. R. Cheesman, A. J. Thomson, T. Kaysser, R. B. Gennis, Q. Peng and J. Peterson: The Haem b_{558} Component of the Cytochrome *bd* Quinol Oxidase Complex from *Escherichia coli* has Histidine-Methionine Axial LIgation. *Biochem J* 308, 641-644 (1995)
DOI: 10.1042/bj3080641

166. S. A. Siletsky, F. Rappaport, R. K. Poole and V. B. Borisov: Evidence for Fast Electron Transfer between the High-Spin Haems in Cytochrome bd-I from Escherichia coli. *PLoS One* 11(5), e0155186 (2016)
DOI: 10.1371/journal.pone.0155186

167. I. Belevich, V. B. Borisov, J. Zhang, K. Yang, A. A. Konstantinov, R. B. Gennis and M. I. Verkhovsky: Time-resolved electrometric and optical studies on cytochrome bd suggest a mechanism of electron-proton coupling in the di-heme active site. *Proc Natl Acad Sci U S A* 102(10), 3657-3662 (2005)
DOI: 10.1073/pnas.0405683102

168. V. B. Borisov, I. Belevich, D. A. Bloch, T. Mogi and M. I. Verkhovsky: Glutamate 107 in subunit I of cytochrome bd from Escherichia coli is part of a transmembrane intraprotein pathway conducting protons from the cytoplasm to the heme b595/heme d active site. *Biochemistry* 47(30), 7907-7914 (2008)
DOI: 10.1021/bi800435a

169. V. B. Borisov: Interaction of bd-type quinol oxidase from Escherichia coli and carbon monoxide: heme d binds CO with high

affinity. *Biochemistry (Mosc)* 73(1), 14-22 (2008)
DOI: 10.1134/S0006297908010021

170. J. J. Hill, J. O. Alben and R. B. Gennis: Spectroscopic Evidence for a Heme-heme Binuclear Center in the Cytochrome *bd* Ubiquinol Oxidase from *Escherichia coli*. *Proc Natl Acad Sci U S A* 90, 5863-5867 (1993)
DOI: 10.1073/pnas.90.12.5863

171. M. Tsubaki, H. Hori, T. Mogi and Y. Anraku: Cyanide-binding site of *bd*-type Ubiquinol Oxidase from *Escherichia coli*. *J Biol Chem* 270, 28565-28569 (1995)
DOI: 10.1074/jbc.270.48.28565

172. V. Borisov, R. Gennis and A. A. Konstantinov: Peroxide Complex of Cytochrome *bd*: Kinetics of Generation and Stability. *Biochem Mol Biol Int* 37(5), 975-982 (1995)

173. V. B. Borisov, R. B. Gennis and A. A. Konstantinov: Interaction of Escherichia coli cytochrome bd with hydrogen peroxide. *Biokhimiia (Biochemistry-Moscow)* 60(2), 315-327 (1995)

174. M. H. Vos, V. B. Borisov, U. Liebl, J. L. Martin and A. A. Konstantinov: Femtosecond resolution of ligand-heme interactions in the high-affinity quinol oxidase bd: A di-heme active site? *Proc Natl Acad Sci U S A* 97(4), 1554-1559 (2000)
DOI: 10.1073/pnas.030528197

175. V. B. Borisov, S. E. Sedelnikova, R. K. Poole and A. A. Konstantinov: Interaction of cytochrome bd with carbon monoxide at low and room temperatures: evidence that only a small fraction of heme b595 reacts with CO. *J Biol Chem* 276(25), 22095-22099 (2001)
DOI: 10.1074/jbc.M011542200

176. V. B. Borisov, U. Liebl, F. Rappaport, J.-L. Martin, J. Zhang, R. B. Gennis, A. A. Konstantinov and M. H. Vos: Interactions between heme *d* and heme b_{595} in quinol oxidase *bd* from *Escherichia coli*: a photoselection study using femtosecond spectroscopy. *Biochemistry* 41(5), 1654-1662 (2002)
DOI: 10.1021/bi0158019

177. A. M. Arutyunyan, V. B. Borisov, V. I. Novoderezhkin, J. Ghaim, J. Zhang, R. B. Gennis and A. A. Konstantinov: Strong excitonic interactions in the oxygen-reducing site of bd-type oxidase: the Fe-to-Fe distance between hemes d and b595 is 10 A. *Biochemistry* 47(6), 1752-1759 (2008)
DOI: 10.1021/bi701884g

178. F. Rappaport, J. Zhang, M. H. Vos, R. B. Gennis and V. B. Borisov: Heme-heme and heme-ligand interactions in the di-heme oxygen-reducing site of cytochrome bd from Escherichia coli revealed by nanosecond absorption spectroscopy. *Biochim Biophys Acta* 1797(9), 1657-1664 (2010)
DOI: 10.1016/j.bbabio.2010.05.010

179. V. B. Borisov and M. I. Verkhovsky: Accommodation of CO in the di-heme active site of cytochrome bd terminal oxidase from Escherichia coli. *J Inorg Biochem* 118, 65-67 (2013)
DOI: 10.1016/j.jinorgbio.2012.09.016

180. S. A. Siletsky, A. A. Zaspa, R. K. Poole and V. B. Borisov: Microsecond time-resolved absorption spectroscopy used to study CO compounds of cytochrome bd from Escherichia coli. *PLoS One* 9(4), e95617 (2014)
DOI: 10.1371/journal.pone.0095617

181. R. D'Mello, S. Hill and R. K. Poole: The Cytochrome *bd* Quinol Oxidase in *Escherichia coli* Has an Extremely High Oxygen Affinity and Two-Oxygen-binding Haems: Implicaitons for Regulation of Activity *in vivo* by Oxygen Inihibition. *Microbiology* 142, 755-763 (1996)
DOI: 10.1099/00221287-142-4-755

182. R. A. Rothery, A. M. Houston and W. J. Ingledew: The Respiratory Chain of Anaerobically Grown *Escherichia coli*: Reactions with Nitrite and Oxygen. *J Gen Microbiol* 133, 3247-3255 (1987)
DOI: 10.1099/00221287-133-11-3247

183. J. Zhang, W. Oettmeier, R. B. Gennis and P. Hellwig: FTIR spectroscopic evidence for the involvement of an acidic residue in quinone binding in cytochrome *bd* from Escherichia coli. *Biochemistry* 41, 4612-4617 (2002)
DOI: 10.1021/bi011784b

184. K. Yang, J. Zhang, A. S. Vakkasoglu, R. Hielscher, J. P. Osborne, J. Hemp, H. Miyoshi, P. Hellwig and R. B. Gennis:

Glutamate 107 in subunit I of the cytochrome bd quinol oxidase from Escherichia coli is protonated and near the heme d/heme b595 binuclear center. *Biochemistry* 46(11), 3270-3278 (2007)
DOI: 10.1021/bi061946+

185. D. Pils and G. Schmetterer: Characterization of three bioenergetically active respiratory terminal oxidases in the cyanobacterium *Synechocystis* sp. strain PCC 6803. *FEMS Microbiol Lett* 203(2), 217-222 (2001)
DOI: 10.1111/j.1574-6968.2001.tb10844.x

186. S. Berry, D. Schneider, W. F. Vermaas and M. Rogner: Electron transport routes in whole cells of *Synechocystis* sp. strain PCC 6803: the role of the cytochrome *bd*-type oxidase. *Biochemistry* 41(10), 3422-3429 (2002)
DOI: 10.1021/bi011683d

187. S. Berry, Y. V. Bolychevtseva, M. Rogner and N. V. Karapetyan: Photosynthetic and respiratory electron transport in the alkaliphilic cyanobacterium *Arthrospira* (*Spirulina*) *platensis*. *Photosynth Res* 78(1), 67-76 (2003)
DOI: 10.1023/A:1026012719612

188. G. I. Kufryk and W. F. Vermaas: Sll1717 affects the redox state of the plastoquinone pool by modulating quinol oxidase activity in thylakoids. *J Bacteriol* 188(4), 1286-1294 (2006)
DOI: 10.1128/JB.188.4.1286-1294.2006

189. F. Gutthann, M. Egert, A. Marques and J. Appel: Inhibition of respiration and nitrate assimilation enhances photohydrogen evolution under low oxygen concentrations in *Synechocystis* sp. PCC 6803. *Biochim Biophys Acta* 1767(2), 161-169 (2007)
DOI: 10.1016/j.bbabio.2006.12.003

190. M. Schultze, B. Forberich, S. Rexroth, N. G. Dyczmons, M. Roegner and J. Appel: Localization of cytochrome b_6f complexes implies an incomplete respiratory chain in cytoplasmic membranes of the cyanobacterium *Synechocystis* sp. PCC 6803. *Biochim Biophys Acta* 1787(12), 1479-1485 (2009)
DOI: 10.1016/j.bbabio.2009.06.010

191. G. A. Peschek, M. Wastyn, S. Fromwald and B. Mayer: Occurrence of heme O in photoheterotrophically growing, semi-anaerobic cyanobacterium *Synechocystis* sp. PCC6803. *FEBS Lett* 371(2), 89-93 (1995)
DOI: 10.1016/0014-5793(95)00821-P

192. S. Fromwald, R. Zoder, M. Wastyn, M. Lubben and G. A. Peschek: Extended heme promiscuity in the cyanobacterial cytochrome *c* oxidase: characterization of native complexes containing hemes A, O, and D, respectively. *Arch Biochem Biophys* 367(1), 122-128 (1999)
DOI: 10.1006/abbi.1999.1236

193. G. A. Peschek, C. Obinger and M. Paumann: The respiratory chain of blue-green algae (cyanobacteria). *Physiol Plant*, 120(3), 358-369 (2004)
DOI: 10.1111/j.1399-3054.2004.00274.x

194. I. Belevich, V. B. Borisov and M. I. Verkhovsky: Discovery of the true peroxy intermediate in the catalytic cycle of terminal oxidases by real-time measurement. *J Biol Chem* 282(39), 28514-28519 (2007)
DOI: 10.1074/jbc.M705562200

195. M. J. Miller and R. B. Gennis: The Purification and Characterization of the Cytochrome *d* Terminal Oxidase Complex of the *Escherichia coli* Aerobic Respiratory Chain. *J Biol Chem* 258(15), 9159-9165 (1983)

196. K. Kita, K. Konishi and Y. Anraku: Terminal Oxidases of *Escherichia coli* Aerobic Respiratory Chain II. Purification and Properties of Cytochrome $b_{558\text{-}d}$ Complex from Cells Grown with Limited Oxygen and Evidence of Branched Electron-Carrying Systems. *J Biol Chem* 259(5), 3375-3381 (1984)

197. A. Jasaitis, V. B. Borisov, N. P. Belevich, J. E. Morgan, A. A. Konstantinov and M. I. Verkhovsky: Electrogenic reactions of cytochrome bd. *Biochemistry* 39(45), 13800-13809 (2000)
DOI: 10.1021/bi001165n

198. T. Mogi, S. Endou, S. Akimoto, M. Morimoto-Tadokoro and H. Miyoshi: Glutamates 99 and 107 in transmembrane helix III of subunit I of cytochrome *bd* are critical for binding of the heme b_{595}-*d* binuclear center and enzyme activity. *Biochemistry* 45(51), 15785-15792 (2006)
DOI: 10.1021/bi0615792

199. Y. Matsumoto, E. Muneyuki, D. Fujita, K. Sakamoto, H. Miyoshi, M. Yoshida and T. Mogi: Kinetic mechanism of quinol oxidation

by cytochrome *bd* studied with ubiquinone-2 analogs. *J Biochem (Tokyo)* 139(4), 779-788 (2006)
DOI: 10.1093/jb/mvj087

200. S. F. Hastings and W. J. Ingledew: A study of the stabilization of semiquinones by the *Escherichia coli* quinol oxidase cytochrome *bd*. *Biochem Soc Trans* 24(1), 131-132 (1996)
DOI: 10.1042/bst0240131

201. S. F. Hastings, T. M. Kaysser, F. Jiang, J. C. Salerno, R. B. Gennis and W. J. Ingledew: Identification of a stable semiquinone intermediate in the purified and membrane bound ubiquinol oxidase-cytochrome *bd* from *Escherichia coli*. *Eur J Biochem* 255(1), 317-323 (1998)
DOI: 10.1046/j.1432-1327.1998.2550317.x

202. K. Kusumoto, M. Sakiyama, J. Sakamoto, S. Noguchi and N. Sone: Menaquinol oxidase activity and primary structure of cytochrome *bd* from the amino-acid fermenting bacterium *Corynebacterium glutamicum*. *Arch Microbiol* 173(5-6), 390-397 (2000)
DOI: 10.1007/s002030000161

203. V. B. Borisov, R. Murali, M. L. Verkhovskaya, D. A. Bloch, H. Han, R. B. Gennis and M. I. Verkhovsky: Aerobic respiratory chain of Escherichia coli is not allowed to work in fully uncoupled mode. *Proc Natl Acad Sci U S A* 108(42), 17320-17324 (2011)
DOI: 10.1073/pnas.1108217108

204. B. C. Hill, J. J. Hill and R. B. Gennis: The Room Temperature Reaction of Carbon Monoxide and Oxygen with the Cytochrome *bd* Quinol Oxidase from *Escherichia coli*. *Biochemistry* 33, 15110-15115 (1994)
DOI: 10.1021/bi00254a021

205. M. I. Verkhovsky, I. Belevich, D. A. Bloch and M. Wikstrom: Elementary steps of proton translocation in the catalytic cycle of cytochrome oxidase. *Biochim Biophys Acta* 1757(5-6), 401–407 (2006)
DOI: 10.1016/j.bbabio.2006.05.026

206. R. J. Pace, R. Stranger and S. Petrie: Why nature chose Mn for the water oxidase in Photosystem II. *Dalton Trans* 41(24), 7179-7189 (2012)
DOI: 10.1039/c2dt30185g

207. M. R. Gunner, M. Amin, X. Zhu and J. Lu: Molecular mechanisms for generating transmembrane proton gradients. *Biochim Biophys Acta* 1827(8-9), 892-913 (2013)
DOI: 10.1016/j.bbabio.2013.03.001

208. V. R. Kaila, M. I. Verkhovsky and M. Wikstrom: Proton-coupled electron transfer in cytochrome oxidase. *Chem Rev* 110(12), 7062-7081 (2010)
DOI: 10.1021/cr1002003

209. G. Renger: Mechanism of light induced water splitting in Photosystem II of oxygen evolving photosynthetic organisms. *Biochim Biophys Acta* 1817(8), 1164-1176 (2012)
DOI: 10.1016/j.bbabio.2012.02.005

210. G. Renger: Light induced oxidative water splitting in photosynthesis: energetics, kinetics and mechanism. *J Photochem Photobiol B* 104(1-2), 35-43 (2011)
DOI: 10.1016/j.jphotobiol.2011.01.023

211. T. Tsukihara, H. Aoyama, E. Yamashita, T. Tomizaki, H. Yamaguchi, K. Shinzawa-Itoh, R. Nakashima, R. Yaono and S. Yoshikawa: The whole structure of the 13-subunit oxidized cytochrome *c* oxidase at 2.8. A. *Science* 272, 1136-1144 (1996)
DOI: 10.1126/science.272.5265.1136

212. B. A. Barry and O. Einarsdottir: Insights into the structure and function of redox-active tyrosines from model compounds. *J Phys Chem B* 109(15), 6972-6981 (2005)
DOI: 10.1021/jp044749y

213. E. A. Gorbikova, I. Belevich, M. Wikstrom and M. I. Verkhovsky: The proton donor for O-O bond scission by cytochrome *c* oxidase. *Proc Natl Acad Sci U S A* 105(31), 10733-10737 (2008)
DOI: 10.1073/pnas.0802512105

214. V. Sharma and M. Wikstrom: The role of the K-channel and the active-site tyrosine in the catalytic mechanism of cytochrome c oxidase. *Biochim Biophys Acta* 1857(8), 1111-1115 (2016)
DOI: 10.1016/j.bbabio.2016.02.008

215. M. R. Blomberg: Mechanism of Oxygen Reduction in Cytochrome c Oxidase and the Role of the Active Site Tyrosine. *Biochemistry* 55(3), 489-500 (2016)
DOI: 10.1021/acs.biochem.5b01205

216. G. Christen and G. Renger: The role of hydrogen bonds for the multiphasic P680(+)* reduction by YZ in photosystem

II with intact oxyen evolution capacity. Analysis of kinetic H/D isotope exchange effects. *Biochemistry* 38(7), 2068-2077 (1999)
DOI: 10.1021/bi982188t

217. J. P. McEvoy and G. W. Brudvig: Water-splitting chemistry of photosystem II. *Chem Rev* 106(11), 4455-4483 (2006)
DOI: 10.1021/cr0204294

218. E. M. Sproviero, J. P. McEvoy, J. A. Gascon, G. W. Brudvig and V. S. Batista: Computational insights into the O2-evolving complex of photosystem II. *Photosynth Res* 97(1), 91-114 (2008)
DOI: 10.1007/s11120-008-9307-0

219. P. E. Siegbahn: Water oxidation mechanism in photosystem II, including oxidations, proton release pathways, O-O bond formation and O2 release. *Biochim Biophys Acta* 1827(8-9), 1003-1019 (2013)
DOI: 10.1016/j.bbabio.2012.10.006

220. R. D. Britt, D. L. Suess and T. A. Stich: An Mn(V)-oxo role in splitting water? *Proc Natl Acad Sci U S A* 112(17), 5265-5266 (2015)
DOI: 10.1073/pnas.1505223112

221. Q. H. Gibson and C. Greenwood: Reactions of cytochrome oxidase with oxygen and carbon monoxide. *Biochem J* 86, 541-554 (1963)
DOI: 10.1042/bj0860541

222. M. I. Verkhovsky, J. E. Morgan and M. Wikstrom: Oxygen binding and activation: early steps in the reaction of oxygen with cytochrome *c* oxidase. *Biochemistry* 33, 3079-3086 (1994)
DOI: 10.1021/bi00176a042

223. M. I. Verkhovsky, J. E. Morgan, M. Verkhovskaya and M. Wikstrom: Translocation of electrical charge during a single turnover of cytochrome *c* oxidase. *Biochim Biophys Acta* 1318(1-2), 6-10 (1997)
DOI: 10.1016/S0005-2728(96)00147-8

224. A. Jasaitis, M. I. Verkhovsky, J. E. Morgan, M. L. Verkhovskaya and M. Wikstrom: Assignment and charge translocation stoichiometries of the electrogenic phases in the reaction of cytochrome *c* with dioxygen. *Biochemistry* 38, 2697-2706 (1999)
DOI: 10.1021/bi982275l

225. C. Ribacka, M. I. Verkhovsky, I. Belevich, D. A. Bloch, A. Puustinen and M. Wikstrom: An elementary reaction step of the proton pump is revealed by mutation of tryptophan-164 to phenylalanine in cytochrome *c* oxidase from *Paracoccus denitrificans*. *Biochemistry* 44, 16502-16512 (2005)
DOI: 10.1021/bi0511336

226. H. Lepp and P. Brzezinski: Internal charge transfer in cytochrome c oxidase at a limited proton supply: Proton pumping ceases at high pH. *Biochim Biophys Acta* 1790, 552-557 (2009)
DOI: 10.1016/j.bbagen.2009.03.023

227. C. von Ballmoos, N. Gonska, P. Lachmann, R. B. Gennis, P. Adelroth and P. Brzezinski: Mutation of a single residue in the ba3 oxidase specifically impairs protonation of the pump site. *Proc Natl Acad Sci U S A* 112(11), 3397-3402 (2015)
DOI: 10.1073/pnas.1422434112

228. J. R. Winkler, D. G. Nocera, K. M. Yocom, E. Bordignon and H. B. Gray: Electron-transfer kinetics of pentaammineruthenium(III) (histidine-33)-ferricytochrome *c*. Measurement of the rate of intramolecular electron transfer between redox centers separated by 15 A in a protein. *J Am Chem Soc* 104, 5798-5800 (1982)
DOI: 10.1021/ja00385a047

229. T. Nilsson: Photoinduced electron transfer from tris(2,2'-bipyridyl)ruthenium to cytochrome *c* oxidase. *Proc Natl Acad Sci U S A* 89, 6497-6501 (1992)
DOI: 10.1073/pnas.89.14.6497

230. L. Geren, B. Durham and F. Millett: Use of ruthenium photoreduction techniques to study electron transfer in cytochrome oxidase. *Methods Enzymol* 456, 507-520 (2009)
DOI: 10.1016/S0076-6879(08)04428-5

231. K. Kobayashi, H. Une and K. Hayashi: Electron transfer process in cytochrome oxidase after pulse radiolysis. *J Biol Chem* 246(14), 7976-7980 (1989)

232. O. Farver, Y. Chen, J. A. Fee and I. Pecht: Electron transfer among the Cu_A-, heme *b*- and a_3-centers of *Thermus thermophilus* cytochrome ba_3. *FEBS Lett* 580, 3417–3421 (2006)
DOI: 10.1016/j.febslet.2006.05.013

233. S. A. Siletsky, A. D. Kaulen and A. A. Konstantinov: Electrogenic events associated with peroxy- to ferryl-oxo state transition in cytochrome *c* oxidase. *Eur J Biophys* 26(1), 98 (1997)

234. S. Siletsky, A. D. Kaulen and A. A. Konstantinov: Resolution of electrogenic steps coupled to conversion of cytochrome *c* oxidase from the peroxy to the ferryl-oxo state. *Biochemistry* 38(15), 4853-4861 (1999)
DOI: 10.1021/bi982614a

235. M. I. Verkhovsky, A. Tuukkanen, C. Backgren, A. Puustinen and M. Wikstrom: Charge translocation coupled to electron injection into oxidized cytochrome *c* oxidase from *Paracoccus denitrificans*. *Biochemistry* 40, 7077-7083 (2001)
DOI: 10.1021/bi010030u

236. S. A. Siletsky, J. Zhu, R. B. Gennis and A. A. Konstantinov: Partial steps of charge translocation in the nonpumping N139L mutant of *Rhodobacter sphaeroides* cytochrome *c* oxidase with a blocked D-channel. *Biochemistry* 49(14), 3060-3073 (2010)
DOI: 10.1021/bi901719e

237. M. Ruitenberg, A. Kannt, E. Bamberg, B. Ludwig, H. Michel and K. Fendler: Single-electron reduction of the oxidized state is coupled to proton uptake via the K pathway in *Paracoccus denitrificans* cytochrome *c* oxidase. *Proc Natl Acad Sci U S A* 97, 4632-4636 (2000)
DOI: 10.1073/pnas.080079097

238. M. Haumann, P. Liebisch, C. Muller, M. Barra, M. Grabolle and H. Dau: Photosynthetic O2 formation tracked by time-resolved x-ray experiments. *Science* 310(5750), 1019-1021 (2005)
DOI: 10.1126/science.1117551

239. M. Haumann, A. Mulkidjanian and W. Junge: Electrogenicity of electron and proton transfer at the oxidizing side of photosystem II. *Biochemistry* 36(31), 9304-9315 (1997)
DOI: 10.1021/bi963114p

240. M. D. Mamedov, O. E. Beshta, K. N. Gurovskaya, A. A. Mamedova, K. D. Neverov, V. D. Samuilov and A. Y. Semenov: Photoelectric responses of oxygen-evolving complexes of photosystem II. *Biochemistry (Mosc)* 64(5), 504-509 (1999)

241. H. Suzuki, M. Sugiura and T. Noguchi: pH dependence of the flash-induced S-state transitions in the oxygen-evolving center of photosystem II from Thermosynechoccocus elongatus as revealed by Fourier transform infrared spectroscopy. *Biochemistry* 44(5), 1708-1718 (2005)
DOI: 10.1021/bi0483312

242. D. J. Vinyard, S. Khan and G. W. Brudvig: Photosynthetic water oxidation: binding and activation of substrate waters for O-O bond formation. *Faraday Discuss* 185, 37-50 (2015)
DOI: 10.1039/C5FD00087D

243. D. A. Pantazis, W. Ames, N. Cox, W. Lubitz and F. Neese: Two interconvertible structures that explain the spectroscopic properties of the oxygen-evolving complex of photosystem II in the S2 state. *Angew Chem Int Ed Engl* 51(39), 9935-9940 (2012)
DOI: 10.1002/anie.201204705

244. N. Cox, M. Retegan, F. Neese, D. A. Pantazis, A. Boussac and W. Lubitz: Photosynthesis. Electronic structure of the oxygen-evolving complex in photosystem II prior to O-O bond formation. *Science* 345(6198), 804-808 (2014)
DOI: 10.1126/science.1254910

245. M. D. Mamedov, V. N. Kurashov, D. A. Cherepanov and A. Y. Semenov: Photosysem II: where does the light-induced voltage come from? *Front Biosci (Landmark Ed)* 15, 1007-1017 (2010)
DOI: 10.2741/3658

246. J. Clausen and W. Junge: Detection of an intermediate of photosynthetic water oxidation. *Nature* 430(6998), 480-483 (2004)
DOI: 10.1038/nature02676

247. A. Klauss, M. Haumann and H. Dau: Seven steps of alternating electron and proton transfer in photosystem II water oxidation traced by time-resolved photothermal beam deflection at improved sensitivity. *J Phys Chem B* 119(6), 2677-2689 (2015)
DOI: 10.1021/jp509069p

248. D. L. Zaslavsky, I. A. Smirnova, S. A. Siletsky, A. D. Kaulen, F. Millett and A. A. Konstantinov: Rapid kinetics of membrane potential generation by cytochrome *c* oxidase with the photoactive Ru(II)-tris-

bipyridyl derivative of cytochrome *c* as electron donor. *FEBS Lett* 359, 27-30 (1995) DOI: 10.1016/0014-5793(94)01443-5

249. S. A. Siletsky: Steps of the coupled charge translocation in the catalytic cycle of cytochrome c oxidase. *Front Biosci (Landmark Ed)* 18, 36-57 (2013) DOI: 10.2741/4086

250. S. A. Siletsky, M. D. Mamedov, E. P. Lukashev, S. P. Balashov, D. A. Dolgikh, A. B. Rubin, M. P. Kirpichnikov and L. E. Petrovskaya: Electrogenic steps of light-driven proton transport in ESR, a retinal protein from Exiguobacterium sibiricum. *Biochim Biophys Acta* 1857(11), 1741-1750 (2016) DOI: 10.1016/j.bbabio.2016.08.004

251. B. Chance, C. Saronio and J. S. Leigh, Jr.: Functional intermediates in the reaction of membrane-bound cytochrome oxidase with oxygen. *J Biol Chem* 250(24), 9226-9237 (1975)

252. B. C. Hill and C. Greenwood: Spectroscopic evidence for the participation of compound A (Fea_3^{2+}-O_2) in the reaction of mixed-valence cytochrome *c* oxidase with oxygen at room temperature. *Biochem J* 215(3), 659-67 (1983) DOI: 10.1042/bj2150659

253. S. Han, Y.-C. Ching and D. L. Rousseau: Primary intermediate in the reaction of oxygen with fully reduced cytochrome *c* oxidase. *Proc Natl Acad Sci U S A* 87, 2491-2495 (1990) DOI: 10.1073/pnas.87.7.2491

254. C. Varotsis, W. H. Woodruff and G. T. Babcock: Direct detection of a dioxygen adduct of cytochrome a_3 in the mixed valence cytochome oxidase/dioxygen reaction. *J Biol Chem* 265(19), 11131-11136 (1990)

255. K. Muramoto, K. Ohta, K. Shinzawa-Itoh, K. Kanda, M. Taniguchi, H. Nabekura, E. Yamashita, T. Tsukihara and S. Yoshikawa: Bovine cytochrome *c* oxidase structures enable O_2 reduction with minimization of reactive oxygens and provide a proton-pumping gate. *Proc Natl Acad Sci U S A* 107(17), 7740-7745 (2010) DOI: 10.1073/pnas.0910410107

256. M. R. Blomberg and P. E. Siegbahn: Quantum chemistry as a tool in bioenergetics. *Biochim Biophys Acta* 1797(2), 129-142 (2010) DOI: 10.1016/j.bbabio.2009.10.004

257. M. Karpefors, P. Adelroth, A. Namslauer, Y. Zhen and P. Brzezinski: Formation of the “peroxy” intermediate in cytochrome *c* oxidase is associated with internal proton/hydrogen transfer. *Biochemistry* 39, 14664-14669 (2000) DOI: 10.1021/bi0013748

258. A. Jasaitis, C. Backgren, J. E. Morgan, A. Puustinen, M. I. Verkhovsky and M. Wikstrom: Electron and proton transfer in the arginine-54-methionine mutant of cytochrome *c* oxidase from *Paracoccus denitrificans*. *Biochemistry* 40, 5269-5274 (2001) DOI: 10.1021/bi002948b

259. E. A. Gorbikova, M. Wikstrom and M. I. Verkhovsky: The protonation state of the cross-linked tyrosine during the catalytic cycle of cytochrome *c* oxidase. *J Biol Chem* 283, 34907-34912 (2008) DOI: 10.1074/jbc.M803511200

260. S. A. Siletsky, I. Belevich, A. Jasaitis, A. A. Konstantinov, M. Wikstrom, T. Soulimane and M. I. Verkhovsky: Time-resolved single-turnover of ba_3 oxidase from *Thermus thermophilus*. *Biochim Biophys Acta* 1767(12), 1383-1392 (2007) DOI: 10.1016/j.bbabio.2007.09.010

261. V. Sharma, K. D. Karlin and M. Wikstrom: Computational study of the activated O(H) state in the catalytic mechanism of cytochrome c oxidase. *Proc Natl Acad Sci U S A* 110(42), 16844-16849 (2013) DOI: 10.1073/pnas.1220379110

262. I. Belevich, M. I. Verkhovsky and M. Wikstrom: Proton-coupled electron transfer drives the proton pump of cytochrome *c* oxidase. *Nature* 440(7085), 829-832 (2006) DOI: 10.1038/nature04619

263. I. Belevich, E. Gorbikova, N. P. Belevich, V. Rauhamaki, M. Wikstrom and M. I. Verkhovsky: Initiation of the proton pump of cytochrome c oxidase. *Proc Natl Acad Sci U S A* 107(43), 18469-18474 (2010) DOI: 10.1073/pnas.1010974107

264. K. Faxen, G. Gilderson, P. Adelroth and P. Brzezinski: A mechanistic principle for proton pumping by cytochrome *c* oxidase. *Nature* 437, 286-289 (2005) DOI: 10.1038/nature03921

265. G. Branden, R. B. Gennis and P. Brzezinski: Transmembrane proton translocation by cytochrome *c* oxidase. *Biochim Biophys Acta* 1757, 1052–1063 (2006)
DOI: 10.1016/j.bbabio.2006.05.020

266. I. Smirnova, P. Adelroth, R. B. Gennis and P. Brzezinski: Aspartate-132 in cytochrome *c* oxidase from *Rhodobacter sphaeroides* is involved in a two-step proton transfer during oxo-ferryl formation. *Biochemistry* 38, 6826-6833 (1999)
DOI: 10.1021/bi982865j

267. A. Namslauer, A. Pawate, R. Gennis and P. Brzezinski: Redox-coupled proton translocation in biological systems: Proton shuttling in cytochrome *c* oxidase. *Proc Natl Acad Sci U S A* 100(26), 15543-15547 (2003)
DOI: 10.1073/pnas.2432106100

268. E. A. Gorbikova, N. P. Belevich, M. Wikstrom and M. I. Verkhovsky: Time-resolved ATR-FTIR spectroscopy of the oxygen reaction in the D124N mutant of cytochrome *c* oxidase from *Paracoccus denitrificans*. *Biochemistry* 46(45), 13141-13148 (2007)
DOI: 10.1021/bi701614w

269. S. A. Siletsky, I. Belevich, M. Wikstrom, T. Soulimane and M. I. Verkhovsky: Time-resolved O_H->E_H transition of the aberrant ba_3 oxidase from *Thermus thermophilus*. *Biochim Biophys Acta* 1787(3), 201-205 (2009)
DOI: 10.1016/j.bbabio.2008.12.020

270. L. Weng and G. M. Baker: Reaction of hydrogen peroxide with the rapid form of resting cytochrome oxidase. *Biochemistry* 30, 5727-5733 (1991)
DOI: 10.1021/bi00237a014

271. D. Zaslavsky, A. Kaulen, I. A. Smirnova, T. V. Vygodina and A. A. Konstantinov: Flash-induced membrane potential generation by cytochrome *c* oxidase. *FEBS Lett* 336(3), 389-393 (1993)
DOI: 10.1016/0014-5793(93)80843-J

272. K. Kirchberg, H. Michel and U. Alexiev: Net proton uptake is preceded by multiple proton transfer steps upon electron injection into cytochrome c oxidase. *J Biol Chem* 287(11), 8187-8193 (2012)
DOI: 10.1074/jbc.M111.338491

273. M. D. Mamedov, A. A. Tyunyatkina, S. A. Siletsky and A. Y. Semenov: Voltage changes involving photosystem II quinone-iron complex turnover. *Eur Biophys J* 35(8), 647-654 (2006)
DOI: 10.1007/s00249-006-0069-3

274. D. M. Medvedev, E. S. Medvedev, A. I. Kotelnikov and A. A. Stuchebrukhov: Analysis of the kinetics of the membrane potential generated by cytochrome *c* oxidase upon single electron injection. *Biochim Biophys Acta* 1710(1), 47-56 (2005)
DOI: 10.1016/j.bbabio.2005.08.008

275. R. Sugitani, E. S. Medvedev and A. A. Stuchebrukhov: Theoretical and computational analysis of the membrane potential generated by cytochrome *c* oxidase upon single electron injection into the enzyme. *Biochim Biophys Acta* 1777(9), 1129-1139 (2008)
DOI: 10.1016/j.bbabio.2008.05.006

276. T. Tsukihara, H. Aoyama, E. Yamashita, T. Tomizaki, H. Yamaguchi, K. Shinzawa-Itoh, T. Nakashima, R. Yaono and S. Yoshikawa: Structures of metal sites of oxidized bovine heart cytochrome *c* oxidase at 2.8. A. *Science* 269, 1069-1074 (1995)
DOI: 10.1126/science.7652554

277. S. S. Kuznetsova, N. V. Azarkina, T. V. Vygodina, S. A. Siletsky and A. A. Konstantinov: Zink ions as cytochrome c oxidase inhibitors: two sites of action. *Biochemistry (Moscow)* 70, 128-136 (2005)
DOI: 10.1007/s10541-005-0091-6

278. M. A. Sharpe and S. Ferguson-Miller: A chemically explicit model for the mechanism of proton pumping in heme-copper oxidases. *J Bioenerg Biomembr* 40(5), 541-549 (2008)
DOI: 10.1007/s10863-008-9182-6

279. P. Adelroth, R. B. Gennis and P. Brzezinski: Role of the pathway through K(I-362) in proton transfer in cytochrome *c* oxidase from *R. sphaeroides*. *Biochemistry* 37, 2470-2476 (1998)
DOI: 10.1021/bi971813b

280. M. K. F. Wikstrom, A. Jasaitis, C. Backgren, A. Puustinen and M. I. Verkhovsky: The role of the D- and K-pathways of proton transfer in the function of the haem-copper oxidases. *Biochim Biophys Acta* 1459, 514-520 (2000)
DOI: 10.1016/S0005-2728(00)00191-2

281. D. Bloch, I. Belevich, A. Jasaitis, C. Ribacka, A. Puustinen, M. I. Verkhovsky and M. Wikstrom: The catalytic cycle of cytochrome

c oxidase is not the sum of its two halves. *Proc Natl Acad Sci USA* 101, 529-533 (2004) DOI: 10.1073/pnas.0306036101

282. H. Lepp, E. Svahn, K. Faxen and P. Brzezinski: Charge transfer in the K proton pathway linked to electron transfer to the catalytic site in cytochrome *c* oxidase. *Biochemistry* 47, 4929-4935 (2008) DOI: 10.1021/bi7024707

283. R. C. Sadoski, D. Zaslavsky, R. B. Gennis, B. Durham and F. Millett: Exposure of bovine cytochrome *c* oxidase to high triton X-100 or to alkaline conditions causes a dramatic change in the rate of reduction of compound F. *J Biol Chem* 276, 33616-33620 (2001) DOI: 10.1074/jbc.M103640200

284. S. A. Siletsky, I. Belevich, N. P. Belevich, T. Soulimane and M. I. Verkhovsky: Time-resolved single-turnover of caa_3 oxidase from *Thermus thermophilus*. Fifth electron of the fully reduced enzyme converts O_H into E_H state. *Biochim Biophys Acta* 1807(9), 1162-1169 (2011) DOI: 10.1016/j.bbabio.2011.05.006

285. M. Wikstrom: Active site intermediates in the reduction of O(2) by cytochrome oxidase, and their derivatives. *Biochim Biophys Acta* 1817(4), 468-475 (2012) DOI: 10.1016/j.bbabio.2011.10.010

286. M. R. Blomberg and P. E. Siegbahn: How cytochrome c oxidase can pump four protons per oxygen molecule at high electrochemical gradient. *Biochim Biophys Acta* 1847(3), 364-376 (2015) DOI: 10.1016/j.bbabio.2014.12.005

287. M. I. Verkhovsky, A. Jasaitis, M. L. Verkhovskaya, L. Morgan and M. Wikstrom: Proton translocation by cytochrome *c* oxidase. *Nature* 400, 480-483 (1999) DOI: 10.1038/22813

288. A. L. Woelke, G. Galstyan and E. W. Knapp: Lysine 362 in cytochrome c oxidase regulates opening of the K-channel via changes in pKA and conformation. *Biochim Biophys Acta* 1837(12), 1998-2003 (2014) DOI: 10.1016/j.bbabio.2014.08.003

289. V. B. Borisov and M. I. Verkhovsky: Oxygen as Acceptor. *EcoSal Plus* 3(2) (2009) DOI: 10.1128/ecosalplus.3.2.7

290. A. Paulus, S. G. Rossius, M. Dijk and S. de Vries: Oxoferryl-porphyrin radical catalytic intermediate in cytochrome *bd* oxidases protects cells from formation of reactive oxygen species. *J Biol Chem* 287(12), 8830-8838 (2012) DOI: 10.1074/jbc.M111.333542

291. N. Azarkina, V. Borisov and A. A. Konstantinov: Spontaneous spectral changes of the reduced cytochrome *bd*. *FEBS Lett* 416(2), 171-174 (1997) DOI: 10.1016/S0014-5793(97)01196-4

292. K. Yang, V. B. Borisov, A. A. Konstantinov and R. B. Gennis: The fully oxidized form of the cytochrome bd quinol oxidase from E. coli does not participate in the catalytic cycle: direct evidence from rapid kinetics studies. *FEBS Lett* 582(25-26), 3705-3709 (2008) DOI: 10.1016/j.febslet.2008.09.038

293. J. G. Koland, M. J. Miller and R. B. Gennis: Reconstitution of the Membrane-Bound, Ubiquinone-Dependent Pyruvate Oxidase Respiratory Chain of *Escherichia coli* with the Cytochrome *d* Terminal Oxidase. *Biochemistry* 23(3), 445-453 (1984) DOI: 10.1021/bi00298a008

294. M. J. Miller and R. B. Gennis: The Cytochrome *d* Complex is a Coupling site in the Aerobic Respiratory Chain of *Escherichia coli*. *J Biol Chem* 260, 14003-14008 (1985)

295. M. J. Miller, M. Hermodson and R. B. Gennis: The Active Form of the Cytochrome *d* Terminal Oxidase Complex of *Escherichia coli* is a Heterodimer Containing One Copy of Each of the Two Subunits. *J Biol Chem* 263, 5235-5240 (1988)

296. A. Puustinen, M. Finel, T. Haltia, R. B. Gennis and M. Wikstrцm: Properties of the Two Terminal Oxidases of *Escherichia coli*. *Biochemistry* 30, 3936-3942 (1991) DOI: 10.1021/bi00230a019

297. Y. V. Bertsova, A. V. Bogachev and V. P. Skulachev: Generation of protonic potential by the *bd*-type quinol oxidase of *Azotobacter vinelandii*. *FEBS Lett* 414, 369-372 (1997) DOI: 10.1016/S0014-5793(97)01047-8

298. J. F. Kolonay, Jr and R. J. Maier: Formation of pH and potential gradients by the reconstituted *Azotobacter vinelandii*

cytochrome *bd* respiratory protection oxidase. *J Bacteriol* 179(11), 3813-3817 (1997)
DOI: 10.1128/jb.179.11.3813-3817.1997

299. A. Jasaitis, F. Rappaport, E. Pilet, U. Liebl and M. H. Vos: Activationless electron transfer through the hydrophobic core of cytochrome c oxidase. *Proc Natl Acad Sci U S A* 102, 10882-10886 (2005)
DOI: 10.1073/pnas.0503001102

300. P. R. Rich and A. Marechal: Functions of the hydrophilic channels in protonmotive cytochrome c oxidase. *J R Soc Interface* 10(86), 20130183 (2013)
DOI: 10.1098/rsif.2013.0183

301. P. Brzezinski and G. Larsson: Redox-driven proton pumping by heme-copper oxidases. *Biochim Biophys Acta* 1605, 1-13 (2003)
DOI: 10.1016/S0005-2728(03)00079-3

302. D. M. Popovic and A. A. Stuchebryukhov: Proton pumping mechanism and catalytic cycle of cytochrome *c* oxidase: Coulomb pump model with kinetic gating. *FEBS Lett* 566, 126-130 (2004)
DOI: 10.1016/j.febslet.2004.04.016

303. M. Wikstrom and M. I. Verkhovsky: Mechanism and energetics of proton translocation by the respiratory heme-copper oxidases. *Biochim Biophys Acta* 1767, 1200-1214 (2007)
DOI: 10.1016/j.bbabio.2007.06.008

304. V. R. Kaila, V. Sharma and M. Wikstrom: The identity of the transient proton loading site of the proton-pumping mechanism of cytochrome c oxidase. *Biochim Biophys Acta* 1807(1), 80-84 (2011)
DOI: 10.1016/j.bbabio.2010.08.014

305. P. Siegbahn and M. R. A. Blomberg: Important roles of tyrosines in Photosystem II and cytochrome oxidase. *Biochim Biophys Acta* 1655(1), 45-50 (2004)
DOI: 10.1016/j.bbabio.2003.07.003

306. N. Capitanio, L. L. Palese, G. Capitanio, P. L. Martino, O. M. Richter, B. Ludwig and S. Papa: Allosteric interactions and proton conducting pathways in proton pumping aa(3) oxidases: heme a as a key coupling element. *Biochim Biophys Acta* 1817(4), 558-566 (2012)
DOI: 10.1016/j.bbabio.2011.11.003

307. J. Lu and M. R. Gunner: Characterizing the proton loading site in cytochrome c oxidase. *Proc Natl Acad Sci U S A* 111(34), 12414-12419 (2014)
DOI: 10.1073/pnas.1407187111

308. R. Liang, J. M. Swanson, Y. Peng, M. Wikstrom and G. A. Voth: Multiscale simulations reveal key features of the proton-pumping mechanism in cytochrome c oxidase. *Proc Natl Acad Sci U S A* 113(27), 7420-7425 (2016)
DOI: 10.1073/pnas.1601982113

309. W. W. Yang, Y. W. Zhong, S. Yoshikawa, J. Y. Shao, S. Masaoka, K. Sakai, J. Yao and M. A. Haga: Tuning of redox potentials by introducing a cyclometalated bond to bis-tridentate ruthenium(II) complexes bearing bis(N-methylbenzimidazolyl)benzene or -pyridine ligands. *Inorg Chem* 51(2), 890-899 (2012)
DOI: 10.1021/ic2016885

310. B. M. Samudio, V. Couch and A. A. Stuchebrukhov: Monte Carlo Simulations of Glu-242 in Cytochrome c Oxidase. *J Phys Chem B* 120(9), 2095-2105 (2016)
DOI: 10.1021/acs.jpcb.5b10998

311. S. de Vries: The role of the conserved tryptophan272 of the *Paracoccus denitrificans* cytochrome *c* oxidase in proton pumping. *Biochim Biophys Acta* 1777, 925-928 (2008)
DOI: 10.1016/j.bbabio.2008.05.008

312. A. Paulus, C. Werner, B. Ludwig and S. de Vries: The cytochrome ba3 oxidase from Thermus thermophilus does not generate a tryptophan radical during turnover: Implications for the mechanism of proton pumping. *Biochim Biophys Acta* 1847(10), 1093-1100 (2015)
DOI: 10.1016/j.bbabio.2015.05.013

313. S. Al-Attar and S. de Vries: Energy transduction by respiratory metallo-enzymes: From molecular mechanism to cell physiology. *Coord Chem Rev* 257, 64-80 (2013)
DOI: 10.1016/j.ccr.2012.05.022

314. S. Yoshikawa: A cytochrome *c* oxidase proton pumping mechanism that excludes the O_2 reduction site. *FEBS Lett* 555, 8-12 (2003)
DOI: 10.1016/S0014-5793(03)01098-6

315. S. Yoshikawa, K. Muramoto, K. Shinzawa-Itoh, H. Aoyama, T. Tsukihara, T. Ogura, K. Shimokata, Y. Katayama and H. Shimada: Reaction mechanism of bovine heart cytochrome c oxidase. *Biochim Biophys Acta* 1757(5-6), 395-400 (2006) DOI: 10.1016/j.bbabio.2006.04.028

316. S. Yoshikawa, K. Muramoto and K. Shinzawa-Itoh: Reaction mechanism of mammalian mitochondrial cytochrome c oxidase. *Adv Exp Med Biol* 748, 215-236 (2012) DOI: 10.1007/978-1-4614-3573-0_9

Abbreviations: PSII, photosystem II; TRO, terminal respiratory oxidases; COX, cytochrome oxidase; BRC, bacterial reaction centre; ET, electron transfer; PLS, proton loading site; BNC, binuclear catalytic centre; Rubpy, tris(2,2-bipyridyl)ruthenium; KIE, kinetic isotope effect.

Key Words: Photosystem, Cytochrome, Oxidase, Protons, Membrane potential, Channels, Electrogenic, Voltage, Electron injection, Review

Send correspondence to: Sergey A. Siletsky, Belozersky Institute of Physico-Chemical Biology, Lomonosov Moscow State University, Leninskie Gory, Moscow 119991, Russian Federation, Tel: 74959395149, Fax: 74959393181, E-mail: siletsky@genebee.msu.su